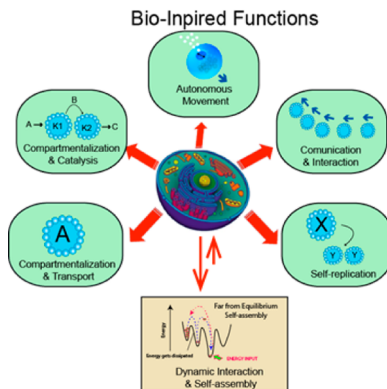


## Mimicking the Cell: Bio-Inspired Functions of Supramolecular Assemblies

Yingfeng Tu, Fei Peng, Alaa Adawy, Yongjun Men, Loai K. E. A. Abdelmohsen, and Daniela A. Wilson\*

Institute for Molecules and Materials, Radboud University, Heyendaalseweg 135, 6525 AJ, Nijmegen, The Netherlands



### CONTENTS

1. Introduction	
1.1. Preface	A
1.2. Inspiration from Nature	A
1.3. Definitions	B
1.4. Scope of this Review	C
2. Functions of Supramolecular Assemblies in Structural Biology	D
2.1. Membrane Proteins: A Challenging Story	D
2.2. Protein Solubilization	D
2.3. Protein Stabilization	D
2.3.1. Amphipols (APols)	E
2.3.2. Nanodiscs (NDs)	E
2.4. Protein Crystallization	F
2.4.1. Lipidic Cubic Mesophases	F
2.4.2. Bicelles	G
2.5. Conclusion	G
3. Bioinspired Functions of Supramolecular Assemblies	G
3.1. Compartmentalization, Transport, and Release	G
3.1.1. Passive Transport and Release	H
3.1.2. Selective Transport and Release	I
3.2. Compartmentalization and Catalysis	T
3.2.1. Micellar-Based Catalysis	V
3.2.2. Polymersomes	V
3.2.3. Virus Capsids	X
3.2.4. Supramolecular Polymeric Based Supra Molecular Catalysis	X
3.3. Autonomous Movement	Z
3.3.1. Polymersome Stomatocyte Nanomotors	Z
3.3.2. Layer-by-Layer Motors	AB
3.3.3. Cell-Based Motors	AB
3.3.4. Metal–Organic Framework (MOF) Motors	AC

3.3.5. Polymer Single Crystals (PSC)-Based Nanomotors	AC
3.4. Interaction and Communication	AD
3.4.1. Chemotaxis	AD
3.4.2. Magnetotaxis	AF
3.4.3. Other Forms of Taxis	AF
3.4.4. Conclusion	AF
3.5. Self-Replication of Supramolecular Assemblies	AG
4. Dynamic Interaction and Self-Assembly	AH
4.1. Far-from-Equilibrium Self-Assembly	AH
4.1.1. Definition of Self-Assembly Far-from-Equilibrium	AI
4.1.2. Light as Energy Source	AI
4.1.3. Electricity as Energy Source	AJ
4.1.4. Magnetic Field as Energy Source	AJ
4.1.5. Catalytic and Fuel Consuming System	AJ
5. Conclusion and Perspective	AK
5.1. Toward Artificial Cell	AL
5.2. Outlook	AN
Author Information	AO
Corresponding Author	AO
Notes	AO
Biographies	AO
Acknowledgments	AP
References	AP

### 1. INTRODUCTION

#### 1.1. Preface

The successful assembly of large supramolecular structures infers a delicate balance between reversible noncovalent interactions which are capable of undergoing correction and reassembly, stereochemical features (chirality), and conformational flexibility.<sup>1</sup> The goal of the supramolecular chemist is to synthesize the simplest molecular structures that are able to form supramolecular assemblies with novel functions that cannot be fulfilled by a single molecule or collection of molecules. The functions that arise from these supramolecular architectures can be as diverse as novel magnetic and optical properties, catalysis, molecular recognition, and transport processes.<sup>2–6</sup> While many excellent reviews focused on the synthesis and characterization of supramolecular architectures from a structural point of view with the aim to design complex

**Special Issue:** Frontiers in Macromolecular and Supramolecular Science

**Received:** June 8, 2015

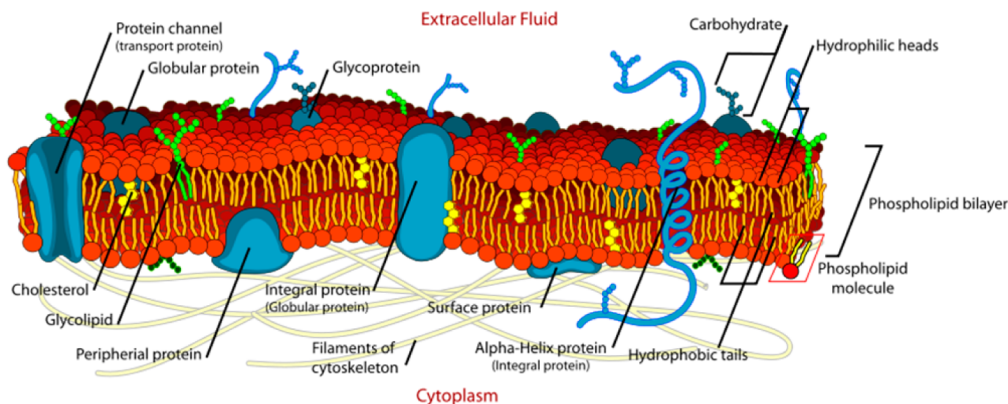


**Figure 1.** Representation of cell membrane. Reprinted from Wikipedia (Auther: LadyofHats). ([http://en.wikipedia.org/wiki/Cell\\_membrane#/media/File:Cell\\_membrane\\_detailed\\_diagram\\_en.svg](http://en.wikipedia.org/wiki/Cell_membrane#/media/File:Cell_membrane_detailed_diagram_en.svg)).

supramolecular assemblies inspired by nature, very few have ventured to look further to combine a complex form and function in one.<sup>7,8</sup> It is the aim of this review to give account of the emerging functions of supramolecular assemblies reported to date in the literature. These assemblies have been already employed as tools to expedite studies in different research fields such as the determination of three-dimensional structures of biological macromolecules by means of different characterization methodologies. Above that, vital bioinspired functions from compartmentalization, transport, regulated transport, catalysis, motion, and collective movement to more challenging approaches such as dynamic and far-from-equilibrium self-assembly have been facilitated and well-investigated in the latest three decades. These bioinspired functions are expected to be potential routes for other emerging properties such as chemotaxis, self-replication, and eventually mimicking of the cellular life cycle in minimal life systems.

## 1.2. Inspiration from Nature

Cellular structures are one of the basic building blocks of life and perhaps the most well-studied collection of complex systems that has inspired many scientific disciplines to design synthetic structures that can mimic their functions. The simple prokaryotic cell has been the inspiration for many of the oldest reports in the literature relating to compartmentalization mimicking cells; however, as the field of bioinspired self-assembly moves forward, there is a drive to strive to reach the complexity of eukaryotic cells containing membrane bound organelles and cytoskeletons that can mediate many complex processes in concert. The living cell is a microconfining space with an outer membrane and multiple internal organelles, which can provide segregation for the different processes that act in concert within the cell. By observing cellular processes, scientists have tried to mimic the design features of such complex structures to create a minimal cell, leading to a new field “bottom-up” synthetic biology.<sup>9</sup> The design of artificial cell membrane was among the first subjects to be investigated.

The cell membrane is an assembly of amphiphilic lipids (mainly phospholipids and cholesterol) as a bilayer with short-range liquid crystalline ordering held together mainly by hydrophobic interactions. The hydrophilic polar heads of the amphiphiles are exposed to the surrounding aqueous environment, while the hydrophobic tails are embedded in the bilayer center (Figure 1).

The main function of the cell membrane is to separate and protect the intracellular compartments. The semipermeable cell

membrane can provide a scaffold for biological macromolecules to selectively mediate the release and uptake of molecules, ions, and particles for intra- and intercellular signaling processes. Small vesicular structures also exist among the intracellular organelles. These vesicles perform a variety of functions, including osmotic control (vacuole), intracellular digestion (lysosomes), transport of molecules between different organelles and secretion of wastes (toxic compounds), hormones, enzymes, and neurotransmitters (secretory vesicles).

Beside compartmentalization, other important molecules like DNA and  $\alpha$ -helices or  $\beta$ -sheets of proteins provide important functions such as transfer and storage of genetic information in nucleic acids and the structural organization of proteins (enzymes) into efficient molecular machines. The most impressive assembly of proteins into a molecular machine is that of the ribosome,<sup>10,11</sup> which is the molecular foundry that processes mRNA sequences, to produce a multitude of proteins with diverse functionalities. Design of structure is the control over the spatial placement of atoms and molecules, which allows for instance the folding of a protein in a specific direction that if misfolded can have dramatic consequences in the biochemical systems.

All above examples among many others in nature have inspired scientists to mimic these compartmentalized structures found within cells via supramolecular assemblies that can perform several bioinspired functions (Figure 2). These supramolecular assemblies such as micelles,<sup>12</sup> unilamellar, lamellar, and multilamellar vesicles (liposomes)<sup>13,14</sup> from amphiphilic (amphipathic) lipids and later also from amphiphilic polymers (polymersomes)<sup>15</sup> and dendrimers (dendrimersomes)<sup>16</sup> are nowadays widely used in different diagnostic and therapeutic medical applications.<sup>17</sup>

In 1878, Louis Henry first proposed the idea of molecular polymerization via associative interactions;<sup>18</sup> however, it was the seminal paper of Jean-Marie Lehn in 1990 that demonstrated the design and synthesis of the first linear supramolecular polymer based on hydrogen bonding among small molecules.<sup>19</sup> Other recent studies also focused on mimicking the transcription and translation of information within ribosomes by designing synthetic analogues of processed enzymes that are able to thread onto biopolymers and to perform stepwise reactions along the polymer chain.<sup>20,21</sup> Nowadays, the functions of the designed structures include (chiral) molecular recognition, (selective) transport, drug delivery, catalysis, and many other industrial applications.<sup>17</sup> In combination with polymolecular organization, they open the path toward molecular and

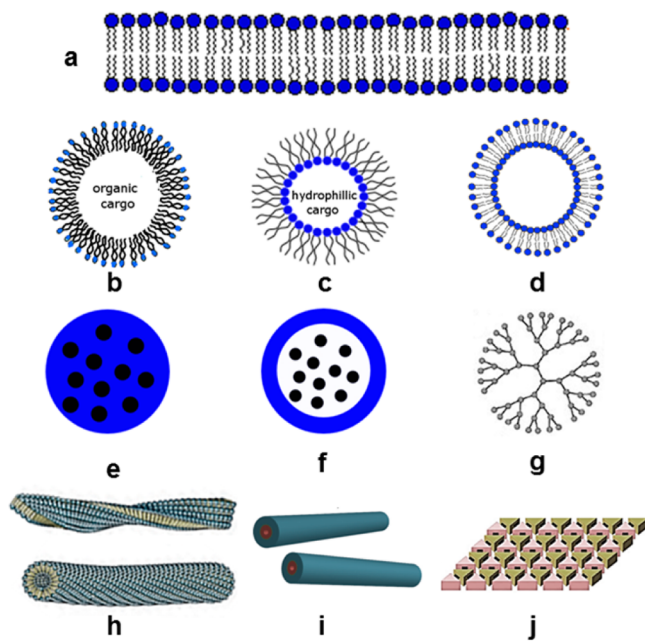


**Figure 2.** Several examples of bioinspired self-assembled structures: (a) planar lipid bilayer, (b) micelles, (c) inverted micelles, (d) liposomes (polymersomes), (e) nanospheres, (f) nanovesicles, (g) dendrimers, (h) nanotubes, (i) nanorods, and (j) 2D crystals.

supramolecular devices for information processing and signal generation.<sup>4</sup>

### 1.3. Definitions

Several concepts and terms are used throughout this review, which require a clear distinction. Herein, we explain the most used terms and the historical development behind them.

Self-assembly is a process by which molecules, ions, or polymers arrange spontaneously or in response to a specific stimuli into supramolecular structures via hydrogen bonding, hydrophobic and electrostatic interactions, and donor–acceptor effects, or metal ion coordination as basic interactions between the components and their media.<sup>4</sup> Self-assembly is generally associated with spontaneous energy-minimization processes and thermodynamic equilibrium and requires the stability of the individual entities throughout the assembly process (in a more accurate sense, it is described as static self-assembly).<sup>22</sup> The

formed product is a single well-defined structure, which stays in thermodynamic equilibrium with its pre-existing components.<sup>23</sup> The term self-assembly is frequently used in supramolecular chemistry to mean largely rigid, organized, synthetic architectures facilitated by molecular receptors using a bottom-up approach.<sup>24–27</sup>

Self-organization is a process by which supramolecular structures or entities in solution or solid state arrange themselves into two-dimensional (2D)- or three-dimensional (3D)-ordered periodic lattices or quasiperiodic arrays with rotational symmetry other than the crystallographically allowed 2-, 3-, 4-, or 6-fold symmetry.<sup>24</sup> While self-assembly implies binding, self-organization additionally implies translation of information.<sup>4</sup> This information is necessary for self-organization to take place, and the algorithm (molecular recognition events) that the process follows must be preprogrammed into the components and operated through selective molecular interactions. Self-organization takes place as a subsequent stage of a nonequilibrium stimulated process, whereas self-assembly occurs spontaneously to move a system toward equilibrium without any predefined molecular algorithm.<sup>28</sup> Therefore, the term self-organization is associated with biological systems (e.g., self-organization of DNA double helix is primarily mediated via positive and negative feedback events, which act as the driving force). The result is the emergence of a pattern from numerous nonlinear interactions between smaller constituents.<sup>29</sup>

Complex systems have been the subject of debate over years resulting sometimes in confusion of this term with that of complicated systems. Like a complex system, complicated systems can have a large plurality of parts and their parts may interact; however, the removal of a single component results in complete failure of the system. Complex systems may be made up of many interacting quasi-equivalent parts while their complexity arises not from the number of parts but rather in the emergence of an evolving structure able to adapt, interact, self-control, and self-heal. Complex systems have been most elegantly described by Ottino<sup>30</sup> as systems “capable of exchanging stimuli with one another and with their environment, with immediate neighbors or with distant ones; display organization without any external organizing principle being applied and learning from past history and modify their states accordingly...” Biological systems and those described herein are examples of complex systems; however, there are many examples of such systems that are emerging in today’s

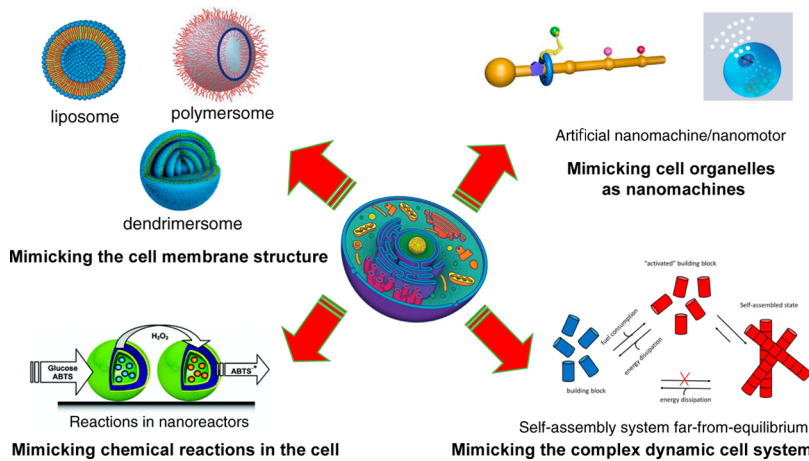


**Figure 3.** Bioinspired concepts originated from cell.

connected society such as financial banking system, social media, and the Internet.

#### 1.4. Scope of this Review

In the following text, different bioinspired functions and applications such as compartmentalization, transport, drug release, catalysis, motion, taxis, and self-replication generated from supramolecular assemblies toward artificial lifelike systems will be reviewed. Before deciding to dive straight into the bioinspired function, we have chosen to review the usage of supramolecular assemblies to assist and accelerate the studies of biological macromolecules and determine their functioning structures. Despite its importance, this topic is usually skipped, though it presents the solid basis for studies concerning protein/peptide–polymer hybrid materials that in turn are reviewed thoroughly elsewhere.<sup>31,32</sup> More detailed and recent specialized reviews on each of the topics will be presented at the beginning of each section. This review does not attempt to address detailed analysis of supramolecular assemblies from a structural point of view reported in the literature<sup>4,24,33–36</sup> but rather look at the functions of such assemblies from a biomimetic point of view (Figure 3).

## 2. FUNCTIONS OF SUPRAMOLECULAR ASSEMBLIES IN STRUCTURAL BIOLOGY

In order to mimic natural assembly and function, a robust understanding of the mechanism of action of biological macromolecules is required.<sup>37</sup> The elucidation of the macromolecular structures to high degree of resolution is heavily utilized in reports that have aimed to duplicate, modify, or expand upon the target structures already observed in nature.<sup>38</sup>

The majority of structures that are available in the protein data bank (PDB)<sup>39</sup> were solved using X-ray diffraction (XRD). Other methodologies such as neutron diffraction (ND), nuclear magnetic resonance (NMR), and electron microscopy (EM) contributed in solving the remaining structures. The same diffraction techniques used by structural biologists have been extended and adapted by supramolecular chemists in the retrostructural analysis of self-organized periodic and quasiperiodic lattices that can mimic biological structures.<sup>16,24,40–43</sup>

Combined with the analysis of functions via physical organic chemistry and other analytical techniques, the supramolecular chemists designed structures to mimic the architectural and functional assemblies found in nature.<sup>24</sup> The ultimate aim of structural biologists as well as the supramolecular chemists is to determine the structural model of the macromolecule or supramolecule under study in order to elucidate how the specific function under study arises from the structure observed.<sup>44</sup> Although there are many interesting examples of proteins incorporated into self-assembled systems, we have chosen to focus on one set in particular that has demonstrated the co-operative effect of self-assembly and natural protein to observe both structure and function in concert. In this section, we focus on the utilization of supramolecular assemblies that have been exploited to facilitate the structural studies of an important category of macromolecules: membrane proteins.<sup>45</sup>

#### 2.1. Membrane Proteins: A Challenging Story

Membrane proteins are vital for the transportation of nutrients and signaling molecules across the cell membrane. These proteins can be peripheral: temporarily associated with the lipid bilayer; membrane-anchored: bound to the lipid bilayer through lipidated amino acid residues; or integral: permanently spanning the entire bilayer and can either be monotopic where they have

only one terminal away from the lipid bilayer (in intra- or extracellular environment) or polytopic (also called transmembrane) where they have both intracellular and extracellular terminals (Figure 1). The tight association of these proteins, especially integral proteins, with other membrane components (mainly lipids) and their possession of hydrophobic surface regions buried in the lipid bilayer core as well as hydrophilic regions with charged or polar residues exposed at the external faces of the membrane reveal that their amphiphilic nature makes them challenging to study.

Membrane proteins represent more than half of the known drug targeting sites. Nevertheless, structure-based drug progress is hindered by the inadequacy of available 3D structural models for these proteins. Given their amphipathic nature and thus their peculiar solubility properties, membrane proteins are not completely compatible with the aqueous-based purification and crystallization conditions used routinely for most globular (water-soluble) proteins. They rather need to be stabilized in conditions resembling their natural microenvironment.<sup>46</sup> These requirements made the first successful crystallization of membrane proteins (bacteriorhodopsin<sup>47</sup> and porin<sup>48</sup>) challenging, the first report of which was not published until 1980, and the first structural model of a membrane protein (a photosynthetic bacterial reaction center)<sup>49</sup> was published five years later in 1985.<sup>50</sup> In order to determine the functional structure of the target membrane protein, it needs to be first isolated from its natural matrix via disruption of the surrounding membrane bilayer, which is mainly facilitated by using surfactants. The second necessary step is stabilization, so that the protein can survive subsequent treatment en-route to structure determination. At this stage of sample preparation, different characterization methodologies can be exploited to derive structural information. Above that, different strategies are nowadays employed<sup>51–53</sup> to enhance the crystallization of these proteins to be characterized by the state-of-art macromolecular crystallography facilities. These strategies employ in some sense the merits of supramolecular assemblies. This will be discussed in the following subsections.

#### 2.2. Protein Solubilization

Inspired by the amphiphilic nature of membrane proteins, detergent micelles, assembled from amphipathic surfactants, have been employed to purify and solubilize these proteins from their membrane bilayer.<sup>54,55</sup> If correctly selected, detergents can maintain with a high degree of equivalence the biological activity of the protein.<sup>56</sup> Detergent micelles form a thin layer around the membrane protein to mimic the phospholipid bilayer found in nature and consequently can disrupt this bilayer forming mixed micelles.<sup>57</sup> It is the separation of mixed micelles to protein–detergent and detergent–lipid micelles that defines the protein solubilization. Unfortunately, the dissociation properties of detergents can also decrease the activity of the proteins and even cause their destabilization and eventual denaturation. At this stage, the essential protein–protein and protein–lipid<sup>58</sup> interactions at the transmembrane region of a membrane protein are disrupted and thus the protein becomes inactivated. Therefore, crystallizing proteins in detergent-based mother liquor, although largely used, does not always correlate well with the intact natural form. In fact, the protein-detergent complex is the entity that crystallizes with high probability of having disordered detergent molecules within the crystals.<sup>59</sup> Mild nonionic detergents<sup>55,60</sup> were found to significantly

increase the success rate of proteins that were crystallized in aqueous-detergent-based conditions.<sup>59</sup>

The challenging aspect when using detergents to crystallize proteins in this application is that the detergent molecules should fit around the hydrophobic regions of the protein without hindering the interprotein contacts. In the presence of membrane proteins, detergent monomers, protein-free detergent micelles, and protein-bound detergents exist in equilibrium. The protein-bound detergent resembles micellar structures: nonpolar portions of the detergent are sequestered by the protein and thus held away from aqueous solvent; however, studies suggest that rather than a micellar structure, a toroidal structure more similar to a monolayer of detergent wrapped around the protein is generally formed.<sup>61,62</sup>

Recently, more promising synthetic detergent micelles based on calix[4]arenes that stabilize the protein not only via hydrophobic interactions but also via a network of salt bridges with basic residues of the protein has been reported (Figure 4).<sup>63</sup>

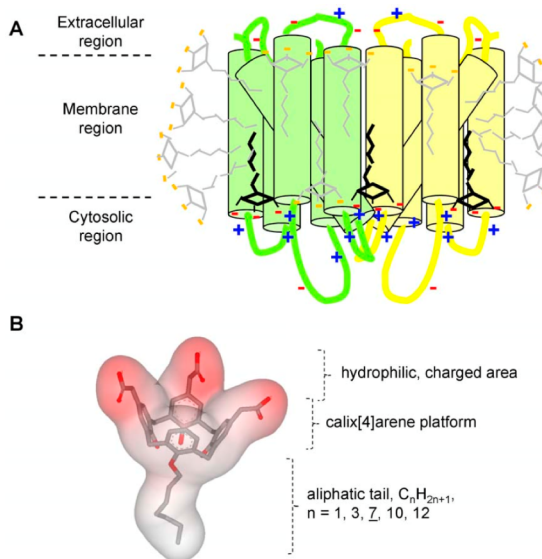


**Figure 4.** Concept of salt bridge network between anionic and amphiphilic molecules and basic residues located at the cytosol–membrane interface of membrane proteins. (A) Scheme of a hypothetical dimeric membrane protein typically displaying basic residues at the cytosol–membrane interface. (B) Chemical structure of the designed molecules, C4Cn. Reprinted from ref 63 under the terms of the Creative Commons Attribution License.

In addition, engineered micelles that form a micellar aggregate when mixed with a hydrophobic metal chelator have been demonstrated to offer great utility in separation of membrane proteins from aqueous soluble proteins (Figure 5).

### 2.3. Protein Stabilization

Concomitant with solubilization of membrane proteins, is their stabilization, that is necessary after extraction from their native environment in order to deliver an intact protein.<sup>65</sup> The natural progression from micellar structures for the encapsulation of membrane proteins is to reconstitute the purified membrane proteins into lipid-based structures. The reconstitution step allows for protein–protein as well as biomimetic protein–lipid interactions. The usage of the reconstitution strategy prevents aggregation of membrane proteins after being solubilized using detergents.<sup>66</sup> For reconstitution, many natural as well as

artificial lipids that spontaneously assemble into lipid bilayers and liposomes were utilized. This facilitated the assembly of membrane proteins into previously inaccessible patterns (e.g., 2D crystals) for electron crystallography, NMR small-angle X-ray scattering (SAXS), and small angle neutron scattering (SANS) and other promising characterization methodologies.<sup>67,68</sup> In this section, we review the most recent achievements in self-assembly-mediated protein stabilization.

**2.3.1. Amphipols (APols).** Amphipols are a class of amphiphilic polymers which provide means for proper folding of membrane proteins after their purification using detergents.<sup>69,70</sup> APols are low molecular weight linear polymers with alternating polar and nonpolar side chains. The key advantage of these polymers is that protein solubility can be preserved by low bulk concentrations of polymer.<sup>71</sup> In the absence of competing surfactants, APols bind to the transmembrane surface of the protein in a noncovalent but quasi-irreversible manner.

Membrane proteins complexed with APols exhibit multipoint interactions and are therefore able to fold into a form that represents a protective and nondenaturing bubble and possess protein–protein interactions, rather than the protein–surfactants ones, as seen in their native state, thus exhibiting higher stability while remaining water-soluble.<sup>72,73</sup> APol A8–35 a poly(acrylic acid) containing octylamine and propylamine grafts allowed both  $\beta$ -barrel and  $\alpha$ -helical membrane proteins to fold to their native state without any detergents or lipids.<sup>74</sup> Many functionalized APols are available and suitable for different aspects of synthetic biology and are reviewed extensively by Martinez.<sup>75</sup> The antiaggregating effect of these APols makes them suitable for NMR studies,<sup>76</sup> however, until recently with limited applicability for crystallization. APols have been successfully used to deliver a membrane protein, diacylglycerol kinase (DAGK), from an octylamine/poly(acrylic acid) APol complex into preformed lipid vesicles to adopt a suitable inserted and folded structural state.<sup>77</sup> Very recently, Gordeliy and co-workers reported that an APol A8–35-trapped Bacteriorhodopsin (BR) can be transferred to bicontinuous  $p\bar{n}3m$  cubic structure (discussed below) and crystallized to high-quality crystals that diffracted beyond 2 Å, with no distinguishable differences between the resultant structural model and the known structure for this protein.<sup>78</sup> The transfer of trapped membrane proteins into lipidic mesophases such as that stated previously may hold significant scope not just for elucidating the structure and function of biological molecules but also in designing materials with both biologically inspired form and function.

**2.3.2. Nanodiscs (NDs).** Discoidal nanometer-sized soluble phospholipid membranes, known as nanolipoprotein particles (NLPs), provide a platform to render membrane proteins soluble in a detergent-free aqueous medium. The membrane diameter is well-defined and, therefore, homogeneous protein solution with high level of monodispersity can be realized. Moreover, simultaneous unrestricted access to both faces of the membrane bilayer is facilitated with the possibility of controlling the composition of the surrounding lipids.<sup>79</sup> NDs are formed upon mixing of buffered saline solutions of phospholipids, purified membrane scaffold protein (MSP), and a detergent<sup>80,81</sup> or by sonication of MSP and phospholipid vesicles<sup>80</sup> in the presence or absence of, for instance, proteins. Upon the removal of the detergent, by dialysis, NDs can self-assemble into multiple disc stacks (Figure 6). A number of membrane proteins have been successfully assembled within these NDs.<sup>82</sup>

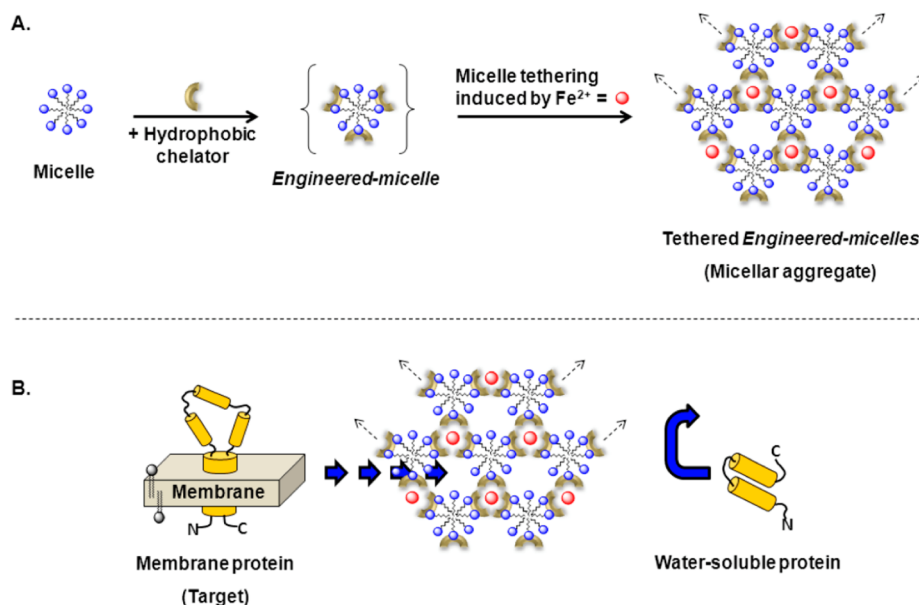


**Figure 5.** Illustration of tethered engineered micelles and their utilization in membrane protein purification. A. Micelles composed of nonionic detergents are transformed into engineered micelles upon incubation with a hydrophobic chelator and specifically cluster in the presence of  $\text{Fe}^{2+}$  ions, thereby forming micellar aggregates interconnected by [metal:chelator] complexes. B. Membrane proteins partition into the micellar aggregate (due to their hydrophobic character) whereas hydrophilic proteins do not. Reprinted from ref 64. Copyright 2013 American Chemical Society.

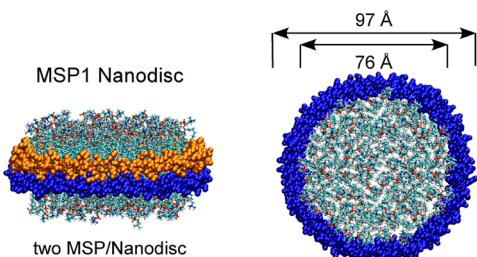


**Figure 6.** Illustrations of Nanodisc structures. Top view shows nanodiscs composed of MSP1D1 and phospholipid shown in side view and top view. The two MSPs are orange and blue. Reprinted with permission from ref 82. Copyright 2010 Elsevier.

NDs facilitate the studies of membrane proteins in different perspectives. Immobilization of NDs containing proteins on surfaces, such as glass or mica, is facilitated through binding of tags on the MSP; this allowed for their orientation into a specific direction, with the bilayer plane parallel to the surface.<sup>83</sup> These immobilized NDs can be examined by several analytical and imaging techniques such as atomic force microscopy (AFM),<sup>84–87</sup> being patterned by microfluidic channels<sup>88</sup> or electron microscopy.<sup>89</sup> NDs can also be used in receptor and enzyme studies and ligand binding.<sup>79</sup> Structural investigations for functionally active membrane proteins embedded in NDs by using magic angle spinning solid state NMR has been reported.<sup>90,91</sup> High throughput screening using solution NMR for structure determination has also been reported.<sup>92</sup> Because NDs have a small fixed diameter, the study of large membrane proteins was not facilitated until the self-assembly of macrodiscs was explored and proven to be possible by increasing the lipid to a MSP ratio during their preparation. This also promoted their investigations by using solid-state NMR.<sup>93</sup> It has been recently shown that, with a little exposure to detergents, an overexpressed fully functional membrane protein can be assembled into soluble lipid NDs, and the resultant level of purification is suitable for functional studies.<sup>94</sup>

## 2.4. Protein Crystallization

**2.4.1. Lipidic Cubic Mesophases.** The assembly of actively functioning membrane proteins into 3D crystals has been facilitated through the use of bicontinuous cubic lipidic phases (CLP) which consists of a lipid, usually Monoolein,<sup>95</sup> and aqueous medium (water or buffer) mixed with the membrane protein.<sup>96,97</sup> This membrane system forms a transparent, toothpaste-like and complex 3D lipidic array permeated by an intercommunicating aqueous channel system.<sup>98</sup> This complex structure provides protein nucleation sites and facilitates crystal growth by lateral diffusion (Figure 7).

Because of the stiffness of these assembled systems, and their possible interference with the hydrophilic domains of membrane proteins, a sponge (liquid) analogue to lipidic

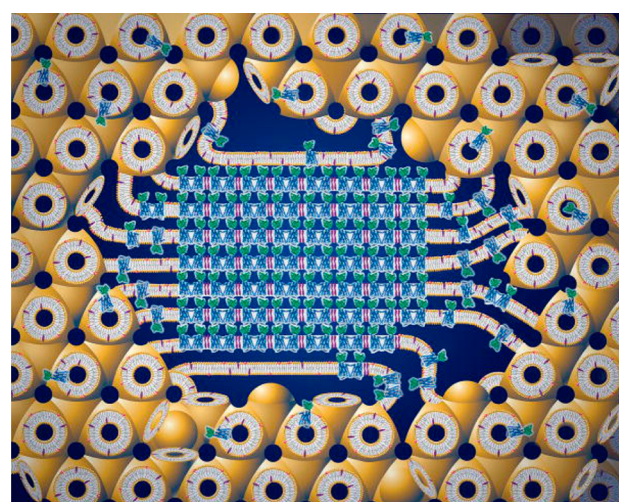


**Figure 7.** Cartoon representation of the events proposed to take place during the crystallization of an integral membrane protein from the lipidic cubic mesophase. Reprinted with permission from ref 99. Copyright 2009 Nature Publishing Group.

cupic mesophase has been explored, so-called lipidic sponge phases (LSP).<sup>100,101</sup>

**2.4.2. Bicelles.** Bicelles are small bilayer discs that form through mixing certain lipid/amphiphiles. They offer membrane proteins a bilayer-like environment much closer to the natural environment than that of detergents. In addition, bicelles encounter phase transition from liquid to gel upon raising the temperature above their transition temperature ( $T_m$ ) and thus can exist in different bicelle-based structures<sup>102</sup> (Figure 8).

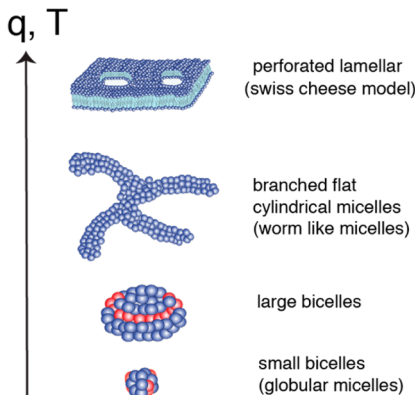


Figure 8. Different phases that can be obtained with bicelle-forming mixtures at different temperatures. Adapted with permission from ref 102. Copyright 2009 Elsevier.

Bicelle phases (liquid or gel) make the use of bicelles much easier than the viscous CLP, resulting in improved crystal packing of the membrane proteins and they are nowadays widely exploited in high-throughput crystallization experiments.<sup>103</sup> This high compatibility with membrane proteins has widened the applications of their utilization in structural biology as extensively reviewed elsewhere.<sup>104</sup>

As stated previously, neither detergents nor lipids can individually and efficiently effectuate crystallization upon mixing with the stabilized membrane protein, however, when used in combination with detergents and lipids have been shown to facilitate access to crystalline structures.<sup>102</sup> This approach has the advantage of promoting the growth of well-diffracting crystals with better packing (Type I) over the poorly diffracting crystals (Type II)<sup>103</sup> (Figure 9).

## 2.5. Conclusion

Drawing on the design principles of self-assembly, structural biologists have been able to extract naturally occurring membrane proteins and integrate them into surrogate membrane mimics and in doing so have been able to retain both the structure and function of the biological system. The incorporation of biologically relevant proteins into artificial membrane mimics has allowed structural biologists to observe the protein in an environment very close to its natural state while allowing them to use existing characterization tool sets to probe structure and function in concert that was previously unobtainable. In the proceeding sections, this review will focus on the application of design principles derived from structural biology in the design of self-assembled systems displaying both form and function found in natural systems.

Conversely, as structural biologists have drawn upon the toolbox of self-assembled systems to allow them to better control the systems of interest, the tools commonly used by crystallographers have been employed by a number of

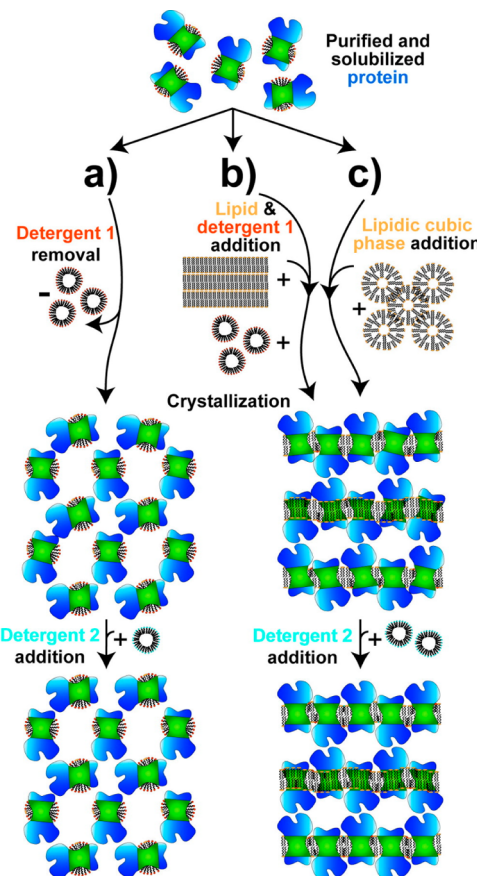


Figure 9. Membrane protein crystallization with high-lipid, high-detergent (HILIDE) concentrations, as compared to traditional techniques. Starting from purified and detergent-solubilized protein, different crystallization approaches are devised: (a) traditional crystallization of delipidated protein in detergents, (b) crystallization of relipidated protein with the HILIDE approach, or (c) lipid cubic phase crystallization. In (a), the detergent levels are typically minimized to generate initial Type II crystals which may be optimized using detergent or lipids screens. In contrast, (b) large amounts of detergent and lipid or (c) specific bicontinuous lipid phases are supplemented prior to crystallization, yielding Type I crystals. The Type I crystals are improved using similar approaches as for Type II crystals, albeit with higher concentrations of detergent. Reprinted with permission from ref 105. Copyright 2011 American Chemical Society.

laboratories in the retrostructural analysis of self-assembled systems. This technique was pioneered by the Percec group and a detailed overview of the application of retrostructural analysis of self-assembled complex systems is covered elsewhere.<sup>24</sup>

## 3. BIOINSPIRED FUNCTIONS OF SUPRAMOLECULAR ASSEMBLIES

### 3.1. Compartmentalization, Transport, and Release

One of the first bioinspired functions to be investigated via supramolecular assemblies was the ability to compartmentalize and confine structures in the same way organelles are able to separate different functionalities and pH inside the cell. While complete mimicking of natural systems has not been explored in great detail within supramolecular assemblies, many examples of using artificial organelles such as endogenous exosomes have been reported,<sup>106</sup> which represent a natural analogue to self-assembled systems. Similar to liposomal structures, bilayer exosomes containing proteins, siRNA, and mRNA in their inner

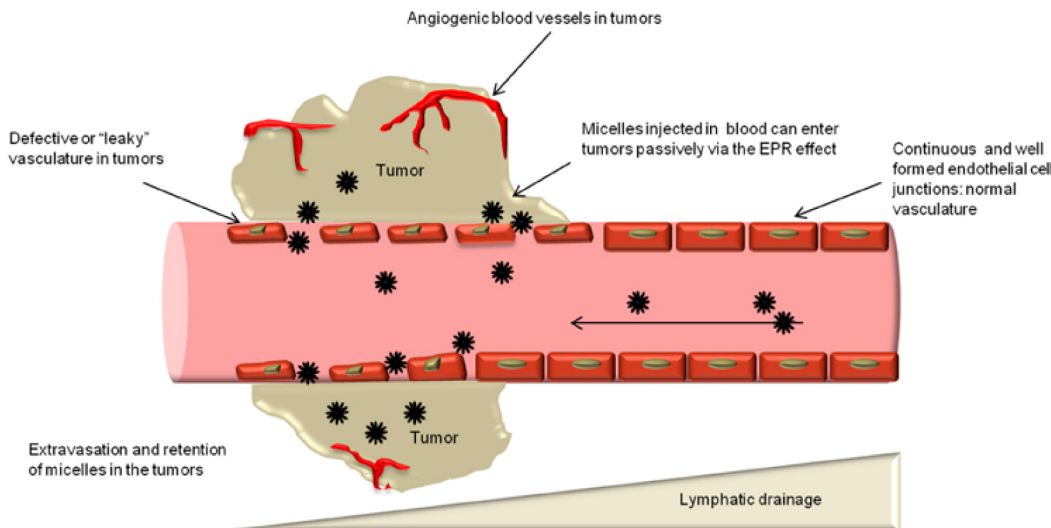


**Figure 10.** Cartoon representation of EPR effect in tumor tissue. EPR effect is mainly caused by leaky blood vessels and inefficient lymphatic drainage of the tumor tissue. Reprinted from ref 143 under the terms of the Creative Commons Attribution License (CC BY).

compartment<sup>107</sup> are widely used for membrane exchange and immunotherapy.<sup>108</sup> As outlined above, self-assembled structures such as liposomes,<sup>109–111</sup> micelles,<sup>112–114</sup> polymerosomes,<sup>15,115–117</sup> proteinosomes,<sup>118,119</sup> dendrimersomes,<sup>16,120</sup> and other vesicles were designed to achieve compartmentalization and mimic the functions of organelles. Furthermore, the compartmentalization approach allows also for sensitive drugs/proteins to be protected inside the self-assembled structures and has triggered their use for diagnostics and interventions in imaging and treatment of tumors. The theranostic drugs/proteins were encapsulated/adsorbed in different compartments of supramolecular assemblies as a simple-level of compartmentalization. Although not a direct mimic of the function of the cells, the use of compartmentalization in drug delivery is an important application of this concept where, as in the cell, separating processes requiring different environmental conditions is crucial. Ideally, supramolecular assemblies with drugs distributed in different compartments should achieve transportation and release of the payloads only to the desired sites without leakage or side effects.<sup>121,122</sup> However, tumor targeting and precise release under the stimuli still require many efforts to achieve this aim.<sup>123,124</sup>

On the basis of their mechanism of action, there are two types of transport,<sup>125</sup> passive and selective transport. Passive transport of supramolecular assemblies relies on diffusion and passive accumulation and is able to reach the target tissue to some extent due to the specific properties of the micro- and nanoscale carriers and certain features of the disease site.<sup>126</sup> Selective transport consists of stimuli-responsive transport<sup>127,128</sup> and active-targeting transport,<sup>129–131</sup> which are more efficient than passive transport. Stimuli-responsive delivery systems are based on physicochemical transformation of the self-assembled structures under different stimuli to achieve the transportation and delivery of loaded cargoes to the desired place.<sup>132</sup> Both applied environmental stimuli, and stimuli provided by diseased site such as lower pH and higher temperature are triggers used for delivery and release of compartmentalized drugs. Active-targeting transport<sup>122,133</sup> relies on specific binding between ligands<sup>134</sup> anchored onto the surface of supramolecular assemblies and receptors expressed on the surface of the desired cells, which results in uptake of the self-assembled

structures via endocytosis. In the following sections of this chapter, we will focus on applying the design principles learned from biological systems to generate mimetic self-assembled systems for passive and selective transport.

**3.1.1. Passive Transport and Release.** Passive transport of self-assembled micro- and nanosystems depends on the structural properties of the assembly and the pathological factors of diseases. A large number of studies have been carried out in the past decades on these kinds of delivery systems using a variety of nano- and microcarriers,<sup>135–137</sup> including vesicles, nanoparticles, and micelles due to the enhanced permeability and retention (EPR) effect<sup>126,138–140</sup> observed in tumor tissue which effectively facilitates the increased retention of large entities up to 400 nm in diameters, including drug-carriers (liposomes), nanoparticles, and macromolecular drugs in solid tumors. The rapid proliferation of tumor cells and their subsequent abnormal need for nutrition allows for the development of rapidly grown and often abnormal vascularization as a result of imbalance in angiogenic regulators. Compared to normal vessels, these newly formed blood vessels are leaky and permeable, as a result of poorly aligned endothelial cells resulting in wide fenestrations in the vessel wall. The well-known EPR effect is one of the most important properties of solid tumors, through which macromolecules and self-assembled structures tend to accumulate (Figure 10). The increased retention of macromolecules and nanoparticles is also enhanced by the lack of efficient lymphatic drainage in tumor tissue. In addition, the EPR effect has also been found in other pathological sites such as infected and inflamed tissues.<sup>141,142</sup>

In order to increase the efficiency of the EPR effect and since this method is based only on passive accumulation of particles circulating in the blood, self-assembled carrier systems were often decorated with poly(ethylene glycol) (PEG) on their surface to prolong their circulation often termed pegylation.<sup>144</sup> PEGylation can avoid both phagocytosis from macrophages and the marking of the antigen for phagocytosis by interactions with opsonin molecules such as antibodies and complement proteins. Compared to normal liposomes, PEG-modified liposomes were observed *in vivo* to circulate up to ten times longer than nonpegylated counter parts, therefore leading to higher retention possibility by EPR effect. On the basis of the

above mechanisms, Doxil, doxorubicin-loaded PEG-modified liposomes, received market clearance as the first commercially available drug-carrying liposomes approved by FDA in 1995.<sup>145</sup> Doxil, with its longer half-life time, can target the tumor site passively and treat the patients efficiently due to the EPR effect. However, this formulation suffers from decreased stability<sup>146</sup> due to the low mechanical properties of the liposomal membrane compared to natural lipid cell membranes. Further studies were directed toward searching for better structural alternatives by designing amphiphiles synthesized from polymers (polymersomes)<sup>15</sup> or from structures closer to phospholipids such as Janus dendrimers (dendrimersomes).<sup>16</sup> While polymersomes suffer from thicker membrane and low permeability, dendrimersomes showed to have thinner and tough membranes (Table 1) that mimic those of natural cell membranes, which allowed the incorporation of membrane proteins within their bilayer.

**Table 1. Membrane Properties of Liposomes, Polymersomes, and Dendrimersomes<sup>16</sup>**

dendrimersome	K <sub>a</sub> (mN/m)	lysis tension (mN/m)	critical $\alpha_c$ (mN/m)
(3,5) 12G1-PE-BMPA-(OH) <sub>8</sub> polymersomes	976	15	0.03
OB <sub>2</sub> (PEO-PBD) liposomes	100	14	0.21
SOPC	193	5.7	0.03
SOPC/50% Cholesterol	781	19.7	0.03

$K_a = \Delta T / \Delta \alpha$ ;  $\alpha_c = \Delta A / A_0$ ;  $\Delta T$  = fractional tension;  $K_a$  = elastic area expansion modulus;  $\Delta \alpha$  = fractional increase in membrane area; and  $\alpha_c$  = critical areal strain.

**3.1.2. Selective Transport and Release.** **3.1.2.1. Stimuli Responsive Transport and Release.** Traditional passive transport systems have facilitated therapeutic application in the clinic in the last few decades in the treatment of cancers. However, passive delivery systems also have limitations such as low selection and associated high systemic toxicity.<sup>147,148</sup> Therefore, self-assembled delivery systems that respond to different stimuli to control properties and transport behaviors are a promising and important field of research that can potentially open a door to more targeted delivery and thus lower systemic toxicity.<sup>148,149</sup> This class of adaptive structures include micro- and nanoscale vehicles based on responsive lipids,<sup>150,151</sup> polymers,<sup>40,152</sup> dendrimers,<sup>153</sup> and other macromolecules that are able to adapt to changes under single or multi stimuli.<sup>154</sup>

Functional vehicles play an important role in the controlled release of molecules in response to applied stimuli. For example, carboxyl<sup>155</sup> or amino groups<sup>156</sup> are generally introduced in pH-responsive self-assembled systems. By applying a pH stimulus at the target site (tumor), the encapsulated molecules were shown to be released in the tumor as a result of reduced stability of the vehicle structure. The stimuli used to trigger transport and release of molecules can be generally classified<sup>127,157</sup> by external physical stimuli (magnetic field, light, ultrasound, and electrical field) and internal stimuli (pH, temperature, redox, and enzymes). The properties and characteristics of different stimuli-responsive systems are reported below.

**3.1.2.1.1. pH-Triggered Transport and Release.** As discussed above, the encapsulation of different intracellular

organelles with their own lipid bilayer allows for the compartmentalization of different pH environments. This is typified by the endosomal transport mechanism whereby concomitant pH changes occur during the process of transport from early endosomes through the fusion with lysosomes and formation of endolysosomes. Early endosomes (EEs) are the compartments that receive the first incoming cargo and fluid from the plasma membrane of the cell. It is thought that EEs are formed largely from primary endocytic vesicles that undergo fusion to form the larger EE structure. This process takes around 10 min during which the fluid is rapidly recycled away and the cargo is retained and accumulated.<sup>158</sup> In the EEs, the pH of the inner compartment drops to around pH 6. EEs have a rich morphology of tubular and vacuolar domains. Maturation of the EEs into late endosomes (LEs) occurs as EEs migrate along microtubules toward the perinuclear space. The EEs fuse and lose their tubular features resulting in first spherical vacuolar structures and as more EEs fuse later, less spherical giant vacuolar structures are obtained. As the maturation process occurs, the pH of the endosomal space progressively becomes acidified, dropping gradually from pH 6 through to pH 4.9. The acidification of LE and EE structures is essential not only for mediating hydrolytic reactions but also for membrane trafficking, sorting of cargo, and for the inactivation of internalized pathogens. The final stage of LE maturation is fusion with lysosomes to acquire the enzymatic payload to form endolysosomes. The progressive decrease of pH in the endocytic pathway acts as a signal to some incoming cargo to give a sense of the location within the pathway as will be discussed below. The maturation process (Figure 11) represents

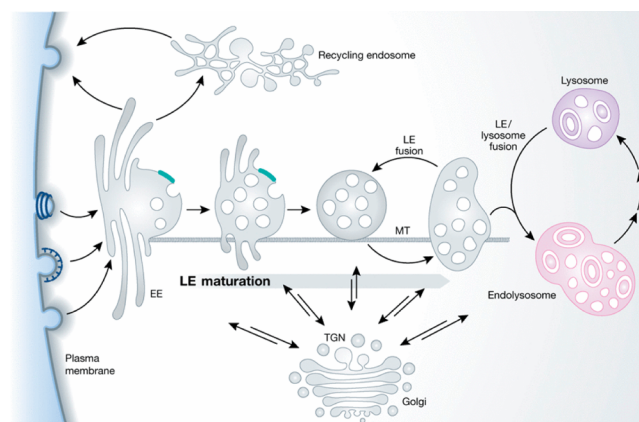


**Figure 11.** Cartoon representation of endosome/lysosome system. Reprinted with permission from ref 159. Copyright 2011 Wiley-VCH.

both an exchange of membrane components and shift in choice of fusion partners from EEs to LEs and acquisition of lysosomal components. The dramatic transformation seen in these structures is a function of the terminal usage of these compartments in the lysosomal degradation of the cargo contained within them.<sup>159</sup>

Transport and pH-mediated delivery of virus vectors is a common trait in the family *flaviviridae*. The *Flaviviridae* family of viruses contains some of the world's most problematic viral disease such as West nile virus, yellow fever, Dengue fever, swine fever, and Hepatitis type C. The utilization of transport followed by pH-triggered release of the Hepatitis C virus (HCV) has been identified as a major route to infectivity requiring an acidified intracellular compartment such as an

endosomal vesicle.<sup>160</sup> Following attachment and endocytosis, the viral particle becomes encapsulated into an early endosomal compartment (Figure 12). A post binding maturation step

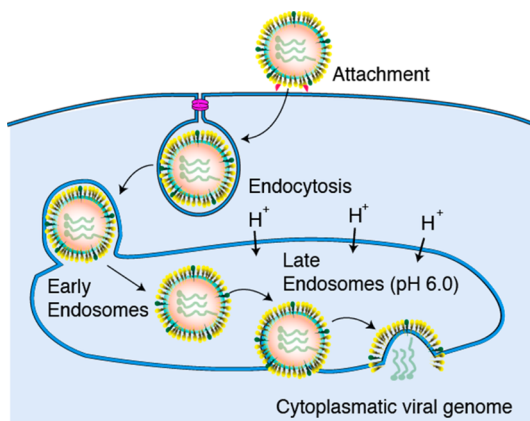


**Figure 12.** Schematic representation of fusion of virus membrane with endosomal membrane. Adapted from Web site [http://viralzone.expasy.org/all\\_by\\_protein/992.html](http://viralzone.expasy.org/all_by_protein/992.html).

results in priming the virus capsule for pH sensitivity, and the low pH of the endosomal compartment results in a conformational change of the viral glycoproteins, allowing for virus-endosomal membrane fusion and ultimate delivery of the viral genomic payload to the cytoplasm.<sup>161</sup>

In contrast, the African Swine Fever Virus (ASFV) enters the cell in a clathrin-coated vesicle, the clathrin coating is shed followed rapidly by colocalization into early endosomes. As the endosome maturation process proceeds, the virus becomes incorporated into multi vesicular bodies and retained through late endosomal progression. Once in the late endosomal compartment and the environmental pH is of a suitable level, desencapsulation takes place and ultimately release of the viral payload<sup>162</sup> (Figure 13).

Synthetic triggered transport systems that are pH-responsive are mainly chosen because of the presence of a pH gradient in the human body. On the systemic level, pH values<sup>163,164</sup> in the digestive system range from strong acidic to basic (stomach: 1.5–3.5; duodenum: 5.0–7.0; jejunum: 6.0–7.0; ileum: 7.0; colon: 5.5–7.0; rectum: 7.0), which can be used as a trigger to activate the release of drugs. In fact, pH gradients have also been observed at the macro level, the cellular level, and the subcellular level. Compared to normal tissue, the pH value of specific pathological sites such as inflamed,<sup>165</sup> infected,<sup>166,167</sup> or tumor tissue<sup>168</sup> is usually more acidic. For instance, the heterogeneous vasculatures in tumors cannot supply enough oxygen and nutrition for the growth of tumor cells because of the rapid proliferation. The lack of oxygen leads to increased levels of anaerobic respiration, and thus lactic acid production increases. The presence of lactic acid in tissues renders the tumor microenvironment acidic. The extracellular pH value in most tumor tissues is around 6.0–7.0, which is lower than physiological pH (7.4).<sup>169</sup> Even in the different compartments of cells, cytoplasm,<sup>170</sup> endosome,<sup>171</sup> endoplasmic reticulum,<sup>172</sup> lysosomes,<sup>173</sup> nucleus,<sup>174</sup> and other organelles have their own pH values. These properties have been taken into consideration for the development of pH-responsive delivery systems. There are two main synthetic strategies that have been employed to achieve pH-sensitive systems: (1) introduce materials with rich acidic and basic functional groups<sup>175,176</sup> and (2) introduce pH-

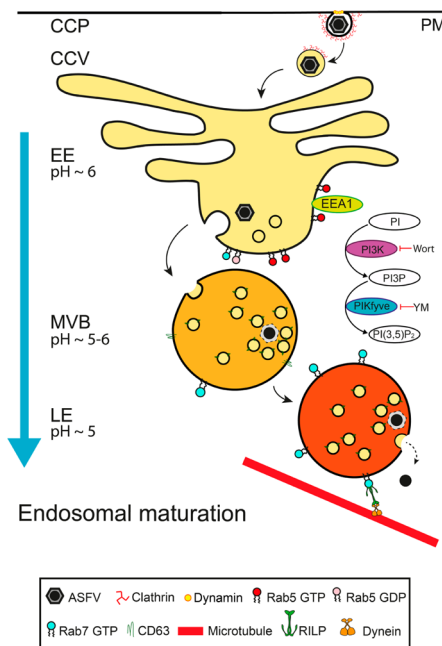


**Figure 13.** Cartoon representation of ASFV infection progress through the endosomal pathway. Reprinted from ref 162 under Creative Commons Attribution License.

responsive bonds,<sup>177,178</sup> which can be cleaved at a target pH value.

Molecules containing acidic and basic functionalities that interact during the self-assembly process are one of the simplest choices for preparing pH-responsive self-assembled systems. Palmitoyl homocysteine (PHC) is pH sensitive lipid and becomes neutral at low pH value. Release of drugs from liposomes containing PHC-doped phospholipid membranes in acidic conditions has been investigated intensively by Shinitzky and co-workers. The neutral liposome formed with PHC at low pH destabilizes the liposome's bilayer.<sup>175</sup> Poly-L-histidine (Poly-His) is a pH-sensitive polymer owing to the presence of an imidazole group, which is widely used for drug delivery and imaging.<sup>179</sup> The responsive range of poly-His is similar to the extracellular pH at a tumor site. The tumor microenvironment can trigger the protonation of imidazole group of Poly-His, resulting in targeted release of drugs. Poly-His-PEG-based micelles reported by Bae and co-workers are stable above pH 8.0. At lower pH (less than 7.2), protonation of the imidazole results in an increase in hydrophilicity and thus destabilization of the micelles.<sup>180</sup> Other attempts to simultaneously introduce an acidic and a basic group in one self-assembled system to accomplish more sophisticated and controllable structures have been reported.<sup>181</sup> As a biamphiphilic polymer, poly(acrylicacid)-*b*-polystyrene-*b*-poly(4-vinylpyridine) triblock copolymer (PAA-PS-PVP) has two different hydrophilic blocks, in which PAA and PVP are the acidic and basic segments, respectively. At low pH, PAA is protonated and becomes more hydrophobic, while PVP accepts a proton to produce a quaternary amine and thus becomes hydrophilic. The reverse occurs however at high pH. Vesicles made from this triblock copolymer can achieve reversible transformation from PAA on the outside structure to PVP outside structure in DMF/THF/water solution upon changing of the environmental pH<sup>182</sup> (Figure 14a). Zwitterionic copolypeptides poly(L-glutamic acid)-*b*-poly(L-lysine) (PGA-*b*-PLys) can spontaneously self-

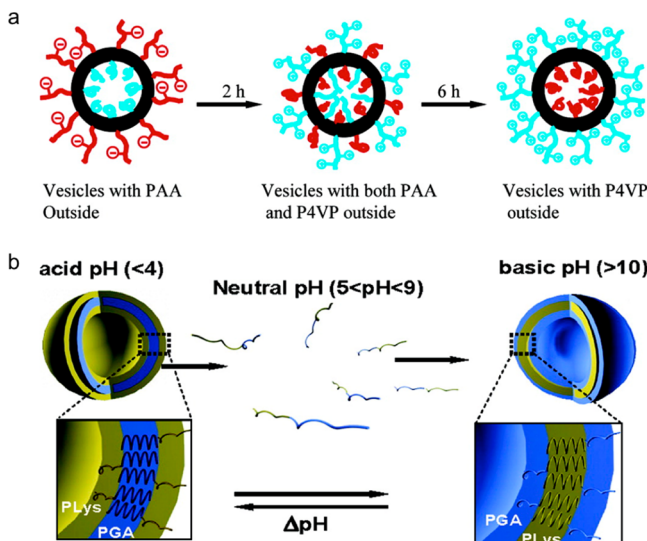


**Figure 14.** Reversible inside–outside structural changes. (a) Schematic representation of inversion of vesicles from PAA outside to P4VP outside. (b) Self-assembled vesicles with the diblock copolymer PGA15-*b*-PLys15 which can change the structure reversible. Reprinted with permission from refs 182 and 183. Copyright 2003 and 2005, respectively, American Chemical Society.

assemble into polymersomes in acidic and basic solutions. Because of the two different types of pH-sensitive polymers, these polymersomes can also undergo reversible inside–outside structural changes (Figure 14b), which could facilitate drug delivery in response to pH changes.<sup>183</sup>

As for self-assembled systems containing pH-cleavable bonds, many studies have been reported for different applications, a selection of the most relevant is presented herein. Core-cross-linked pH sensitive micelles were synthesized based on acid-labile acetal group and photocross-linkable hydrophobic polycarbonate for encapsulating paclitaxel.<sup>184</sup> After cross-linking, the micelles are stable at physiological pH, however, the acetal groups are hydrolyzed at moderately acidic pH 4.0–5.0, which leads to the release of paclitaxel. pH Sensitive dynamic covalent bonds, especially hydrazone bonds which can be cleaved at low pH, are one of the most versatile models of cleavable self-assembled systems.

Acid sensitive hydrazine linkers were introduced to link hydrophobic polybutadiene (PBD) with hydrophilic poly(ethylene glycol) (PEG). Polymersomes made from these dynamic diblock copolymers PBD-*r*-PEG and noncleavable copolymers PBD-PEG showed high stability even when 95% PEG was cleaved at low pH.<sup>185</sup> Polystyrene(PS)-*b*-PEG via an acylhydrazone bond linker was also used to prepare polymersomes under neutral and basic conditions. This pH sensitive vesicle can release cargoes upon addition of TFA (pH = 4.0).<sup>186</sup>

On the other hand, dynamic covalent bonds have also been used as a driving force for preparation of self-assembled systems. Van Esch et al. observed that small amphiphiles based on dynamic covalent bonds could form micelles at physiological pH.<sup>187</sup> 4-(Decyloxy) benzaldehyde (DBA) was used as a hydrophobic segment to react with PEG-*b*-poly(L-lysine hydrochloride) (PEG-*b*-PLKC) to make benzoic imine bonds. Reversible self-assembly and disassembly can be observed when the pH changes.<sup>188</sup> Molecules can also be conjugated to self-assembled units by pH-cleavable hydrazine linkers.<sup>189</sup> Elastin-like polypeptides (ELP) have been conjugated with antitumor

drugs such as doxorubicin via pH-labile linker hydrazone bond by Chilkoti et al. The conjugates, named chimeric polypeptides (CPs), can self-assemble into 100 nm nanoparticles in which ELP and doxorubicin act as the hydrophilic and hydrophobic parts, respectively. These CPs nanoparticles possess four times higher maximum tolerated dose than free DOX and have also demonstrated higher efficiency to the murine cancer model.<sup>190</sup>

Morphological transformation for self-assembled systems can also be induced by pH. Hydrophilic β-cyclodextrins with hydrophobic tails can self-assemble into bilayer cyclodextrin vesicles (CDVs). In order to form β-sheet-like domain on the surface of CDVs, octapeptide functionalized adamantine was introduced via host–guest interactions.<sup>191</sup> Decreasing the pH (pH = 5.0) in this system can induce the formation of the secondary structure of the octapeptide, changing from random coil into β-sheet, thus leading to reversible transformation of spherical CDVs into fibers (Figure 15). During the shape

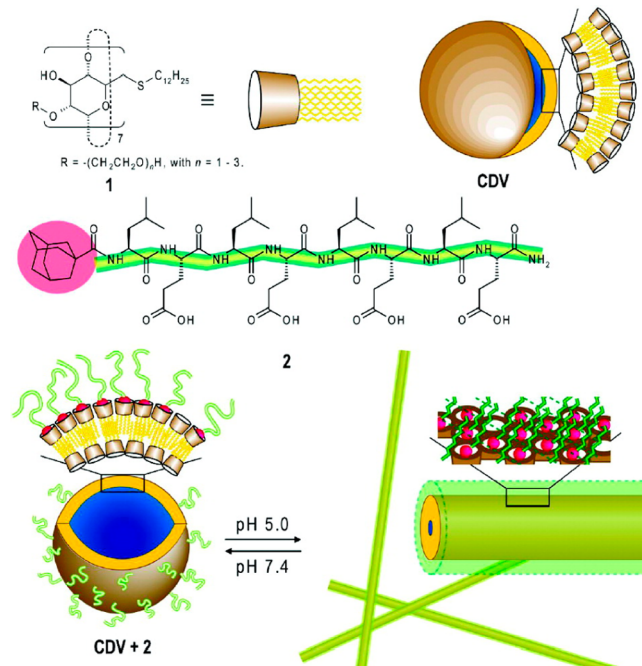


**Figure 15.** Representation of shape transformation between spheres and fibers based on self-assembly of β-CD derivative and adamantine modified octapeptide. Reprinted from ref 191. Copyright 2009 American Chemical Society.

transformation process, loaded cargoes can be transported and released at the desired site to decrease the toxicity.<sup>192</sup> Peptide amphiphiles consisting of pH-sensitive amino acid sequences, β-sheet forming peptide sequences, and alkyl tails can self-assemble into micelles or present as single components in solution.<sup>193</sup> Increasing the acidity to pH 6.6, which is quite similar to the microenvironment of tumor tissues, causes the shape transformation from micelles or single components into nanofibers.

**3.1.2.1.2. Temperature-Triggered Transport and Release.** Temperature response is generally viewed as a protective mechanism in most biological systems. A number of mechanisms involving self-assembly processes are notable including polysaccharide complexation and encapsulation, complexation and formation of supramolecular aggregates of proteins. The simple disaccharide trehalose has a dual function in nature. The first and most widespread use of trehalose is to

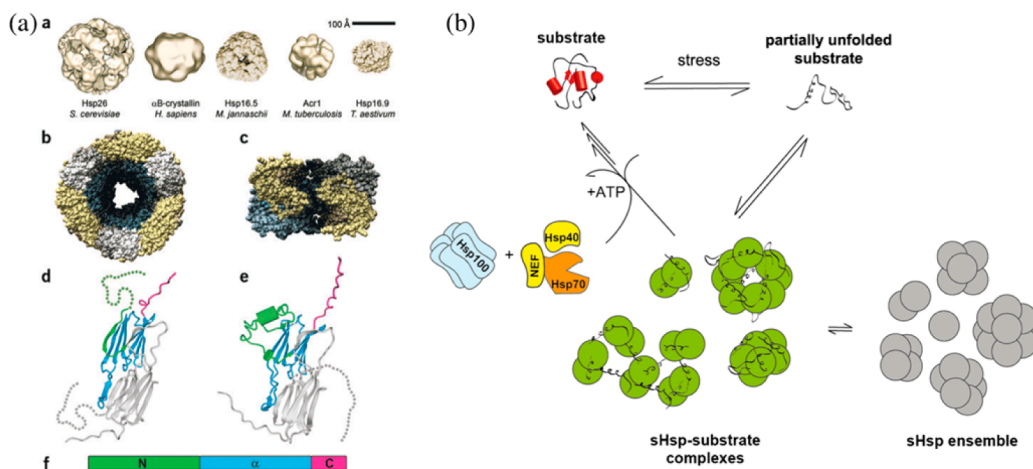


**Figure 16.** Representation of sHsps. (a) Features of sHsps structures. (b) Model for the chaperone function of sHsps. Reprinted with permission from ref 196. Copyright 2005 Nature Publishing Group. Reprinted with permission from ref 197. Copyright 2015 Elsevier.

act as an explosive source of glucose. Many flying insects use this mechanism to release two molecules of glucose per molecule of trehalose when metabolized by trehalase. The second ability of trehalose that is of significance to temperature-triggered biological events is that of the nonreducing sugar to encapsulate proteins in extreme heat shock conditions and in this way to stabilize proteins by replacing the aqueous shell around the protein with a more heat-resistant matrix of the disaccharide.<sup>194,195</sup>

Another supramolecular complexation reaction employed in nature is that of the heatshock or chaperone proteins. Instead of clustering around single proteins as for disaccharides, the heat shock proteins actively complex multiple proteins to prevent unfolding and denaturation in extreme heat shock events. Heat shock proteins are hollow ball or barrel-like structures that bind to unfolded (denatured) proteins and prevent irreversible aggregation via temporary complexes<sup>196,197</sup> (Figure 16).

Finally, perhaps the most investigated strategy to synthetically mimic bioinspired responses is changing the membrane fluidity and examining the thermal effects on the membrane stability in vesicular systems. The self-assembled cellular membrane exists in a liquid crystalline state<sup>198</sup> whose fluidity increases as a function of temperature until complete lysis is obtained.<sup>199–201</sup> Natural systems use membrane response and engineering as a way to resist and protect against external thermal stimuli. In many plants such as mosses, changes in temperature have been shown to lead to increase in membrane fluidity. As a consequence, fluidity responsive protein channels open resulting in calcium influx to signal the plant cell to induce a heat shock response.<sup>202,203</sup> On a more fundamental level, it is also known that many cell membranes adapt to the environmental conditions they are in, via genotypic alterations or as a result of short-term changes in local environmental conditions via phenotypic alterations in membrane composition. The most striking variety of membrane composition adaptation is that of the domain of bacteria, which can survive in a nondormant state in some of the most extreme environmental conditions (Table 3.2). Many ways of modulating membrane fluidity exists, such as changes in lipid headgroup, protein content of the cell membrane, composition of carotenoids, acyl chain length, fatty acid isomerization, and changes in fatty acid unsaturation. However, it is the changes in degree and position of fatty acid unsaturation that has the most pronounced effect and is

**Table 3.2. Classification of Bacteria Based on Growth Temperature<sup>204</sup>**

category	growth temperature (°C)		
	minimum	optimum	maximum
mesophile	10–15	30–40	45
psychrophile	≤ 0	10–15	20
psychrotolerant	≤ 0	20–25	30
thermophile	45	50–70	80
hyperthermophile	55	80–110	113

exploited by almost all bacteria especially in cold climate adaptation.<sup>204</sup>

From all the examples shown, the effect of thermal stimuli on membrane properties has been most intensively studied in synthetic systems, and so it is this aspect that this review shall focus upon. It should be however noted that the mechanisms employed by heat shock proteins and disaccharide systems are significantly underexplored in the domain of bioinspired self-assembly especially focusing on combining both form and function into a single system.

Thermoresponsive self-assembled nanocarriers are one of the most investigated systems for delivery, because tumor, infected inflammatory tissues are more hyperthermic than normal tissue,<sup>169,205</sup> but also it is relatively simple to locally heat the tumor site to trigger the release of transported molecules.<sup>206–209</sup> In addition, abnormal tumor cells are more sensitive to higher temperature,<sup>210</sup> resulting in bigger interval between microvasculature. In temperature-sensitive delivery systems, thermoresponsive units undergo physicochemical transformation along with the changes in ambient temperature to release the payload.<sup>211</sup> For drug delivery, it is ideal that temperature-responsive delivery systems are stable at 37 °C and sharply release the loaded molecules in the locally heated site. Many reviews<sup>212,213</sup> focus on other temperature-responsive systems such as gels; in our review, we only focus on the self-assembled system.

Poly-*N*-isopropylacrylamide (PNIPAM) has a lower critical solution temperature (LCST), close to physiological temperature (32 °C), making the polymer potentially useful for biomedical application. PNIPAM chains show high solubility below LCST, whereas they become hydrophobic rapidly above the LCST. When combined with hydrophilic PEG, PNIPAM-

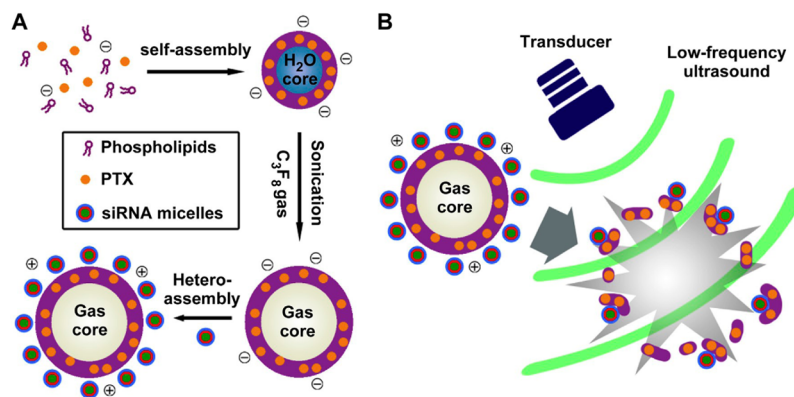


**Figure 17.** (A) Illustrative preparation of PTX–NBs/siRNA by heteroassembly of positively charged siRNA micelles and negatively charged PTX-loaded gas-cored liposomes (PTX–NBs). (B) Illustrative principle of the destruction of PTX–NBs/siRNA under external low-frequency US force. Reprinted with permission from ref 249. Copyright 2009 Elsevier.

PEG can form micelles (PNIPAM as core) at high temperatures.<sup>214</sup> When NIPAM is copolymerized with *N,N*-dimethylacrylamide (DMAM), the LCST of P(NIPAM-*co*-DMAM) changes to around 40 °C. In addition, biodegradable poly(d,L-lactide) (PLA), poly(*ε*-caprolactone) (PCL), and poly(d,L-lactide-*co*-*ε*-caprolactone) (P(LA-*co*-CL)) have been used as the hydrophobic segment in the preparation of micelles, which have been demonstrated to be a biodegradable thermosensitive self-assembled system for drug delivery.<sup>215</sup> PNIPAM was successfully grafted to biocompatible hyperbranched poly(3-ethyl-3-octanemethanol) (HBPO) to obtain amphiphilic copolymer, which can also self-assemble into micelles depending on temperature.<sup>216</sup>

Conversely, some polymers have upper critical solution temperature (UCST), which means that they become soluble upon heating. The UCST of these polymers is strongly dependent on their molecular weight and concentration.<sup>217</sup> Methoxy-PEG-*b*-poly(acrylamide-*co*-acrylonitrile) (mPEG-*b*-P(AAm-*co*-AN)) was used to prepare doxorubicin-encapsulated micelles for antitumor therapy. The UCST of micelles raised from 43.1 to 65 °C when increasing the concentration of mPEG-*b*-P(AAm-*co*-AN) from 0.3 to 1 mg/mL. The accumulative release of drugs increased when the micelles were heated and the polymers became more soluble.<sup>218</sup>

The bilayer lipid membrane of liposomes can undergo phase transitions such as liquid-crystalline transition<sup>219</sup> and lamellar-hexagonal phases<sup>220</sup> at elevated temperature, the phase transitions lead to leaky membranes toward molecules encapsulated inside of the liposomes. To realize more thermal sensitivity, some researchers also incorporated thermosensitive polymers into the membrane of liposomes to achieve temperature-triggered properties. Thermosensitive polymers of *N*-(2-hydroxypropyl) methacrylamide/dilactate (PHPMA-lac) were synthesized with cholesterol anchor by Hennink et al.<sup>221</sup> These complexes can be introduced into the bilayer membrane of doxorubicin-loaded liposomes by thin lipid film hydration method. The release of doxorubicin from these novel liposomes was shown to be related to the composition and grafting density of chol-PHPMAlac. Liposomes with 5% PHPMAlac-modified ratio showed a rapid release upon increasing temperature, which is promising for local drug delivery using hyperthermia. In order to make the systems more biocompatible, thermosensitive leucine zipper peptides can also be incorporated into the bilayer during the formation of traditional temperature-responsive liposomes.<sup>222,223</sup> Leucine

zipper peptides dissociate when temperature exceeds their melting point (around 40 °C) to release the cargoes from liposomes. The high stability and dual thermo responsiveness of hybrid liposomes leads to high retention of drug in tumor site following hyperthermia. Sung et al. reported ammonium bicarbonate as a pH gradient source for loading doxorubicin. After hyperthermia treatment, ammonium bicarbonate decomposed into ammonia and carbon dioxide bubbles, leading to permeable defects in liposomes for rapid drug delivery.<sup>224,225</sup>

**3.1.2.1.3. Ultrasound-Triggered Transport and Release.** The ultrasound frequency domain is above the threshold of normal human hearing.<sup>226</sup> Because of its high penetration,<sup>227</sup> spatial and temporal control,<sup>228,229</sup> tuning frequency,<sup>230</sup> and noninvasiveness,<sup>127,231</sup> ultrasound provides a potential application in triggering the release of molecules from self-assembled structures for drug delivery, imaging, and diagnosis.<sup>232–235</sup> The most important mechanism of ultrasound-sensitive transport systems is cavitation effect,<sup>236</sup> which can induce destabilization of nanocarriers and also increase the permeability of tissue.<sup>235,237–239</sup> To decrease the threshold for cavitation, ultrasound contrast agents such as perfluorocarbons (PFC)<sup>240,241</sup> are widely used for acoustic sound triggered systems. PFC emulsions can undergo conversion into microbubbles after treatment of ultrasound. These microbubbles lead to the release of encapsulated drugs or imaging agents. Furthermore, high-intensity focused ultrasound (HIFU)<sup>242</sup> can also induce the local hyperthermia effect<sup>232,243</sup> to release the loaded molecules, therefore some reports have introduced a thermosensitive polymer such as PNIPAM into the membrane of liposomes to decrease the thermo dose.<sup>231,244</sup> Detailed information about ultrasound-sensitive systems is out of the scope of this review, and we refer the readers to more comprehensive studies.<sup>235,245</sup> Ultrasound however does represent an interesting enhancing modality to increase efficacy and delivery efficiency of vesicle-bound drugs, and so its utility in this respect shall be briefly discussed for completeness.

Recently, magnetic resonance imaging (MRI) and single-photon emission computed tomography (SPECT) combined with ultrasound have been used to visualize and guide the release from self-assembled systems for theranostics.<sup>246–248</sup> Gadoteridol (gadolinium-based MRI contrast agent), a clinically approved paramagnetic agent, has been encapsulated as a model drug in the liposomes to investigate the release property in vivo under MRI. An enhancement of up to 35% of the MRI signal was observed when pulsed low-intensity nonfocused ultrasound

(pLINFU) was applied. Following metabolism, signal observed in the kidneys, calyx, and bladder were detected and confirmed that gadoteridol is released as a result of exposure to pLINFU. SPECT of radioactive In<sup>111</sup> in labeled doxorubicin and [Gd(HPDO3A)(H<sub>2</sub>O)]-loaded liposomes under HIFU treatment demonstrated that the tumor area retained 4.4 times higher liposomes uptake than the control, which is promising for tumor therapy.

In the attempt to overcome drug resistance in tumor cells, heteroassembly of positively charged siRNA-entrapped micelles with negatively charged paclitaxel-loaded liposomes with gas cores (Figure 17) have been used for carcinoma treatment.<sup>249</sup> Under low-frequency ultrasound for triggering the *in vivo* release, intratumoral distribution of paclitaxel and siRNA in mice was increased, leading to a significant decrease in tumor size and higher survival rate after treatment when compared with control mice. Z. Dai et al. incorporated polyorganosiloxane into liposomes by mixing *N*-[*N*-(3-triethoxysilyl)-propylsuccinamoyl]-dihexadecylamine (cerosome-forming lipid, CFL), lipids and a temperature sensitive, 1-stearoyl-2-hydroxy-*s*-glycero-3-phosphocholine (MSPC) lipids together, forming hybrid liposomal cerasomes.<sup>250</sup> Inorganic polyorganosiloxanes can maintain the stability of liposomes and have also shown utility for bioconjugation. The temperature responsive doxorubicin-loaded cerasomes with 43.25% CFL release more than 90% drugs in 1 min, due to hyperthermia caused by HIFU treatment. Ultrasound has also been investigated to trigger the shape transformation of self-assembled structures.<sup>251</sup> Amphilic molecule LA-(CD)<sub>2</sub> was synthesized by alkyne–azide click chemistry between LA-(N<sub>3</sub>)<sub>2</sub> (LA, lithocholic acid) and  $\beta$ -CD ( $\beta$ -cyclodextrin) possessing an alkyne, which were then self-assembled into micelles at room temperature in water. These micelles undergo shape transformation from spherical micelles into irregular micelles and branched structures depending on the applied ultrasound time. The main mechanism behind is the hydrophilic–hydrophobic interaction (guest–host interaction) present between LA and  $\beta$ -CD, which can be destroyed by ultrasound.

**3.1.2.1.4. Light-Triggered Transport and Release.** Photosensitive self-assembled systems responding to specific wavelength (visible light,<sup>252,253</sup> ultraviolet,<sup>254–256</sup> and near-infrared<sup>257,258</sup>) have attracted the attention in the latest decade because of their safety, easy application, and spatiotemporal control.<sup>259,260</sup> Most of these self-assembled structures draw inspiration from the same functional design parameters as outlined in the discussion on temperature sensitive delivery, namely they depend on light-cleavable linkers,<sup>261,262</sup> light-induced cross-linking,<sup>263,264</sup> light-induced degradation,<sup>265</sup> or light-responsive conformational change of groups like azobenzene,<sup>266</sup> which can lead to the change in hydrophilic–hydrophobic balance<sup>267,268</sup> or interaction between host and guest.<sup>269</sup> Most commonly used, azobenzenes can undergo photoisomerization<sup>270</sup> from trans to cis by applying UV at 300–380 nm and from cis to trans reversibly under visible light. Light-responsive structures and their underlying mechanisms have been reviewed intensively,<sup>271–274</sup> therefore we only highlight the most current developments.

Spiropyran (SP) a photosensitive hydrophobic molecule that can undergo transformation into hydrophilic merocyanine (MC) upon irradiation with 365 nm UV light. Introduction of SP at the hydrophobic terminus of biodegradable poly(ethylene glycol)-*b*-poly(5-methyl-5-propargylxycarbonyl-1,3-dioxane-2-one) (PEG–PMPC) via click chemistry by Y. Lu et

al. lead to the formation of PEG-PMPC-SP.<sup>275</sup> Micelles formed with PEG-PMPC-SP together with coumarin 102 disassembled and aggregated after applying UV, and reassembly into micelles was observed when exposing the aggregates to visible light of 620 nm. These UV-triggered release and visible light-induced reload systems may show utility in theranostic applications where it is necessary to retrieve samples of the local environment following drug delivery. Host–guest systems incorporating photosensitive units have also shown potential for light-triggered systems.<sup>276,277</sup> Hybrid polymers formed by hydrophilic pillar[6]arene and trans azobenzene-based amphiphilic polymers via host–guest interaction have been observed to self-assemble into bilayer vesicles (Figure 18). Upon applying

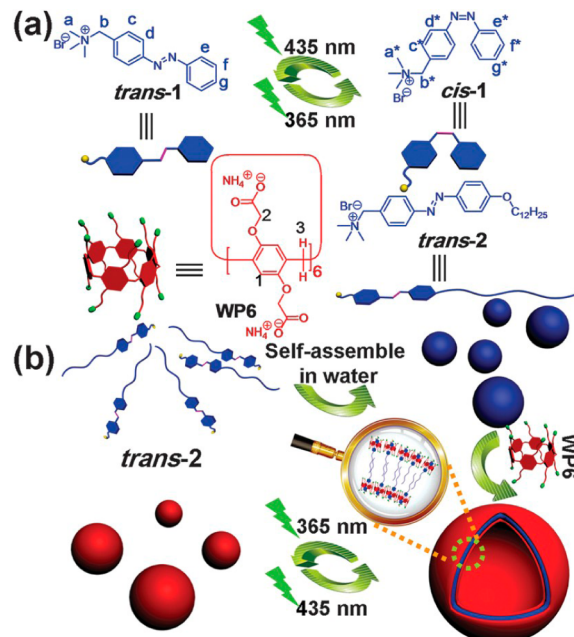


**Figure 18.** (a) Chemical structures of 1, 2, and WP6. (b) Cartoon representation of the photoresponsive self-assembly between WP6 and 2 in water. Reprinted with permission from ref 276. Copyright 2014 Royal Society of Chemistry.

UV, azobenzene changes from trans to cis, thus interfering with the host–guest interaction. The azobenzene-based amphiphiles detach from the cavity of pillar[6]arene and self-assemble into micelles. The transformation from vesicle to micelle is reversible under UV and visible light excitation.<sup>276</sup> The main disadvantage of visible light and ultraviolet-triggered systems is their low penetration depth into tissue. As a consequence, their application is limited to directly accessible tissues such as eye and skin. On the other hand, near-infrared light possesses deeper penetration depth and less harm to the human body; this makes near IR a plausible alternative to UV. Y. Zhao and his co-workers prepared micelles based on poly(ethylene oxide)-*b*-block-poly(4,5-dimethoxy-2-nitrobenzyl methacrylate) (PEO-*b*-PNBMA).<sup>257</sup>

Nanoparticles capable of upconverting IR radiation into the UV-vis range (NaYF<sub>4</sub>: TmYb) (UCNPs) together with the hydrophobic molecule Nile Red were encapsulated in the hydrophobic core of micelles to achieve cascade excitation. UCNPs were chosen as internal visible light or ultraviolet sources for near-infrared light excitation. Upon excitation with 980 nm near-infrared light, UCNPs were able to emit UV-vis

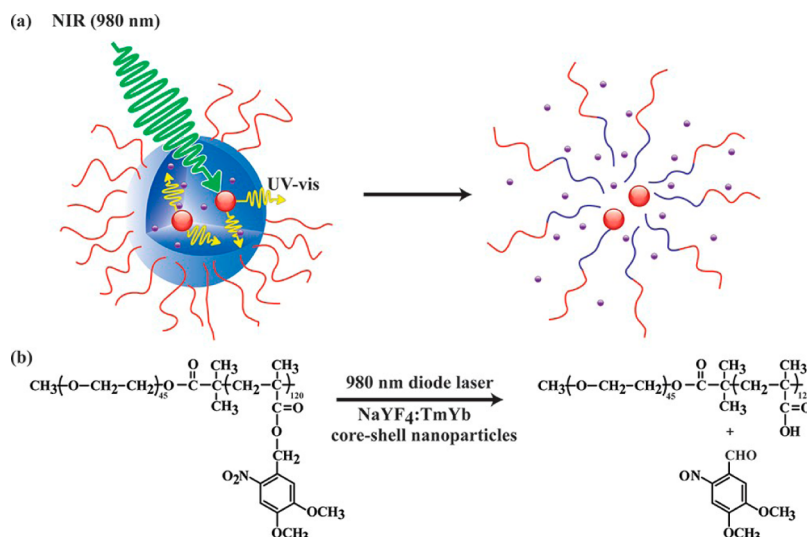


**Figure 19.** (a) Schematic illustration of using NIR light excitation of UCNPs to trigger dissociation of BCP micelles. (b) NIR light-triggered photoreaction with the used BCP of PEO-*b*-PNBMA and UCNPs of NaYF<sub>4</sub>:TmYb. Reprinted from ref 257. Copyright 2011 American Chemical Society.

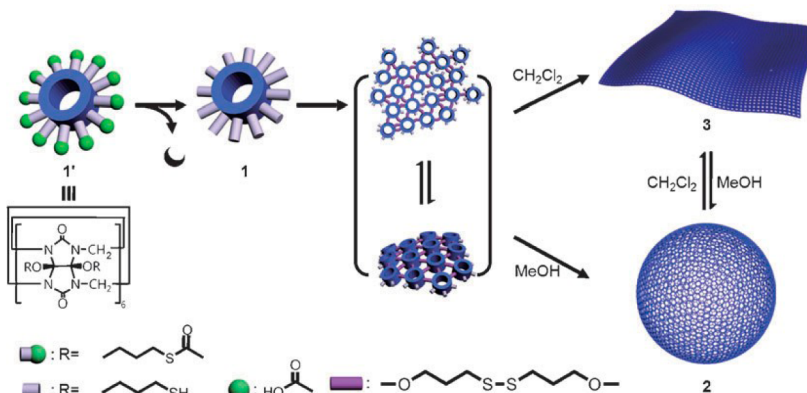


**Figure 20.** Formation of 2D polymer film 3 and polymer nanocapsule 2 through reversible disulfide bond formation and reversible morphological transformation between them. Reprinted with permission from ref 291. Copyright 2015 Wiley-VCH.

wavelength light, which was subsequently absorbed by light sensitive nitrobenzyl units. Consequently, the cleavage of nitrobenzyl groups from PNBMA block revealed the underlying hydrophilic poly(methacrylic acid), leading to disassembly of micelles and the release of Nile Red as a model drug during the process of disassembly (**Figure 19**).

Gold nanoparticles irradiated with near-infrared light transduce the light to heat via surface plasmons in light-responsive systems.<sup>278</sup> Amphiphilic complexes are made by the conjugation of hydrophilic poly(2-(2-methoxyethoxy)ethyl methacrylate (PMEO<sub>2</sub>MA) and hydrophobic poly( $\epsilon$ -caprolactone) (PCL) onto the surface of 14 nm gold nanoparticles via thiolation.<sup>279</sup> These hybrid polymers can self-assemble into different structures by varying the ratio of PCL to PMEO<sub>2</sub>MA. Such self-assembled structures demonstrated strong near-infrared light absorption. Owing to their high X-ray absorption, gold nanoparticles are also used as potential contrast agents for computed tomography (CT).<sup>280,281</sup>

**3.1.2.1.5. Redox-Triggered Transport and Release.** Disulfide bonds<sup>282,283</sup> are the most widespread linking and regulatory units in biological redox-responsive systems; they can be rapidly cleaved by using glutathione.<sup>284,285</sup> The latter, is one of the most important natural antioxidants helping to keep the human

body from free radicals and peroxides.<sup>286,287</sup> The sulphydryl group of glutathione can donate a reducing equivalent to reactive oxygen, after which it becomes reactive, forming together with another glutathione a disulfide.<sup>288</sup> Compared to extracellular microenvironments ( $\sim 2\text{--}10 \mu\text{M}$ ), the intracellular compartments ( $\sim 2\text{--}10 \text{ mM}$ ) possess a higher concentration of glutathione, which can be the trigger for the release of molecules from redox-sensitive delivery systems.<sup>289,290</sup>

Mercaptopropylcucurbit[6]uril was demonstrated to function as a monomer to self-assemble into nanocapsules and films by forming a dynamic covalent disulfide linkage.<sup>291</sup> The films can undergo reversible morphological transformation into nanocapsules by changing of the solvents used (Figure 20). These kinds of structures are suitable for cargo release from hollow nanosapsules under reducing conditions, such as in the presence of glutathione. J. Li et al. prepared self-assembled supramolecular system based on host–guest interaction between  $\beta$ -CD and adamantyl group for gene therapy.<sup>292</sup> Bioreducible disulfide bonds have been used to link  $\beta$ -CD with poly(2-dimethylaminoethyl methacrylate) (pDMAEMA) to form the host polymer  $\beta$ CD-SS-pDMAEMA.

The guest polymer is a complex in which the adamantyl group is conjugated with zwitterionic phosphorylcholinepoly(2-

methacryloyloxyethyl phosphorylcholine) (pMPC). The lipid pMPC, quite similar to its natural cell membrane equivalent, can protect the whole systems from protein adsorption and increase the cellular uptake. The high level of glutathione in the cytosol cleaves the disulfide bonds and has been shown to result in the release of the DNA cargoes from these polyplex nanoparticles and their up-take by the MCF-7 cells. In another development, polylactic acid (PLA) and PEG have been linked through complementary hydrogen bonds and double disulfide bonds to form amphiphilic PLA–PEG.<sup>293</sup>

The synthesized block copolymer can self-assemble into micelles with the model anticancer drug doxorubicin, which can be rapidly released under extracellular stimuli into tumor cellular nuclei. Ferrocenium-capped amphiphilic pillar[5]arene (FCAP) has been also synthesized by Pei and co-workers and shown to self-assemble into cationic vesicles with high loading efficiency for polyanionic siRNA.<sup>294</sup> Ferrocenium can change to a ferrocenyl group when exposed to a reducing agent, leading to the disassembly of cationic vesicles (Figure 21). During the

mechanisms of action of these nanocarrier systems is either through magnetic guidance,<sup>300,301</sup> induced temperature increase<sup>302–304</sup> (magnetic materials are prone to convert magnetic energy into heat), or a combination of both. In accordance with magneto-induced hyperthermia, thermoresponsive components were combined with magnetic nanoparticles for further applications.<sup>305</sup> In our review, we only briefly introduce the current progresses for magnetic-sensitive delivery.

Iron oxide nanoparticles are one of the most widely used magnetic nanoparticles because of its biocompatibility and biodegradability.<sup>306</sup> Iron oxide nanoparticles showed strong potential in magnetic-guidance, MRI imaging, and magnetic-induced hyperthermia. Anderson et al. developed lipidoids-coated iron oxide nanoparticles for DNA and siRNA delivery.<sup>307</sup> Lipidoids<sup>308</sup> as cationic lipids were used as reservoirs for loading because of electrostatic interaction between the lipid and DNA or siRNA. After applying an external magnetic field, the release increased, which was better than commercial Lipofectamine 2000. S. Jin and co-workers prepared magnetic  $\text{Fe}_3\text{O}_4$  beads and camptothecin-coencapsulated lipid-polymer hybrid systems for magnetic field triggered drug delivery.<sup>309</sup> The hybrid structures were based on the self-assembly of poly(lactic-*co*-glycolic acid) (PLGA) (as core), soybean lecithin, carboxyl-terminated 1,2-distearoyl-*sn*-glycero-3-phosphoethanolamine-*N*-carboxy-(polyethylene glycol) (DSPE-PEG) and  $\text{Fe}_3\text{O}_4$  beads. Controlled release behavior of camptothecin was observed under remote radio frequency magnetic field because hyperthermia induced by built-in  $\text{Fe}_3\text{O}_4$  beads led to leaky structures. Magneto-induced thermosensitive supramolecular magnetic nanoparticles loaded with anticancer drug doxorubicin (DOX-SMNPs) were prepared by host–guest interaction between adamantine and  $\beta$ -CD using four building blocks: (1) adamantine-modified polyamidoaminodendrimers (Ad-PAMAM), (2) 6 nm adamantine-grafted  $\text{Zn}_{0.4}\text{Fe}_{2.6}\text{O}_4$  superparamagnetic nanoparticles (Ad-MNP), (3) adamantine-modified polyethylene glycol (Ad-PEG), and (4)  $\beta$ -CD-grafted branched polyethylenimine (CD-PEI) (Figure 22).<sup>310</sup> 6 nm Ad-MNP was functioned as built-in transformer in the whole systems, which can convert the energy from alternating magnetic field (AMF) into local heat, as stimuli for triggering release. After applying AMF for 2 min, around 50% of doxorubicin was released from disassembled SMNPs structures. DOX-SMNPs also showed efficient inhibition in tumor growth at even very low concentration of doxorubicin (2.8  $\mu\text{g}/\text{kg}$  DOX per injection) compared to normal protocols, which have the advantage of decreasing the toxicity.

We have recently demonstrated that not only paramagnetic or superparamagnetic materials can be efficient carriers for magnetic manipulation but also diamagnetic structures assembled from amphiphilic block copolymers.<sup>311</sup> Bowl shape polymeric stomatocytes with a small opening assembled from polystyrene-polyethylene glycol block copolymers were shown to reversibly open and close in homogeneous magnetic fields (Figure 23, panels a–g).

Polymer stomatocytes were previously obtained from polymersomes via an osmotically driven shape transformation.<sup>312–314</sup> Strict control over the size of the opening was obtained during the shape transformation under osmotic stress depending on condition of formation. However, once formed, the morphological change into stomatocytes was irreversible, unless more plasticizing solvent and osmotic shock was applied to the membrane. In the magnetic field, these structures were

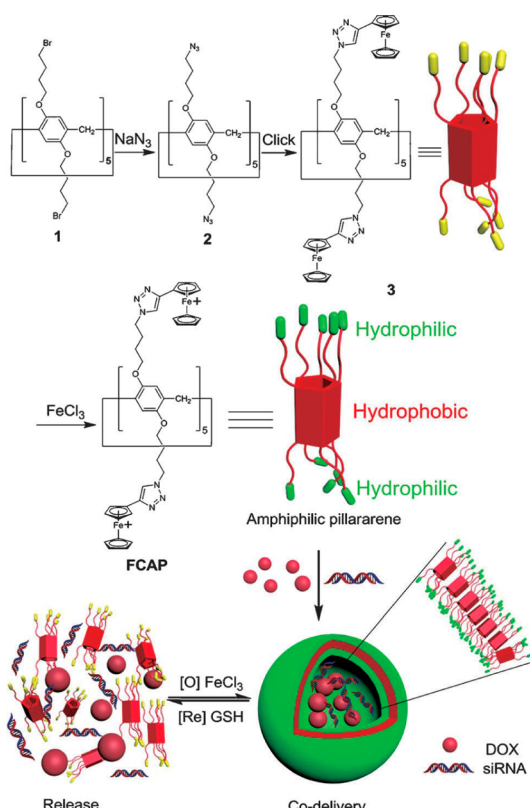


**Figure 21.** Illustration of the synthesis of FCAP, formation of cationic vesicles, and their redox-responsive drug/siRNA release. Reprinted with permission from ref 294. Copyright 2014 Wiley-VCH.

disassembly, 92% of the model drug DOX is released to cancer cells from the vesicles upon the addition of 10 mM glutathione. Combined with drug resistance gene silencing siRNA, these systems can efficiently inhibit the growth of SKOV-3 cells.

**3.1.2.1.6. Magnetically Sensitive Transport and Release.** Magnetic fields<sup>295</sup> have been widely used for therapy, imaging, and diagnosis due to its noninvasive nature, high penetration, and ease of control.<sup>296</sup> To combine the advantages of self-assembled structures with magnetic stimuli, paramagnetic or superparamagnetic materials were incorporated in the self-assembled systems to achieve magneto-responsive prop-

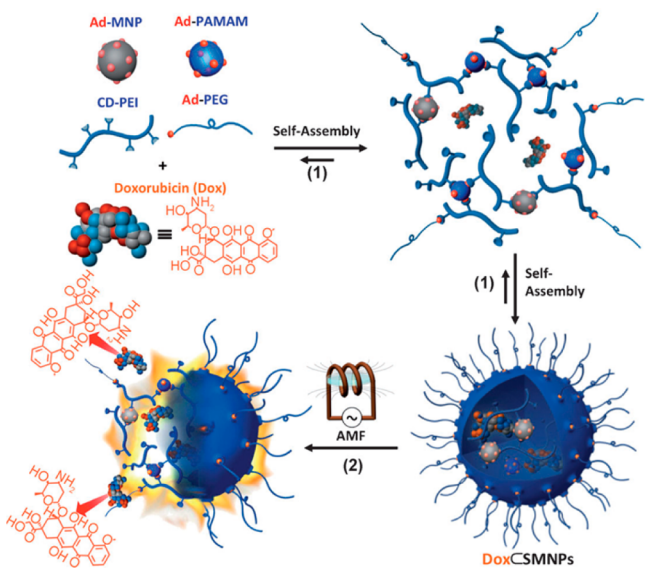


**Figure 22.** Molecular design, self-assembly, and function of magnetothermally responsive doxorubicin (Dox)-encapsulated supramolecular magnetic nanoparticles (Dox-SMNPs). (1) The self-assembled synthetic strategy is employed for the preparation of Dox-SMNPs, which is made from a fluorescent anticancer drug (Dox) and four molecular building blocks: Ad-PAMAM, 6 nm Ad-grafted Zn<sub>0.4</sub>Fe<sub>2.6</sub>O<sub>4</sub> superparamagnetic nanoparticle (Ad-MNP), CD-PEI, and Ad-PEG. (2) The embedded Ad-MNP serves as a built-in heat transformer that triggers the burst release of Dox molecules from the magnetothermally responsive SMNP vector, achieving on-demand drug release upon the remote application of an alternative magnetic field (AMF). Reprinted with permission from ref 310. Copyright 2013 Wiley-VCH.

shown to reversibly increase the size of their opening with increasing the intensity of the magnetic field and were able to

return to the initial closed opening once the field was removed (Figure 23g).<sup>311</sup>

This behavior was due to the highly anisotropic magnetic susceptibility of the building blocks within the self-assembled structure leading to their collective perpendicular alignment in magnetic field and, subsequently, a stretching of the membrane resulting in a deformation of the structure and increase in the opening.<sup>315,316</sup> Since the size of the opening was directly related to the intensity of the magnetic field, the self-assembled structures were further demonstrated to capture and release cargo via the reversible magnetic valve (Figure 23i).

#### 3.1.2.1.7. Electro Responsive Transport and Release.

Remote electric field can be used as a trigger to release the payloads from self-assembled systems containing ionizable groups.<sup>317</sup> Electrochemical reduction–oxidation and motion of charged molecules or particles driven by the electric field are the main mechanisms for electroresponsive systems.<sup>318</sup> However, electro-responsive delivery systems, like light-responsive ones, have the disadvantage of the low penetration ability.

Thin films consisting of positive antibiotic gentamicin and negative Prussian blue (PB) nanoparticles made through layer-by-layer (LBL) self-assembly have been prepared.<sup>319</sup> The PB nanoparticles charge changed from negative to neutral under +0.5 V voltage due to oxidization, which leads to the dissolution of thin films. The release rate of gentamicin can be controlled by choosing films with different thicknesses and applied voltage strengths. These structures suit implantable medical application and transdermal drug delivery systems. Hydrophobic polymers modified with  $\beta$ -CD and hydrophilic polymers with ferrocene tails can form amphiphilic block copolymer due to the host–guest interaction between  $\beta$ -CD and ferrocene, which can further self-assemble into polymersomes.<sup>318,320,321</sup> The +1.5 V voltage can induce the oxidization of ferrocene into charged ferrocenium, which dissociates from  $\beta$ -CD, thus disrupting the stability of vesicles (Figure 24). Increasing the voltage resulted

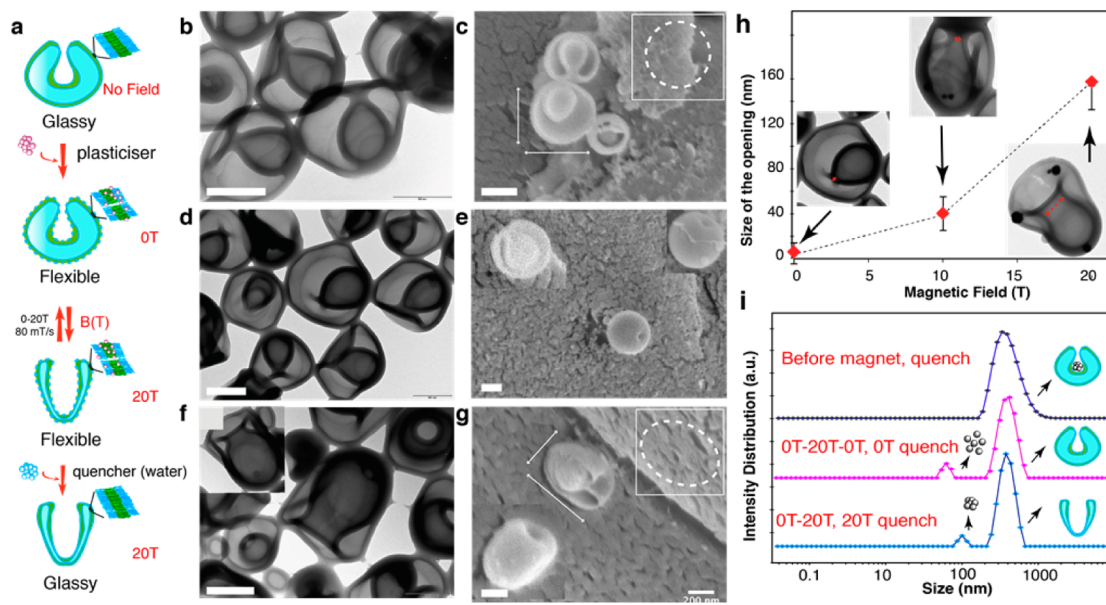


**Figure 23.** (a–g) Schematic representation, TEM, and SEM of the deformation in a high magnetic field of spherical narrow-opening stomatocytes into prolate wide-opening structures and their fixation via membrane quenching. (h) Size of the opening of the stomatocytes at 0, 10, and 20 T and their TEM images, demonstrating the gradual opening and development of shape asymmetry of the objects during the process. (i) Schematic representation of the deformation in a high magnetic field of spherical narrow-opening stomatocytes into prolate wide-opening structures and their fixation via membrane quenching. Reprinted from ref 311 in nature communication under a Creative Commons CC-BY license.

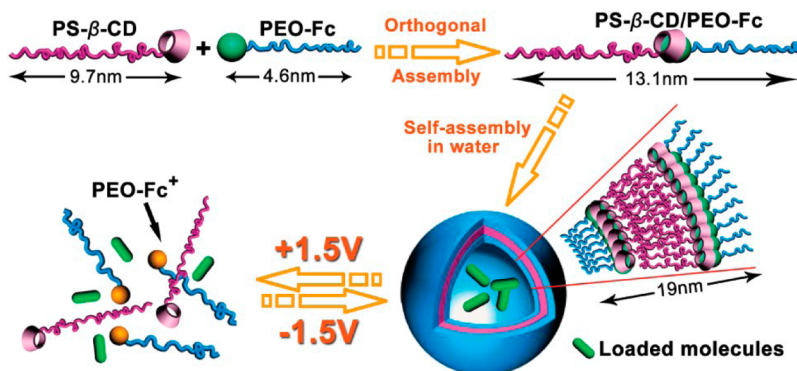


**Figure 24.** Structure of PS- $\beta$ -CD and PEO-Fc and schematic of the voltage-responsive controlled assembly and disassembly of PS- $\beta$ -CD/PEO-Fc supramolecular vesicles. Reprinted from ref 318. Copyright 2010 American Chemical Society.

in disassembly of the structures. The reassembly was subsequently achieved by applying  $-1.5$  V over the system rendering these structures reversible.

**3.1.2.1.8. Enzyme-Sensitive Systems.** Enzyme-driven reactions are usually highly efficient and substrate selective. Some enzymes are overexpressed in certain pathological regions such as at tumor and inflammation sites.<sup>322–324</sup> As a result, a growing number of scientists are integrating specific enzyme reactions or degradation<sup>325,326</sup> points into self-assembled structures to achieve on-site release and transport of drugs, imaging, and diagnosis.<sup>327–329</sup> In this section, we have chosen a selection of recent developments; more information about enzyme-responsive self-assembled systems were intensively reviewed by Liu et al.<sup>330</sup>

Amphiphilic hybrids made from linear water-soluble PEG and enzyme sensitive water-insoluble dendrons can self-assemble into micelles.<sup>329,331</sup> Hydrophobic phenyl acetamide is chosen as the end group to the four-armed dendron, which can be cleaved by penicillin G amidase (PGA). By stimulation, these enzyme responsive micelles can disassemble into hybrids and then release payloads under stimuli. By utilizing this motif, the release rates of encapsulated cargoes from micelles can be adjusted depending on the critical micelle concentration (CMC) of amphiphilic hybrids by selecting different PEG lengths. Alternatively, the cargoes can also be conjugated to the end of the dendron.<sup>329</sup> It was found that oligomeric glutaraldehyde (2GA, 3GA) can react with cationic diphenylalanine (CDP) by forming Schiff base covalent bonds, which can self-assemble into nanocarriers.<sup>332</sup> Notably, the systems display autofluorescence because of the n- $\pi^*$  transitions of the C=N bonds in the Schiff base. When doxorubicin was encapsulated, the systems showed higher cytotoxicity toward tumor cells compared to the free drug.

Moreover, enzymes can also trigger the self-assembly behavior by cleavage to form amphiphilic components.<sup>333,334</sup> Block copolymers, which can transform into micelles by the action of enzymes, have been synthesized. The structure of the copolymer consists of two hydrophobic segments: polystyrene (PS) and polymethacrylate (PMA) with azobenzene side chains (after modification with azobenzene, the PMA became water-insoluble). The azobenzene side chains are cleaved by the cascade reaction with azoreductase (enzyme) and NADPH (coenzyme) to form the hydrophilic PMA part, which enable their subsequent assembly (PS-PMA) into micelles (Figure 25).

**3.1.2.1.9. Glucose Responsive Drug Delivery Systems.** Diabetes mellitus is a metabolic disease which is characterized

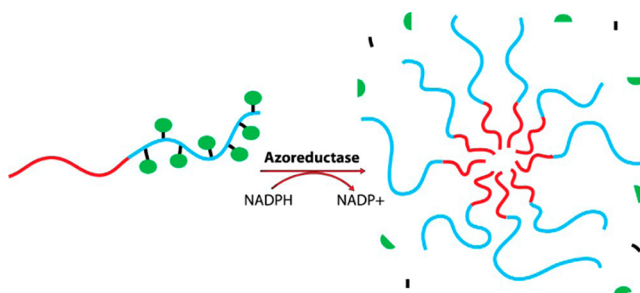


**Figure 25.** Schematic representation of a polymer building block and its assembly into a micellar nanostructure upon enzymatic activation in water. Reprinted from ref 334. Copyright 2014 American Chemical Society.

by high blood glucose levels because of the insufficient insulin produced by the pancreas or lack of response of cells to the produced insulin.<sup>335,336</sup> High blood glucose over extended periods of time leads to many complications<sup>337,338</sup> like eye damage, foot ulcers, cardiovascular disease. Increasingly, researchers are investigating the capability of novel delivery systems, especially of self-assembled structures, to release insulin according to blood glucose level as self-regulated systems;<sup>339,340</sup> this topic is already reviewed by Wang et al.<sup>341</sup> Here, we focus on the current state of the art.

Phenylboronic acid (PBA) and its derivative-based systems are mainly used for glucose-triggered insulin release.<sup>339,342–344</sup> However, responsiveness of PBA for glucose is not that sensitive. Also, insulin possesses high efficiency to the treatment of diabetes, the release of insulin should be controlled precisely. In order to increase the sensitivity and control, glucose oxidase/catalase (GOx/CAT) and insulin have been encapsulated in polymersomes based on pH sensitive amphiphilic block copolymer PEG-poly(Ser-Ketal).<sup>345</sup> Negligible leak of insulin was observed due to the compact and stable bilayer of polymersomes. Glucose diffused across the polymersomes and oxidized into gluconic acid and water and oxygen by GOx/CAT, resulting in acidic pH in the inner lumen of polymersomes (Figure 26).

Low pH led to hydrolysis of poly(Ser-Ketal) into hydrophilic polyserine and induced the disassembly of structures, thus triggering the release of insulin. This system could maintain the blood glucose at normal level for 5 days. To mimic the endogenous release of insulin, multilayer film based on pH responsive 21-arm poly[2-(dimethylamino)ethyl methacrylate] (star PDMAEMA), insulin and GOx was prepared via LBL

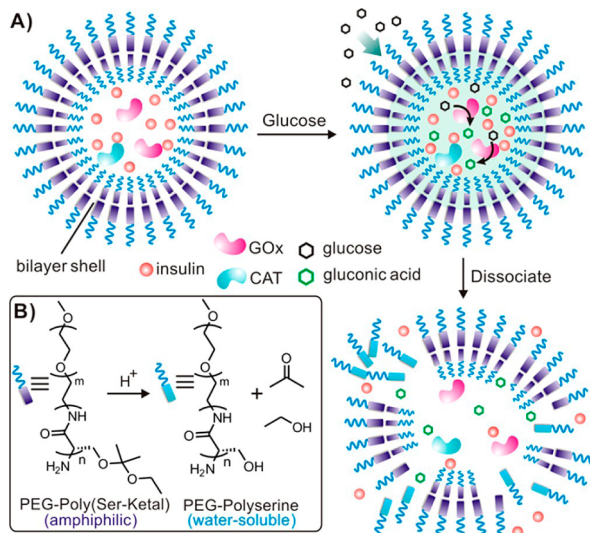


**Figure 26.** Schematic of the enzyme-based glucose-responsive nanovesicle. (A) GOx converts glucose into gluconic acid and acidifies the aqueous core of polymersome nanovesicle, leading to hydrolysis of the polymeric bilayer shell and subsequent dissociation of vesicles. (B) The chemical structure of the pH-sensitive diblock copolymer PEG-poly(Ser-Ketal), which can be hydrolyzed into water-soluble PEG-polyserine and acetone/ethanol in an acidic environment. Reprinted from ref 345. Copyright 2014 American Chemical Society.

assembly, which can function for at least 2 weeks to streptozotocin-induced diabetic rats.<sup>346</sup> Moreover, GOx/CAT induced acidic microenvironment can also be used in combination with pH-triggered biodegradable systems. Two oppositely charged dextran nanoparticles (coated with chitosan or alginate) loaded with insulin and GOx/CAT can self-assemble into a polymeric network by electrostatic forces (Figure 27).<sup>347</sup> Gluconic acid produced by GOx led to the degradation of dextran to release the insulin. These networks show high effectiveness in type 1 diabetic mice models for 10 days.

**3.1.2.1.10. Combining Two or More Different Stimuli-Sensitive Approaches.** Dual- and multistimuli responsive self-assembled systems that are sensitive to two or more stimuli are a high-profile area in supramolecular assemblies.<sup>128,348–350</sup> Combining different advantages of stimuli in one system is a promising way to control the transport of cargoes and trigger the release at the desired site. The most commonly used dual sensitive nanocarriers are based on pH and temperature responsiveness.<sup>351–353</sup> pH and temperature stimuli are easy to achieve in concert and also can be found in some pathological areas such as tumor tissues (acidic microenvironment, hyperthermia), which can autonomously induce the release of payloads targeted at these stimuli. Stimuli like ultrasound, magnetic field, and light possess high spatiotemporal control and are also very popular as one component of multistimuli.

H. Xia et al. introduced redox sensitive disulfide bonds and mechano-labile ester bonds in copolymer PEG-COO-SS-poly(propylene glycol) (PEG-COO-SS-PPG).<sup>354</sup> The addition of reducing agent D,L-dithiothreitol (DTT) into micelles based on these multifunctional copolymer caused the breakage of disulfide bonds, leading to slow release of cargoes. The micelles underwent fast release when remote HIFU treatment was applied, due to the cavitation produced by ultrasound. These

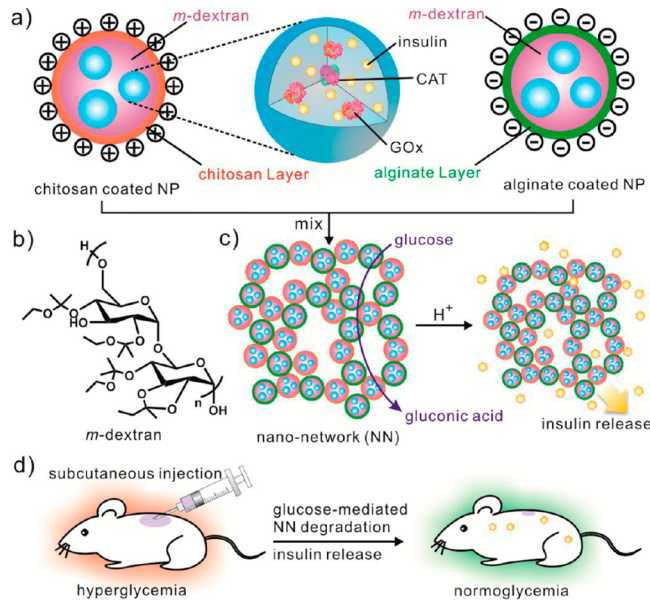


**Figure 27.** Schematic of the glucose-responsive nanonetwork. (a) Nanoparticles (NPs) encapsulating insulin and glucose-specific enzymes (GOx, glucose oxidase; CAT, catalase) are made of (b) acidic sensitive acetal-modified dextran and coated with chitosan and alginate, respectively. (c) Nanonetwork (NN) is formed by mixing oppositely charged nanoparticles together and efficiently degrades to release insulin upon the catalytic generation of gluconic acid under hyperglycemic conditions. (d) Schematic of glucose-mediated insulin delivery for type 1 diabetes treatment using the STZ-induced diabetic mice model. Reprinted from ref 347. Copyright 2013 American Chemical Society.

dual responsive systems provided controlled release profiles for drug delivery according to adjusting different stimuli.

Temperature and light stimuli can be also combined in one system. Supra-amphiphilic polypseudorotaxane based on the host–guest interaction between temperature responsive pillar[7]-arene (WP7) (as hydrophilic part) and photo sensitive azobenzene derivative (as hydrophobic part) can form vesicles in aqueous solutions.<sup>355</sup> When temperature was increased above LCST of WP7 or 365 nm UV light was applied, the interaction between azobenzene and WP7 broke down, leading to the disassembly of vesicles, therefore nanospheres based on the single self-assembly of azobenzene derivatives were formed. These transformations were shown to be reversible from formed nanospheres to vesicles upon removing the heat or applying 435 nm visible light. X.-Z. Zhang and his coworkers developed novel matrix metalloproteinases (MMPs) sensitive and UV light responsive microcapsules via LBL assembly.<sup>356</sup> These microcapsule systems relied on host–guest interaction between adamantine grafted onto poly(acrylic acid) via MMPs cleavable short peptide and  $\beta$ -CD grafted onto poly(aspartic acid). The peptide between the  $\beta$ -CD and adamantine layer was cleaved by MMPs, leading to disassembled structures (Figure 28). Macromolecular drugs loaded in the cavity of microcapsules can be released from the systems during that time.  $\alpha$ -CD modified with drugs (small molecules) can attach to the azobenzene also grafted on poly(acrylic acid) as the outer layer, which can be triggered by UV irradiation.

**3.1.2.2. Active Targeting.** In traditional intravenous delivery systems used for therapy, imaging, and diagnosis, the molecules are distributed throughout the whole body by blood circulation. For most agents, only a small amount of given molecules reach

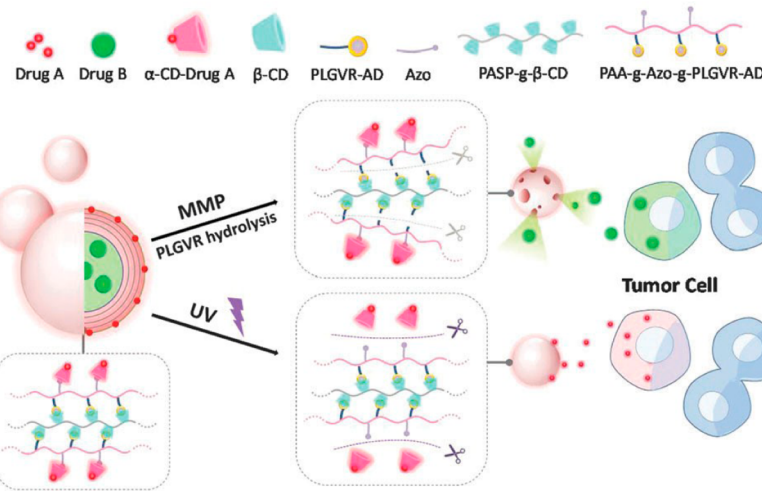


**Figure 28.** Schematic illustration of the codelivery system to individually release loaded drugs. Reprinted with permission from ref 356. Copyright 2015 Royal Society of Chemistry.

to the desired site, which in turn results in many unwanted side effects. Although stimuli-responsive systems can achieve some desired goals, active targeting is a smart method to deliver molecules or macromolecules to the specific site most commonly by coupling specific ligands to the surface of the self-assembled nanocarriers.<sup>131,357,358</sup> Modified ligands can be selectively recognized by receptors on the surface of desired cells. For instance, tumor cells overexpress many classes of receptors such as integrin receptors,<sup>359,360</sup> folic acid,<sup>361</sup> transferrin receptors,<sup>362,363</sup> epidermal growth factor receptors,<sup>364,365</sup> etc., all of which can be used for targeted transport.

Linear RGD (Arg-Gly-Asp) or cyclic RGD peptide is one of most simple ligands for targeting  $\alpha_5\beta_1/\alpha_5\beta_5$  integrins, which are overexpressed in tumor tissues. Cyclic RGD was introduced via maleimide-sulphydryl reaction onto surface of micelles based on metal-driven self-assembly of PEG-poly(L-glutamic acid) (PEG-PGlu) in (1,2-diaminocyclohexane)platinum(II) (DACHPt, antitumor drug).<sup>366</sup> These smart self-assembled systems showed higher therapeutic efficiency in both in vitro and in vivo experiments compared to nontargeted micelles. A combination of the superiority of ligand-mediated active targeting and the advantages of stimuli triggered structures in one multifunctional system has been reported.<sup>367</sup> Z. Gu et al. developed folic acid-modified DNA nanocomposites incorporated with acid sensitive deoxyribonuclease (DNase) nano-capsules (NCa).<sup>368</sup> Folic acid on the outer surface can guide the DNA complex to actively bind onto the overexpressed folate receptors of tumor cells to cause endocytosis. The acidic microenvironment of the endosome induced the release of DNase from the polymeric shell of NCa, thus leading to self-degradation of DNA nanocomposites to release cargoes (Figure 29). Another example, coated mesoporous silica nanoparticles based on the lectin-sugar interaction between glycogen and Concanavalin A (Con A) were prepared by C. Liu and his co-worker.<sup>362</sup> Transferrin was introduced in the outside of the coating layer, and model drug doxorubicin was loaded into silica nanoparticle cores (Figure 30). It was found that low pH can induce the disassembly of Con A and glycogen coating systems to trigger the release of doxorubicin.

### 3.2. Compartmentalization and Catalysis

Utilization of compartmentalization, transport, and catalysis is employed extensively in the eukaryotic cell. The most elaborate

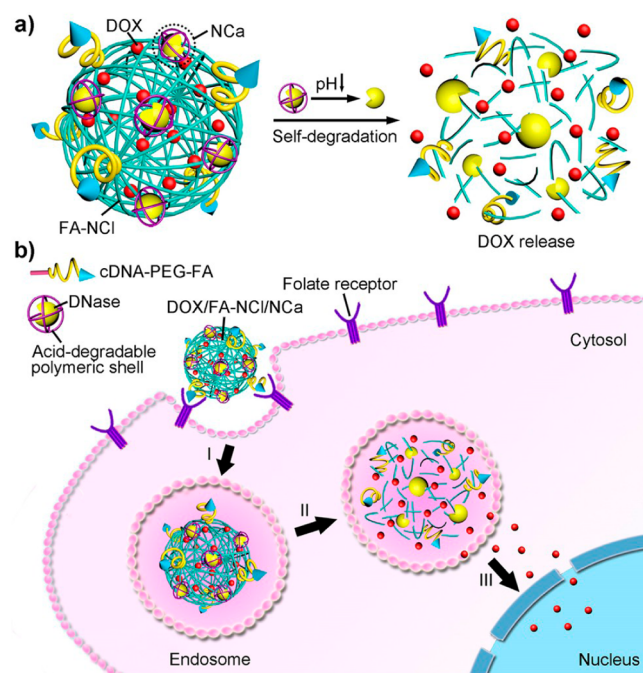


**Figure 29.** (a) Main components of the cocoon-like self-degradable DNA nanoclew, consisting of DOX/FA-NCl/NCa and acid-triggered DOX release. (b) Schematic illustration of efficient delivery of DOX by DOX/FA-NCl/NCa to nuclei for cancer therapy: (I) internalization in endosomes, (II) pH-triggered degradation of the NCl for DOX release, and (III) accumulation of DOX in cell nuclei. Reprinted from ref 368. Copyright 2014 American Chemical Society.

example is the complete synthesis of a protein beginning with mRNA delivery to the ribosome and the commencement of translating the mRNA into a protein; this process occurs in the cytosol. The first 5–10 residues code for the signal peptide that is in turn bound to signal recognition particle that then slows down the protein transcription and locates the ribosome as a temporary stud on the rough endoplasmic reticulum. mRNA continues to transcribe into a protein chain that is then delivered by the endoplasmic membrane wall to the rough endoplasmic reticulum lumen where folding begins. Once complete, the protein sequence is processed and folding is

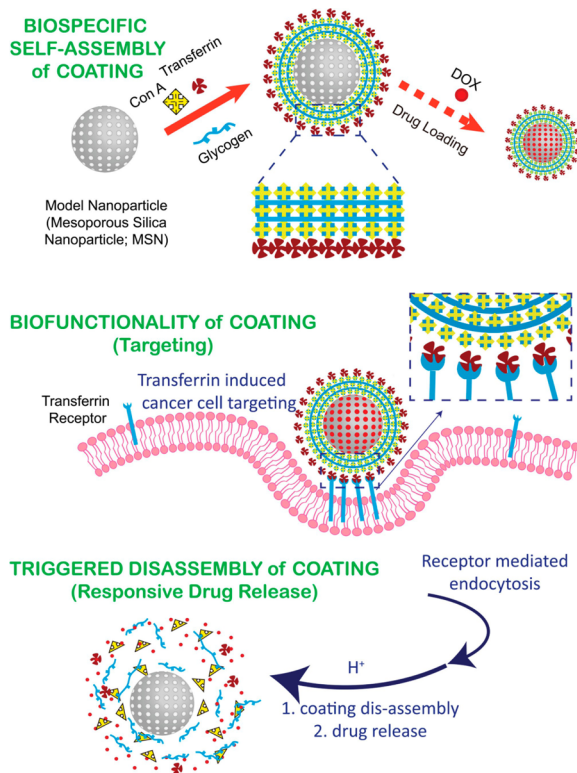


**Figure 30.** Biology as a source of materials and mechanisms for functional coatings. Biospecific interactions are used to self-assemble a nanoparticle coating and incorporate biofunctionality, while the coating's responsive properties allow its disassembly to be triggered by biologically relevant cues. Reprinted with permission from ref 362. Copyright 2015 Wiley-VCH.

completed.<sup>369</sup> The folded protein is then transported within a vesicle coated with coat protein I (COPI) to the golgi apparatus<sup>370–374</sup> (Figure 31). The protein passes through the various membranes of the golgi apparatus via vesicular transport from the cis-golgi proximal to the endoplasmic reticulum

toward the final stage of the trans-golgi. Each membrane compartment contains different golgi enzymes that catalyze distinct reactions (Figure 32). Once delivered to the golgi

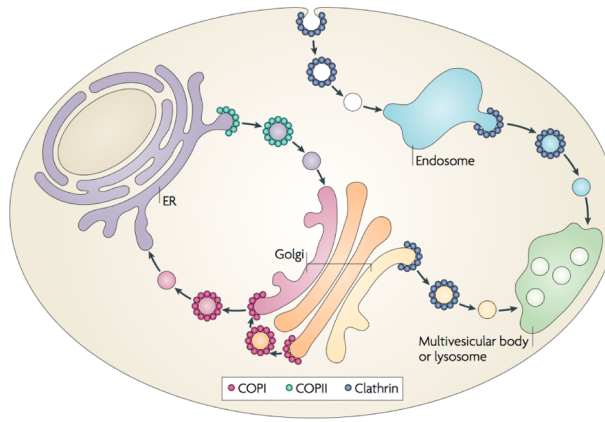


**Figure 32.** Pathways of vesicular transport by the coat protein. Reprinted with permission from ref 370. Copyright 2009 Nature Publishing Group.

apparatus membranes, the protein undergoes a series of post translational modifications most commonly the addition and modification of core glycans (O-linked oligosaccharides) attached in the endoplasmic reticulum during the transcription process resulting in a heterogeneous array often quite complicated branched structures<sup>370,375,376</sup> (Figure 33). The final step in traversing the Golgi apparatus ends in the trans-golgi where the protein is packaged up for delivery either in secretory vesicles or into lysosomes for delivery to late endosomes.<sup>370,377</sup>

The importance of catalysis to many life aspects renders the development of new catalytic systems highly attractive.<sup>378</sup> Industrial and academic research have drawn on bioinspired catalysis for many decades and focus on performing catalytic reactions with high enantioselectivity and efficiency,<sup>379,380</sup> while taking biocompatibility and cost into account.<sup>381,382</sup> Green

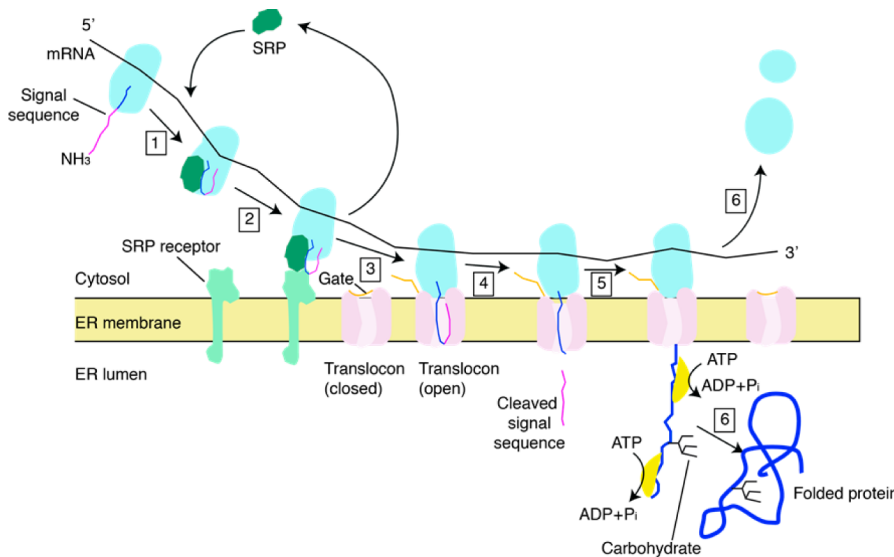


**Figure 31.** Synthesis of secretory proteins on the rough endoplasmic reticulum (ER). Synthesis begins on an unattached ribosome in the cytosol. The complete N-terminal signal sequence emerges from the ribosome only when the polypeptide is about 70 amino acids long because about 30 amino acids remain buried in the ribosome. Adapted from ref 374. Copyright W. H. Freeman 2000.

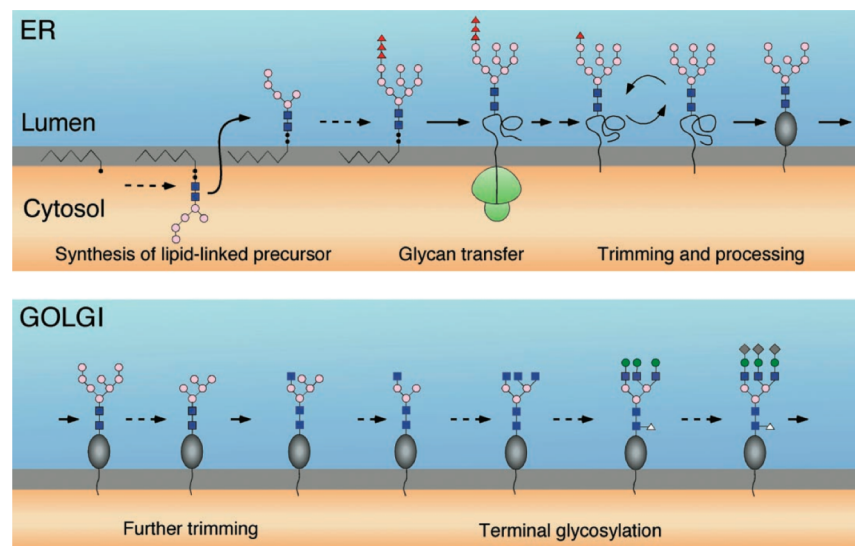


**Figure 33.** Biosynthesis of the N-linked core oligosaccharide. Synthesis starts on the cytosolic surface of the ER membrane by the addition of sugars, one by one, to dolichylphosphate. Reprinted with permission from ref 375. Copyright 2001 American Association for the Advancement of Science.

chemistry has been a crucial chemistry discipline that dictates certain advances in catalysis research topics.<sup>381</sup> Examples of high cost catalysis are represented in enzymatic and chiral catalysis, while the latter type is usually performed in organic toxic solutions which is not preferred in biorelated applications.<sup>383,384</sup> Enzymatic catalysis has overcome many challenges; however, enzymes cost is still rather high. Performing reactions with low cost while minimizing the use of toxic reaction solvents as well as a high degree of control over their rates and outcome has been extensively explored in the scientific literature.<sup>384–387</sup> An emerging strategy that could be applied to circumvent many remaining problems is the use of site-isolated techniques<sup>3,388,389</sup> (i.e., creating separated micro- or nanoenvironments for catalysts that boosts their performance in different media while facilitating catalyst recycling).<sup>390</sup> Supramolecular nanoreactors can be expected to contribute not only to catalyst isolation and catalyst recycling but also to combine two incompatible catalysts to performing a highly controlled crucial cascade or biomimetic reactions,<sup>391,392</sup> or defining some important aspects such as role of confinement on reactions rates.<sup>393–396</sup>

**3.2.1. Micellar-Based Catalysis.** Micelles are amphiphilic molecules that tend to intercede between organic and aqueous phases.<sup>397</sup> Above the critical micelle concentration (c.m.c.), surfactants that are usually neutral, anionic, and cationic with hydrophobic chains based on carbohydrates, amino acids lipopeptides, lipids, glycolipids, phospholipids, and fatty acids yield micelles with hydrophobic core and hydrophilic surface.<sup>398</sup> Depending on the concentration of surfactant, shapes of micelles can vary from spherical to ellipsoidal and rods.<sup>399</sup> Micelle-based catalysis is a well-established field since they represent a unique nanoreactor that facilitates catalysis in water with improved yields.<sup>400,401</sup> During reactions in water, apolar species are attracted toward micelles, which leads to a higher local concentration that increases reactions rates in several order of magnitudes.<sup>402</sup> Micellar-based catalysis does not only show an intrinsic enhancement of some reactions yields but also in performing more environment friendly reactions in aqueous media and the potential for recycling of the catalyst.<sup>400</sup> For example, acylation products of Friedel-crafts reactions between acetyl chloride and halo- and alkyl-methoxynaphthalanes using

cationic surfactants such as hexadecyltrimethylammonium bromide (CTAB) and hexadecyltrimethylammonium chloride (CTAC) led to isolation of excellent yields compared to the traditional reactions in organic solvents.<sup>403</sup> Also, mixing metal catalysts with sodium dodecyl sulfate (SDS)-based micellar aggregates showed an enhanced Friedel–Crafts alkylation of indoles in aqueous media.<sup>402</sup> Rate enhancement of the latter alkylation reaction is a consequence of the micellar aggregates ability to host the R-enone derivatives, and thus, more hydrophobic aryl derivatives showed a five-time higher acceleration rate compared with the methyl-enones. Blum et al. showed the ability of substituting toxic transition metal catalysts with surfactants micro emulsion in acid-catalyzed hydration of alkyne reactions.<sup>404</sup> Uozumi et al. described a self-assembled nitrogen-carbon-nitrogen (NCN) pincer Pd-amphiphile that allowed catalysis of reactions involving water-insoluble substrates in water.<sup>405,406</sup> Inspired by that work, O'Reilly and co-workers prepared a self-assembled sulfur-carbon-sulfur (SCS) pincer Pd- nanoreactor.<sup>407</sup> The self-assembled SCS pincer catalyst showed more than a 100 times increase in the rate of reaction compared to the nonassembled analogues. Unfortunately, this system did not show recycling ability because of palladium leaching and formation of Pd<sup>0</sup>.

Lipshutz et al. reported a newly designed platform for micellar catalysis called PQS and is a structure which dissolves readily in water forming nanomicelles.<sup>408</sup> The PQS allows for ring-closing metathesis of dienes in water with the ability to be recycled up to 10 times. This performance can be concluded from the PQS structure, which has a lipophilic component that acts as a reaction solvent for water insoluble organic substrates besides a free –OH moiety that allow covalent linkage to a Grubbs catalyst.

**3.2.2. Polymersomes.** As elaborated in numerous previous examples, polymersomes are bilayer structures with a spherical morphology made from block copolymers with hydrophobic and hydrophilic covalently linked chains.<sup>409</sup> They are composed of three different compartments represented by an inner aqueous lumen, hydrophobic bilayer (membrane), and a hydrophilic outer surface. Utilizing polymersomes for catalysis was achieved by means of encapsulation of material such as enzymes in their lumen and membrane or covalent attachment

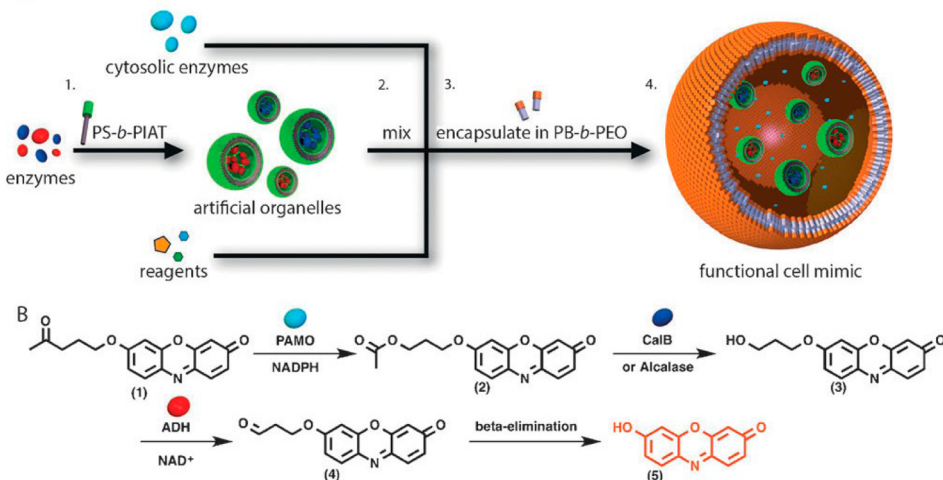


**Figure 34.** Concept of the cell mimic, which shows the initial encapsulation of different enzymes in polystyrene-*b*-poly(3-(isocyano-L-alanyl-aminoethyl)-thiophene) (PS-*b*-PIAT) nanoreactors (1), followed by mixing of the organelle mimics, cytosolic enzymes, and reagents (2), before encapsulation of the reaction mixture in polybutadiene-*b*-poly(ethylene oxide) (PB-*b*-PEO) vesicles (3) to create the functional cell mimic (4), inside which enzymatic multicompartment catalysis takes place. (B) Detailed cascade reaction scheme. Profluorescent substrate undergoes a Baeyer–Villiger reaction catalyzed by phenylacetone monooxygenase (PAMO), with one unit of the reduced form of nicotinamide adenine dinucleotide phosphate (NADPH) being consumed, to yield ester 2, which is subsequently hydrolyzed by *Candida antarctica* lipase B (CalB) or alcalase to provide primary alcohol. Alcohol dehydrogenase (ADH) oxidizes the alcohol, by using the cofactor nicotinamide adenine dinucleotide ( $\text{NAD}^+$ ), to give aldehyde, which then undergoes spontaneous  $\beta$ -elimination to yield resorufin as the final fluorescent product. Reprinted with permission from ref 411. Copyright 2014 Wiley-VCH.

of catalytic molecules onto polymersomes functional surface or bilayer.<sup>389</sup>

Van Hest et al. exploited the potential and the power of polymersomes as a successful nanoreactor candidate. They described a three-step cascade reaction promoted by the use of different compartments of polymersomes.<sup>410</sup> They designed polymersomes with surface functionality to anchor HRP on. Moreover, they inserted CalB in the membrane while GOx was encapsulated in the lumen. This state-of-the-art allowed the conversion of glucose acetate by CalB into glucose, which was oxidized by GOx into glucolactone and hydrogen peroxide that was subsequently oxidized by the available ABTS. The concept of catalysis in polymersomes was also used as a tool to mimic cells by compartmentalizing different enzymes in different polymersome's confined space and performing a sequential cascade reaction<sup>411</sup> (Figure 34). Different enzymes were encapsulated in small polymersomes, which was subsequently encapsulated in a large polymersome. A sequential enzymatic cascade reaction was performed in different polymersomes, as such that every step of the cascade was separated in different polymersomes; the enzymes remain in place while the substrates and products diffuse freely across membranes of the small polymersomes. As a starting point, a Baeyer–Villiger monooxygenase and a cofactor were used to form an ester, which is subsequently diffused into a polymersome subcompartment to form an alcohol through a hydrolysis reaction by a lipase. In another polymersome subcompartment, previously generated alcohol is oxidized by alcohol dehydrogenase to an aldehyde that further undergoes a spontaneous  $\beta$ -elimination to yield a fluorescent dye used for confirmation of the completion of the cascade.

Polymersomes have shown a great capacity in stabilizing emulsions, as so-called Pickering emulsions, which accordingly led to an increase of the contact area between the organic and aqueous phase<sup>412</sup> (Figure 35A). This approach was used for

optimization of biocatalyst activity for reactions involving substrates that are poorly soluble in water.

CalB was encapsulated in the aqueous lumen of the polymersomes or in the emulsion's water phase. After 24 h,

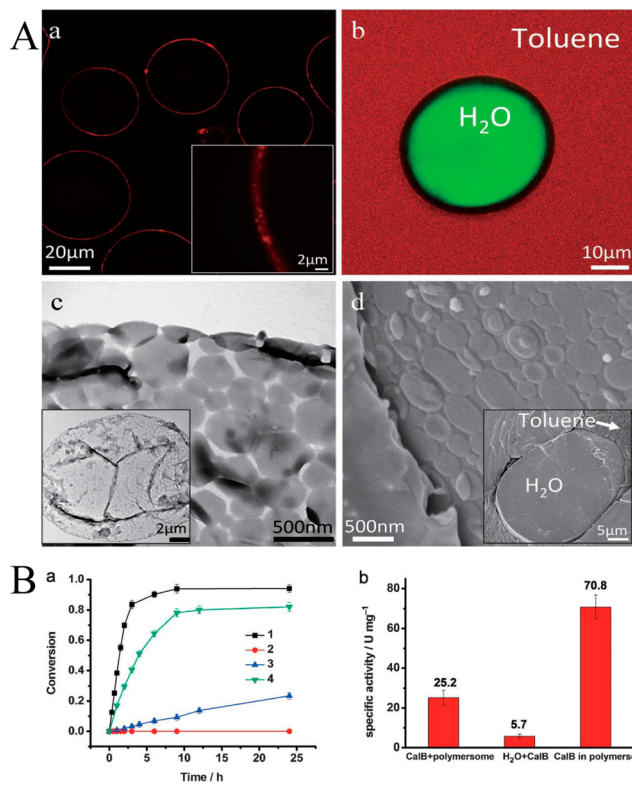


**Figure 35.** CLSM images and catalytic performance of polymersome Pickering emulsions (water in toluene). Reprinted with permission from ref 412. Copyright 2012 Wiley-VCH Verlag.

the enzyme did not show any diffusion into the organic phase from either the water phase or the lumen of polymersome. Authors investigated the ability of this system in the esterification reaction of 1-hexanol and hexanoic acid. Interestingly, they obtained conversions as high as 80–90% compared to 25% conversion obtained from classic biphasic reaction (Figure 35B). The Pickering emulsion polymersome stabilized system showed a high degree of recyclability (seven cycles) without any loss in the final conversion.

Encouraged by their previous results, the same authors aimed to extend the methodology of using polymersomes as a potent site isolated nanoreactor toward transition metals by performing organic reactions in aqueous media.<sup>390</sup> They cross-linked the polymersome membrane with chiral bis-oxazolines copper ligands and performed cyclopropanation of alkenes in water. The mechanism of action was based on attracting hydrophobic alkene substrates into the hydrophobic domain of the cross-linked polymersomes. Catalysis using these copper cross-linked polymersomes showed conversion of broad substrates scope for aqueous asymmetric cyclopropanation reactions with high enantioselectivity comparable to traditional cyclopropanation in organic solvents and much higher than those performed with only bis(oxazoline) in water.

**3.2.3. Virus Capsids.** Protein cages, like virus capsids, are self-assembled structures made up of protein and nucleic acids with remarkable monodispersity.<sup>413–417</sup> These protein cages not only can hold enzyme(s) inside their compartments but also can incorporate a range of metal ions and molecular catalysts within them<sup>388,418</sup> (Figure 36). The virus capsids biological

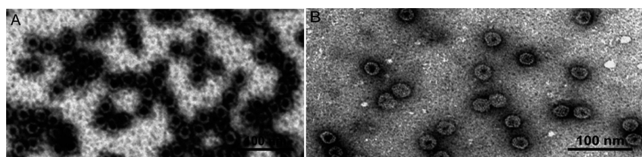


**Figure 36.** TEM micrographs of uranyl acetate-stained capsids: (A) empty wild-type capsids and (B) capsids filled with ~15 EGFP proteins per capsid. Reprinted from ref 418. Copyright 2009 American Chemical Society.

nature and their extreme monodispersity allows for excellent biomimetic properties that make them ideal models for use as nanoreactors that contribute to a better understanding of the role of confined space in determining reaction rates.<sup>394</sup> One example of artificial virus capsid is Cowpea Chlorotic Mottle virus (CCMV), which is composed of 180 identical proteins surrounding a single strand RNA. CCMV possess a capsid diameter of 28 nm when the pH is lowered to 5.0, while it disassembles into 90 proteins if the pH is increased to 7.5.<sup>419</sup> This unique feature allows for encapsulation of negative charged polymers,<sup>420</sup> inorganic materials, and enzymes.<sup>421,422</sup>

Early literature in the field described encapsulation of enzymes in CCMV capsids by normal statistical procedures, however, more controlled methods have since been reported. Cornelissen et al. demonstrated the encapsulation of PalB enzyme by attaching it into the capsid protein dimer before self-assembly using the coiled-coil motif. This study aimed to investigate change in the rate of reactions as a result of the confinement and number of enzymes encapsulated.<sup>394</sup> Interestingly, apparent catalysis rate increased significantly as a consequence of enzyme confinement, this was found to be independent of the number of enzymes encapsulated within the

capsid. These results were explained as a consequence of confinement on increasing enzyme concentration in the capsid, which led to a rapid formation of enzyme–substrate complex.

Other cages were used to investigate the role of confinement for catalytic reactions. One example is nanocage based ferritin,<sup>423</sup> a natural occurring intracellular protein that has 24 subunits. It assembles into 12 nm cages with a very high stability in a broad pH range (2–11) and high temperature tolerance. One intrinsic property of apo-ferritin is its ability in transferring ions from and into the cage;<sup>424</sup> this is because of its composition, which is eight 3-fold and six 4-fold channels that are connected to the interior cage.<sup>425,426</sup> Since these cages have an uniform form and can also incorporate different metals, they are used in many reports to prepare homogeneous nanoparticles.<sup>423,426,427</sup> Such properties qualify apo-ferritin-based nanocages as excellent nanoreactors for a plurality of catalytic purposes. Nie et al. reported the use of the apo-ferritin as a scaffold for designing 1–2 nm platinum (Pt) nanoparticles, which is used to mimic natural occurring enzymes to control oxidative stress in living cells.<sup>428</sup>

As mentioned previously, apo-ferritin has the capacity to consolidate metal complexes within its cage until they are immobilized on the interior surface of the cage to finally become water-soluble. Various examples of metal apo-ferritin were reported such as Pd(allyl).apo,<sup>429</sup> which was used in Suzuki-Miyaura cross-coupling reactions (Figure 37). Another example is Rh(nbd).apo-ferritin,<sup>430</sup> which was used in the synthesis of poly(phenylacetylene) with a superior control over polymer molecular weight distribution.

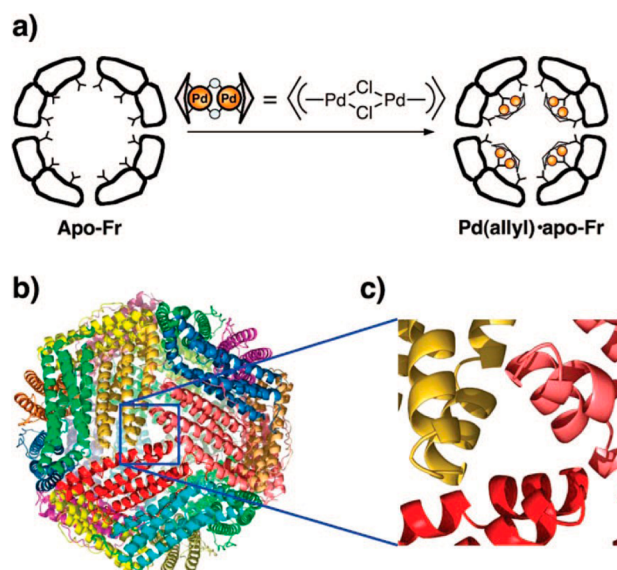


**Figure 37.** (a) Reaction scheme for the preparation of Pd(allyl)-apo-Fr, (b) entire structure of apo-Fr viewed down a 3-fold axis (PDB ID: 1DAT), and (c) close-up view of the 3-fold axis channel. Reprinted from ref 429. Copyright 2008 American Chemical Society.

**3.2.4. Supramolecular Polymeric Based Supra Molecular Catalysis.** **3.2.4.1. Dendrimers.** Dendrimers are highly branched molecules consisting of a different number of generations in which every generation has twice the molecular weight of the previous generation.<sup>431,432</sup> Structurally, dendrimers contain three zones: the core, inner shell, and outer shell.<sup>433,434</sup> The functionalities of these areas determine the properties of dendrimers such as hydrophobicity and thermal

stability.<sup>435</sup> Usually these properties are taken into account before their design, and thus, synthesis procedures and reagents are chosen accordingly.<sup>434</sup> Two strategies toward dendrimer growth are available, which are opposite to each other regarding the synthetic approach; however, they are meant to yield a similar product. In the divergent method, dendrimers are built up from a functional core, while dendrimers yielded as a result of the convergent approach are initially assembled from small molecules that will be located on the surface of the final dendrimer.

Dendrimers can be water-soluble such as Diederich's dendrophanes;<sup>436</sup> however, they contain a hydrophobic zone at their inner core which plays a big role in substrate concentration and transition state stabilization. Water-soluble dendrophanes are as similar to globular protein shells in establishing a microenvironment within their constructs, and thus they were utilized as functional artificial enzyme mimics. Other examples of water-soluble dendrimers are peptide- and glycol-based dendrimers, one fascinating example being the apple trees dendrimer in which amino acids are arranged on dendrimer branches in a similar way to an apple tree.<sup>437</sup> Reymond et al. extensively studied the synthesis and purification of more than 400 peptide and glycol-peptide-dendrimers using solid phase peptide synthesis.<sup>438</sup> Apple trees are excellent candidates for enzyme model comparison, whereas an intrinsic apparent rate enhancement was observed compared to their counter enzyme model. For example, the hydrolysis of 8-acyloxypyrene-1,3,3-trisulfonates using multivalent esterase dendrimer proceeded much faster than the classical enzyme catalyzed reaction. The calculated  $k_{\text{cat}}/k_{\text{uncat}}$  of this reaction was as high as 90000 with the butyryl ester substrate.<sup>439</sup> This high apparent rate acceleration of this system is attributed to the increased apparent reactivity of the catalytic site (18000 per catalytic site). Structures of peptide-dendrimers vary, and subsequently, they possess different properties, functions, and applications. Many examples were screened in catalysis-based applications such as esterase and aldolase enzyme model for efficient catalytic hydrolysis and aldolase reactions. Also, some of the peptide-dendrimers are involved in biorelated applications such as cancer cells labeling, being cytotoxic to cancer cells, antimicrobial reagents, and for drug delivery.<sup>439</sup>

**3.2.4.2. Poly(ethylene-imine) Supra Molecular Catalysis.** Poly(ethylene-imine) (PEI) is a highly branched polymer with primary, secondary, and tertiary amine groups, which allows the polymer to be modified for further property modulation such as their hydrophobicity.<sup>440</sup> Various reports have described catalysis of different reactions in an efficient manner by only changing the hydrophobic groups.<sup>441–444</sup> In 1971, Scarpa et al. reported the first model of dodecyl modified PEI as a supramolecular catalyst. Interestingly, the hydrolysis of 2-hydroxy-5-nitrophenyl sulfate in the presence of PEI proceeded  $10^{12}$  times faster than traditional reaction that is catalyzed by free imidazole.<sup>445</sup> Following this report, many papers were published about the role of PEI in acceleration of some reaction compared to classical reactions without the polymer.<sup>446,447</sup> Enantiomeric forms of PEI were reported and their intrinsic role in increasing some reaction rates such as Michael reaction, condensation of benzoin,<sup>448</sup> decarboxylation,<sup>449</sup> and racemization of amino acids was studied. Utilizing PEI in tandem catalysis was also studied extensively by McQuade et al., whereas PEIs were encapsulated in microcapsules ( $\mu$ cap) that facilitated their isolation from other incompatible catalyst (e.g., nickel catalyst). Thus, tandem catalysis between two incompat-

ible catalysts for Michael addition of a Malonate ester was possible<sup>450</sup> (Figure 38).

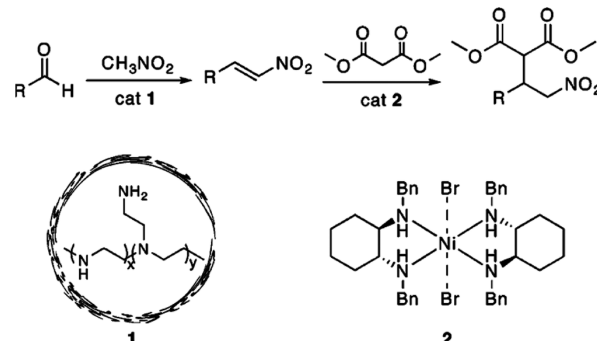


**Figure 38.** Transformation of an aldehyde to a nitroalkene and subsequent Michael addition of a malonate ester can be performed in tandem through the use of a site-isolated catalyst. Reprinted from ref 450. Copyright 2007 American Chemical Society.

Moreover, PEIs were endorsed in many applications such as solubilizing carbon nanotubes<sup>451,452</sup> or delivering siRNA to cells.<sup>453</sup>

**3.2.4.3. Synthetic Cavitands.** Cavitands are supramolecular structures that contain a hydrophobic aromatic bottom and functionalized or nonfunctionalized rims, which in both cases determines the depth of the cavitand cavity.<sup>454</sup> Starting materials used to synthesize cavitands determine the depth of its cavity. For instance, condensation of benzaldehyde and resorcinol form resorcinarene produce cavitand with very small cavity; however, functionalization of the rims of resorcinarene via its condensation with 1,2-difluoro-4,5-dinitro-benzene leads to formation of highly polar rims and thus a deep cavitand cavity.<sup>446</sup> Rebek et al. extensively studied catalysis by cavitands<sup>455</sup> and reported their use as a supramolecular catalysts for many reactions such as Diels–Alder, carbonate hydrolysis, 1,3-dipolar cycloaddition, and nucleophilic aromatic substitution.<sup>456</sup>

**3.2.4.4. Organometallic Macrocycles.** Many macrocycles are commercially available supramolecular materials that were extensively studied and reviewed.<sup>457</sup> They can be formed as a result of molecular self-assembly which is guided by non-covalent interactions, some as weak as van der Waals attractions. Fujita et al. reported the first self-assembled molecular square “clips” directed by metal–ligand binding.<sup>458,459</sup> Palladium-directed self-assembly of the kinetic labile bipyridine led to the formation of rapid and reversible bonds until the most stable structure (molecular square) was formed.<sup>458</sup>

A range of metal–ligand binding was adopted to design three-dimensional nanocages by mixing metal complexes with some organic ligands. These nanocages attracted many scientists due to their outstanding features such as their hydrophobic cavity and their ability to be dissolved in water.<sup>460</sup> Nanocages are outstanding nanoreactors for catalysis of some reaction as it provides an unusual rare regio-selectivity.<sup>461</sup> For instance, during the reaction of naphthalene with maleimide, substrates were encapsulated in a way that forced the maleimide to be positioned above the nonsubstituted naphthalene ring, which led to an efficient reaction on the naphthalene ring.<sup>461</sup>

Other tetrahedral nanocages with the general formula M4L6 (M = Al<sup>3+</sup>, In<sup>3+</sup>, Fe<sup>3+</sup>, Ga<sup>3+</sup>; L = bis-catechol naphthalene) were comprehensively studied and reviewed.<sup>462</sup> These nanocages are

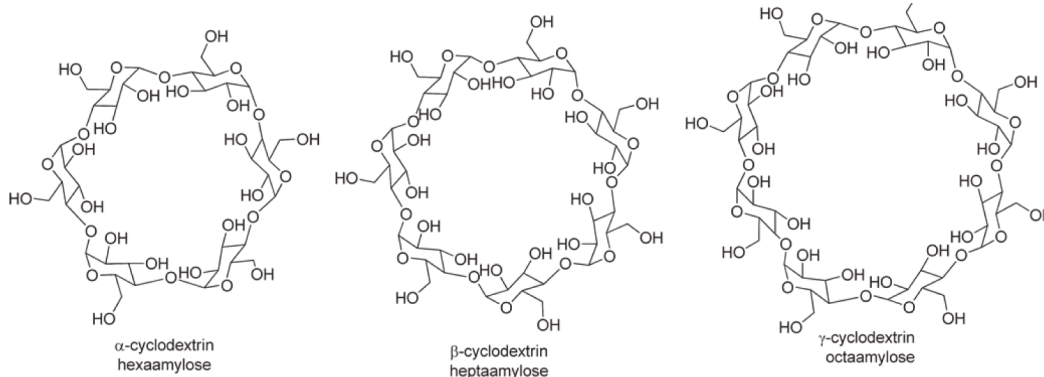


**Figure 39.** Structures of the commonly used  $\alpha$ ,  $\beta$ , and  $\gamma$ -cyclodextrin. Reprinted from ref 446. Copyright 2011 American Chemical Society.

chiral as a consequence of ligand arrangement around the metal center. The ability of these nanocages to stabilize cationic intermediates led reactions to proceed faster as a result of lowered reaction activation energy.

**3.2.4.5. CycloDextrins.** CycloDextrins are cyclic oligosaccharides made from glucose monomers.<sup>391</sup> Cyclodextrins have a hydrophobic cavity, which allows binding to hydrophobic guests.<sup>463</sup>  $\alpha, \beta, \gamma$ -Cyclodextrins are common dextran structures, which are used for catalysis.<sup>446, 464</sup> For example,  $\beta$ -cyclodextrins were reported to efficiently catalyze reactions such as Diels–Alder; as such it provides a well-defined geometry for the reactants to bind in.<sup>465</sup> Also,  $\beta$  cyclodextrins were reported to be recycled<sup>466</sup> and accelerates some reactions in water as in the case of furan-2(5H)-one synthesis.<sup>467</sup>

Cyclodextrins were also used to covalently bind some transition metals ligand in order to accelerate reactions rates.<sup>391</sup> For instance, copper(II)-cyclodextrins (Figure 39) adduct were reported to catalyze the hydrolysis of *p*-nitrophenyl acetate with 6 times faster than the copper(II) complex counterpart.<sup>446</sup> Also, copper(II) linked cyclodextrins was the first example for the so-called “artificial enzymes” because of its successful mimic of artificial metallo-enzymes.<sup>468, 469</sup> Another example of metal bound cyclodextrin as an artificial enzyme mimic is iron-containing cyclodextrin.<sup>470</sup> The structure is an excellent mimic of P450<sup>471, 472</sup> that was used for some oxidation reaction with high regioselectivity resembling the ones performed with the aid of natural P450. The iron center was also successfully exchanged with some other metals such as rhodium<sup>472</sup> and manganese.<sup>473</sup> Other reports have shown lucrative examples of cyclodextrins mimicking other artificial enzymes such as esterases, phospholipases, and nucleases.<sup>468</sup>

### 3.3. Autonomous Movement

In nature, the ability to migrate enables cells to change locations according to changes of the chemical/physical cues of their environment. Such migration guiding cells to a specific location, is essential for immune response and tissue formation.<sup>474</sup> Research into the migrating mechanisms not only shed light on wound healing<sup>475</sup> and embryonic development<sup>476</sup> but also lead to interest in developing motile synthetic particles based on the understanding of the cell motion. Fabricating particles with self-propelling behavior, which could convert energy into autonomous movement,<sup>265, 477–485</sup> has the potential to revolutionize drug delivery<sup>486–491</sup> and environmental remediation.<sup>492–496</sup> In nature, cell polarity caused by the dynamic assembly of actin and rearrangement leads to eukaryotic cell locomotion.<sup>497, 498</sup> In vitro asymmetric electric field or chemical gradient generated by asymmetric synthetic motors induces

directed motion. Besides the self-generating gradient, continuous movement could also be induced by applying an external adhesion gradient, pressure gradient, and electric or magnetic gradient.<sup>499</sup> A decade after the pioneering work of Whiteside's on centimeter-sized self-propelled plate,<sup>477</sup> more precise regulation of the motor speed and direction is now achieved for practical applications in bio environment. For instance, introducing a temperature sensitive polymer such as PNIPAM to the outlayer of tubular motors, temperature increase led to unfolding of motors, slowing down its speed.<sup>500</sup> It was also demonstrated that the speed of electrochemically driven motors could be reversibly changed when the potential of the motor was altered. Furthermore, control over the direction of the motors was also achieved in the presence of external magnetic fields by incorporating ferromagnetic segments into the motor leading to a change in the motor direction on demand. While external stimuli have been demonstrated to achieve spatial and temporal control, there is still controversy over the practicability of its application and relevance in biological systems. Increasing efforts have been devoted to achieve control in directionality by utilizing a more bioinspired approach such as chemotactic behavior, which is directional movement in a gradient of fuel. Several groups have observed independently, for different motor designs, a biased motion of the motors toward higher level of fuel.<sup>501, 502</sup> The mechanism of directional movement was proposed to be due to the enhanced diffusion of the motors at higher fuel concentrations, as the motors demonstrated linear increase in their speed with increasing the fuel concentration. In this chapter, we will focus on self-assembly techniques used to construct supramolecular structures with autonomous movement and their potential applications. Further control in the direction of movement of motors via chemotaxis will be presented in the following section.

From a practical point of view, self-assembled motors provide several advantages in terms of size tunability, easy fabrication, surface modification, cargo loading, and biodegradability. Furthermore, from a material perspective, the self-assembly technique allows for the design of soft supramolecular structures with unique shapes that can facilitate a better interface with biological systems. Therefore, such structures can be potentially great candidates for applications in biological media such as active drug delivery.

**3.3.1. Polymersome Stomatocyte Nanomotors.** Our group is interested in exploring the use of self-assembly as a tool to construct not only active delivery systems for chemotherapeutics but also structures with emergent functions such as motion, regulated transport, or controlled transport. Starting

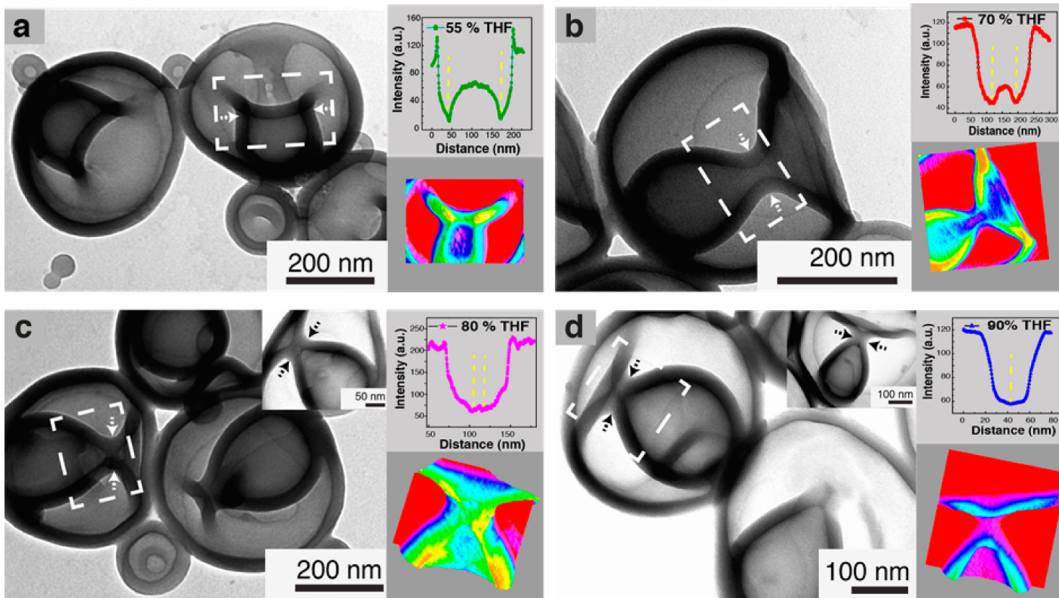


**Figure 40.** Shape transformation of polymersomes assembled from poly(ethylene glycol)<sub>44</sub>-*b*-polystyrene<sub>177</sub> into stomatocytes with controlled opening. The TEM images show the change in the size of the opening according to the percentage of THF by volume in the THF/dioxane solvent mixture used for polymer dissolution. (a) 55% THF, (b) 70% THF, (c) 80% THF, and (d) 90% THF. The upper inset shows the intensity profile as measured by TEM across the stomatocyte “neck” at the narrowest opening indicated by the arrows. The lower inset shows the 3D intensity profile of the neck area. Adapted with permission from ref 314. Copyright 2012 Nature Publishing Group.

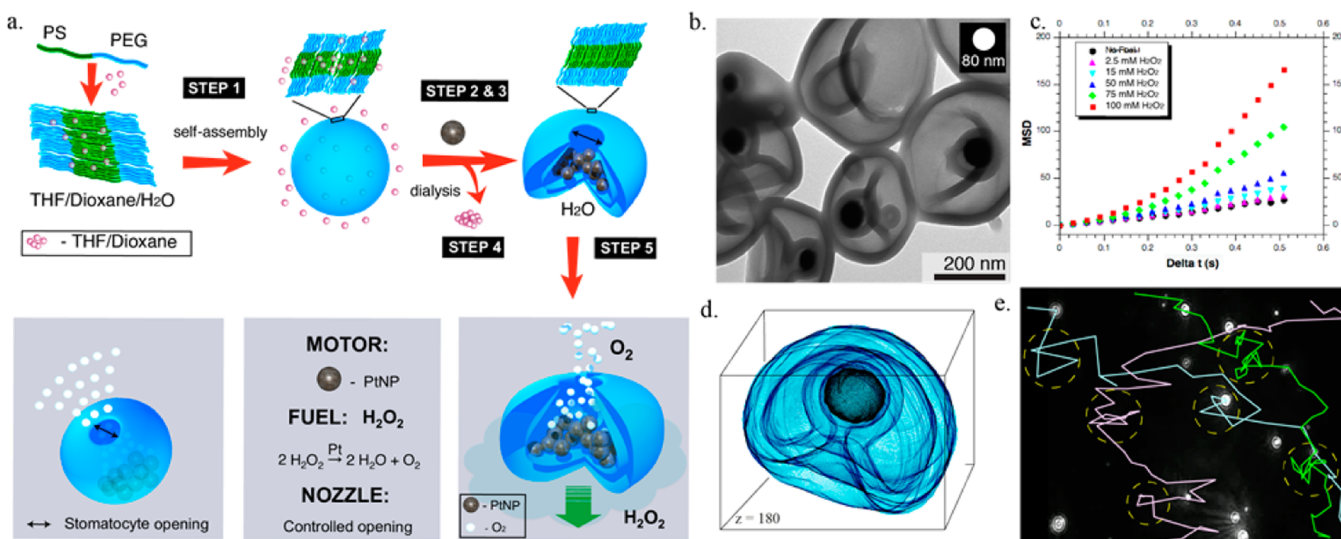


**Figure 41.** (a) Supramolecular nanomotor design; strategy for entrapping preformed PtNPs during the shape transformation into stomatocytes. (b) TEM image showing the entrapment of 80 nm PVP-capped PtNPs during the shape transformation of polymersomes. (c) Average mean square displacement of the supramolecular nanomotors as a function of fuel concentration. (d) 3D Electron reconstruction of the platinum-filled stomatocyte nanomotore. (e) Typical trajectories of the supramolecular nanomotors in 50 mM H<sub>2</sub>O<sub>2</sub> (fuel) concentration. Reprinted with permission from ref 314. Copyright 2012 Nature Publishing Group. Reproduced from ref 503 with permission from The Royal Society of Chemistry. Copyright 2013 Royal Society of Chemistry.

from small polymeric building blocks predisposed to associate, we engineered asymmetric supramolecular bowl-shape structures (stomatocytes) with a narrow opening and an active catalyst (PtNPs) placed inside the structures.<sup>314,503</sup> Spherical polymersomes composed of amphiphilic block copolymer poly(ethylene glycol)-*b*-polystyrene were first prepared via the self-assembly of the amphiphiles in the presence of organic solvents. The design of the amphiphile allowed for a strict control over the mechanical properties of the self-assembled structure with its membrane, rigid and glassy in water, and

flexible and semipermeable in the presence of plasticizers such as THF and dioxane. Dialysis of flexible polymersomes assembled in the presence of organic solvent induced differences in the osmotic pressure over the membrane and consequently a sudden fold of the membrane inward due to the inability of the semipermeable membrane to equilibrate the pressure.<sup>504</sup> Bowl-shape stomatocyte structures with a controlled opening were generated depending on the amount of plasticizer used for the shape transformation (Figure 40).

However, for the structures to become effective nanomotors, an active catalyst capable of generating propelling gas during the catalytic reaction was required. The assembly of the nanomotor was performed in several crucial steps which first necessitated the assembly of the block copolymers into spherical vesicular structures (polymersomes) followed by the loading of catalytically active nanoparticles inside of the structures during the shape transformation of the vesicles into stomatocytes and finally the diffusion of the fuel inside the assembly to generate propelling gas. The structures obtained resemble with “miniature rockets” in which the catalytic decomposition of the fuel results in a fast-moving jet of gases through an outlet “nozzle” (Figure 41).

Such bottom-up supramolecular nanomotors are functional, effective, real nanometre-sized transporters, which we believe will become the constituents of next-generation nanoengineered delivery systems. Polymersomes and liposomes are already used routinely in the clinic for drug delivery due to their ability to enclose different type of drugs; however, they have a limited efficiency and they cannot actively target the diseased tissue. With nanomotor-based drug delivery agents, more rapid and targeted delivery could be achieved. The constituents of stomatocytes nanomotors are not limited to poly(ethylene glycol)-*b*-polystyrene; biodegradable stomatocytes are also under investigation.

Future research is focused on demonstrating the propelling of the stomatocyte nanomotors in biological media and their collective locomotive abilities in a gradient of fuel as intelligent, self-propelled, and self-guided drug carriers that can follow the chemical clues given by tumor cells.

**3.3.2. Layer-by-Layer Motors.** Developed by He and co-workers, polyelectrolyte hollow capsules are fabricated by consecutive absorption of oppositely charged polyelectrolytes to sacrificial templates (layer-by-layer technology).<sup>505</sup> After deposition of polystyrenesulfonate/poly(allylamine hydrochloride) (PSS–PAH) onto sacrificial silica particles, the top surface was modified with dendritic platinum nanoparticles (PtNPs) using microcontact printing technique. Afterward, silica was dissolved to give the asymmetric polyelectrolyte capsules. At 30% H<sub>2</sub>O<sub>2</sub>, maximum velocity of PtNPs-modified Janus capsule exceeded 1 mm/s. FITC-dextran was encapsulated and released as a model cargo. Upon addition of ethanol, the capsule transformed from “closed” to “open” state and facilitated the release of FITC-dextran. Furthermore, negatively charged magnetic particles were added during the self-assembly process allowing for magnetic control over the directionality of the motors. Besides PtNPs modification with microprinting technology, Janus motors were also fabricated through PSS and PAH alternative deposition on a silica template followed by sputtering of 20 nm PtNPs.<sup>506</sup> After dissolution of the silica template, PSS/PAH Janus capsule motor decorated with PtNPs was obtained. Meanwhile, other examples of self-assembled Janus motor appeared from the same group.<sup>507</sup> PAH and PSS were alternatively deposited onto silica particles with a diameter of 8 μm. Then Cr (adhesion layer), Ni (ferromagnetic), and Au were deposited at an incidence angle of 30 degree on the surface of the particles, resulting in Janus particles. After modification of the Au layer with 3-MPA, catalases were conjugated to the surface through a sulfo-EDC/NHS activation. Compared with its PtNPs counterparts, the catalase-modified Janus motor showed a higher catalytic efficiency. After removing the silica templates, Janus capsule motors were obtained. The Ni-capped Janus motors were further guided toward Hela cells under a

magnetic field of 0.02 T. The positively charged PAH motors were shown to interact with the negative surface of the Hela cells via electrostatic interactions and allowed the accumulation of the motors onto the surface of the cells. NIR laser was then employed to trigger the release of the loaded anticancer drug doxorubicin by taking advantage of the heat generated by the gold-coated layer under NIR irradiation, which induced a complete collapse of the structure.

Besides Janus motors, He and co-workers later reported the fabrication of tubular motors using the same layer-by-layer technique.<sup>508</sup> Positively charged chitosan and negatively charged sodium alginate were alternatively deposited into a porous polycarbonate template membrane before adding poly(diallyl dimethylammonium chloride) stabilized PtNPs. After the removal of polycarbonate membrane, PtNPs-loaded chitosan/sodium alginate tubular motors were obtained. The tubular motor could move at a stable speed of 74 μm/s in 15% of hydrogen peroxide solution for over 30 min and a speed of 22 μm/s in 3% of hydrogen peroxide in the presence of Hela cells. In the same fashion as the previous study, iron oxide particles integrated into the motors allowed the guiding of the motors toward Hela cells via magnetic field. In this case, the tubular nanomotors with a length of 8–10 μm were found to partially penetrate the cell membrane. The authors used then ultrasound at 59 kHz and 40 W for several seconds to release the anticancer drug doxorubicin loaded into the outer layer of the tubular motors. As confirmed by SEM, the roughness of outer surface and reduced height indicated the partial rupture of the tubular motors caused by the sonication treatment. The ultrasonic treatment alone did not show any obvious cellular structure damage. A similar report used poly(allylamine hydrochloride) (PAH)/poly(styrene sulfonic acid) (PSS) to assemble a microtubular engine through the same layer-by-layer technique.<sup>509</sup> Poly(diallyl dimethylammonium chloride) stabilized PtNPs were assembled in the inner surface. Then gold nanoparticles were grown on the outer surface, and a layer of thiol-T7 peptide/thiol PEG<sub>2000</sub> was immobilized. (Figure 42) T7 peptide (HAIYPRH) was known to facilitate the specific binding to human transferrin receptors, which were overexpressed in certain tumor cells. With a focused near-infrared (NIR) light projected on the gold nanoparticles containing motors, the gold monolayers heated up within a few picoseconds due to the plasmon resonance. As a consequence, the sharp increase in the environmental temperature induced an elevated catalytic activity and an increased velocity of the motor. The residual heat could still propel the motor for a certain period of time after the motor left the laser point. The T7 peptide/PEG<sub>2000</sub> modified tubular motors were able to attach to Hela cells but unable to bind to red blood cells, which do not express transferrin receptors on the surface. In addition, application of focused NIR on the motors when in the vicinity of Hela cells led to a temperature increase over 10 degrees in the local environment, possibly facilitating the Hela cell apoptosis.

**3.3.3. Cell-Based Motors.** Wang's group has recently reported red blood cell (RBC) motors decorated with 20 nm iron oxide particles using a hypotonic dilution/encapsulation method<sup>510</sup> (Figure 43). In a hypo-osmotic lysing buffer, the influx of outer medium and outflow of the inner medium resulted in formation of pores into the cell membrane, thus allowing for encapsulation of iron oxide particles from the surrounding medium. Upon reaching again the osmotic equilibrium, the cell membrane resealed, entrapping the iron

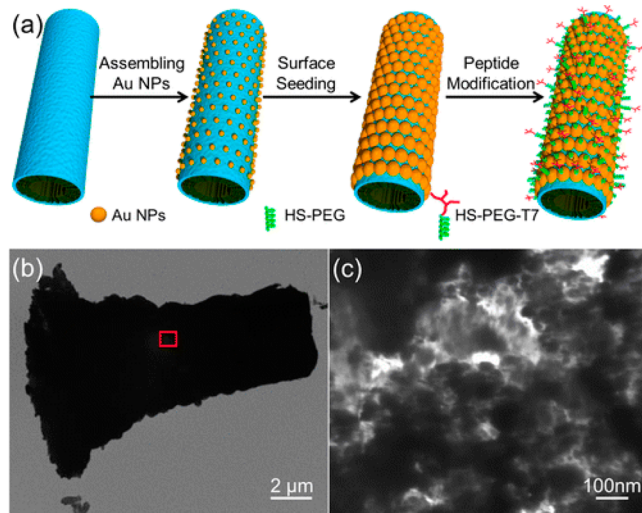


**Figure 42.** (a) Scheme of the fabrication process of the PtNPs-modified polyelectrolyte multilayer microengines coated with a thin AuNS and a tumor-targeted peptide: (i) assembling gold nanoparticles on the outer surface of the tubes, (ii) growth of gold nanoparticles, and (iii) immobilization of the mixed thiol-PEG and thiol-peptide monolayer. (b) TEM image of a T7 AuNS ( $\text{PAH}/\text{PSS}$ )<sub>20</sub> PtNPs microengine. (c) Enlarged image of the indicated region with a red frame in (b). Reprinted from ref 509. Copyright 2014 American Chemical Society.

oxide particles inside. Since iron oxide nanoparticles were unevenly distributed in the RBC since the structure is inherently asymmetric, the iron oxide loaded RBC could be propelled by pressure imbalance produced by acoustic waves.

The RBC motors could move at a speed of 5  $\mu\text{m}/\text{s}$  in the whole blood. The asymmetric distribution of iron oxide nanoparticles also made magnetic navigation possible. Switching on/off external magnetic field could reversibly orient the RBC motors. In the whole blood, the RBC motor could move in a controlled way with orthogonal turning. The RBC motors not only moved in a real biological environment but also experienced no obvious velocity reduction, indicating the absence of salt effects and protein fouling. As immunosuppressive antigen CD47 is present on the surface of RBC, the chance of iron oxide particles being taken up by macrophages is greatly reduced after loading into RBC, ensuring a prolonged lifetime in the blood circulation system.

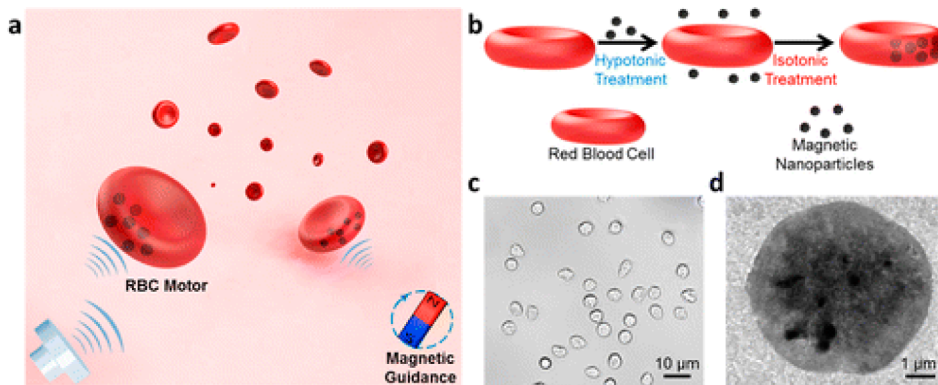


**Figure 43.** Red blood cell (RBC) motors. (a) Schematic illustration of magnetically guided, ultrasound-propelled RBC micromotors in whole blood. (b) Preparation of the RBC motors: magnetic nanoparticles are loaded into regular RBCs by using a hypotonic dilution encapsulation method. (c) Optical and (d) transmission electron microscopy images of the RBC motors. Reprinted from ref 510. Copyright 2014 American Chemical Society.

**3.3.4. Metal–Organic Framework (MOF) Motors.** Hiroshi's group discovered that diphenylalanine (DPA) peptides assembled in the nanometer size pores of MOF could be released and reorganized again at the MOF/water interface (Figure 44).

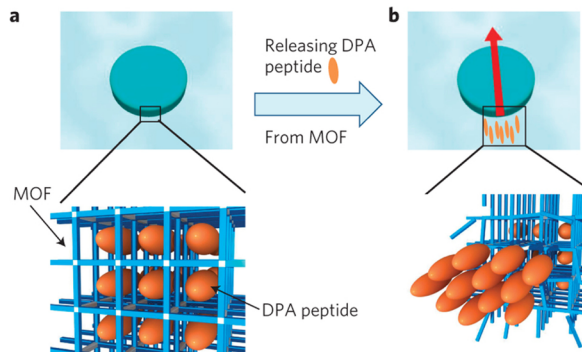


**Figure 44.** Illustration of the mechanism of DPA–MOF motion. (a) Before releasing DPA peptides, MOF incorporates DPA peptides in a well-ordered alignment in the nanoscale pores. (b) After releasing DPA peptides, the reassembly of DPA peptides creates a hydrophobic domain at the end of the MOF particle. Because this domain lowers the surface tension of the MOF on the release side, the MOF particle moves in the direction of the red arrow as a result of the surface tension gradient via the Marangoni effect. Reprinted with permission from ref 511. Copyright 2012 Nature Publishing Group.

Such reconfiguration of the hydrophobic peptides created large enough surface tension gradient to propel the MOF.<sup>511,512</sup> The  $[\text{Cu}_2\text{L}_{2,\text{ted}}]_n$  based metal organic framework first incorporated DPA peptides within its 0.75 nm sized pore. After removing the solvent, the DPA incorporated MOF was placed into a solution of EDTA. EDTA could couple with copper ions and destabilize the frame, thus triggering the release and reconfiguration of the DPA peptide. The DPA-MOF motor system was shown to move on the surface of the solution with speed as high as 35  $\mu\text{m}/\text{s}$ . The moving direction of the motor was determined by the first impulse of released DPA and the tension gradient established.

**3.3.5. Polymer Single Crystals (PSC)-Based Nano-motors.** Li et al. used the self-assembly technique to fabricate a polymer single crystal based motor system.<sup>513</sup> Polymer single crystals of  $\alpha$ -hydroxyl- $\omega$ -thiol-terminated polycaprolactone with

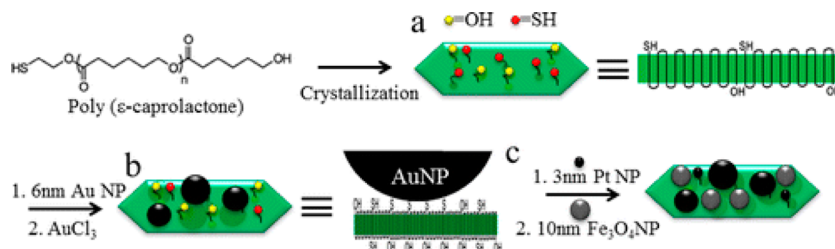


**Figure 45.** Schematic illustrates the fabrication process of a nanoparticle-based nanomotor. Reprinted from ref 513. Copyright 2013 American Chemical Society.

a thickness of 8 nm were formed via a self-seeding solution crystallization technique. The thiol groups on the surface of the polycaprolactone PSC were then used for immobilization of Au nanoparticles and PtNPs. The remaining hydroxyl groups were further used for the immobilization of Fe<sub>3</sub>O<sub>4</sub> nanoparticle (Fe<sub>3</sub>O<sub>4</sub> NP) for guidance under magnetic field (Figure 45).

The surface plasmon resonance absorption of the Au nanoparticles facilitated both the imaging and tracking of the motors under the optical microscope. Although the motor was 100 times heavier than the PtNPs, it was still able to move at considerable high speeds of 30  $\mu\text{m}/\text{s}$  in 15% of the hydrogen peroxide solution. Although the PtNPs were homogeneously distributed on the PSC surface, momentum generated by bubble release still propelled the motor system forward. Furthermore, since the PSC was also decorated with high density superparamagnetic Fe<sub>3</sub>O<sub>4</sub> NP, magnetic steering of the PSC-based motors toward a magnetic polystyrene bead and picking it up as a cargo was also possible.

In nature, the movement of bacteria and sperm is facilitated by rotation of flagella. Several research groups have constructed motors with biomimetic shape to achieve movement. Bibette et al. fabricated a chain of streptavidin coated magnetic particles with biotin-ended double-stranded DNA acting as a linker. The flagella-like magnetic particles chain was attached to the red blood cells. Oscillating magnetic field was then used to induce beating motion of the magnetic chain which propelled the red blood cells<sup>514</sup> (Figure 46). Takeuchi et al. isolated flagella from a single cell based algae *Chlamydomonas reinhardtii*. Through

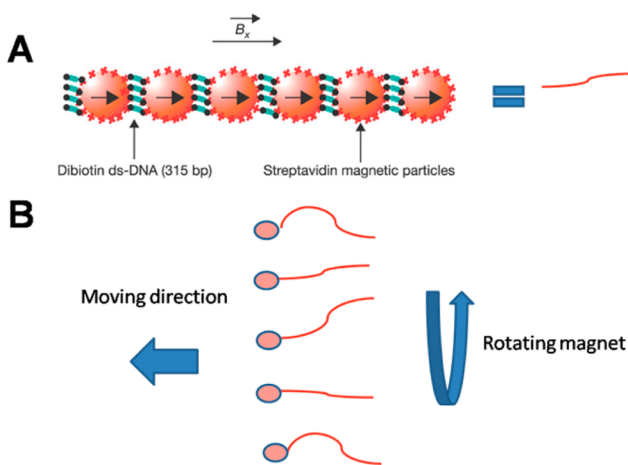


**Figure 46.** (a) Preparation of a magnetic filament and (b) beating pattern of the motion of a magnetic flexible filament attached to a red blood cell. The blue arrow on the top shows the direction of motion. The filament length is  $L = 24 \mu\text{m}$ . Adapted with permission from ref 514. Copyright 2005 Nature Publishing Group.

biotin–streptavidin interaction, dismantled flagellum was attached to liposomes. After reactivation, the flagella attached to the liposome were shown to facilitate the motion of the entire structure.<sup>515</sup>

### 3.4. Interaction and Communication

Interaction and communication are complex functions of biological systems where not only movement is achieved but also directional movement during which sensing and transfer of information is carried out. Random motion is rarely seen in biological systems, in fact seemingly random motion is often a concert of interactions and communication processes leading to a directed motion. For example, while observing swarming bacteria at one magnification may show a random motion of moving bodies viewing the cluster as a whole reveals a highly coordinated translational motion.

Thus, in this chapter, we focus on motility of self-assembled systems in response to stimuli and the relation of these systems to biologically motile systems. Emphasis will be given to directional control of movement in synthetic systems via various forms of taxis.

**3.4.1. Chemotaxis.** Chemotaxis, a common phenomenon observed in nature, is in fact a navigation technique for cells and other microorganisms. Chemotaxis, is a process in which cells/organisms sense and respond to the local physical/chemical stimuli gradient. For instance, neutrophils outside blood vessels migrate along the gradient of N-formyl-methionine-leucine-phenylalanine, a peptide secreted by bacteria.<sup>516</sup> The migration of organisms along the chemical gradient takes place either toward attractant or away from repellent. Motion toward high concentration of chemicals is defined as positive chemotaxis, while the opposite, directed motion is so-called negative chemotaxis. This ability of spatial/temporal sensing and responding enables organisms to find food and escape from toxins, as well as signaling to isolated cells to perform collective tasks. In prokaryotic cells and flagella-carrying eukaryotic cells, chemical attractants/repellants can bind with the receptor on the cell surface, activating Che protein. By interacting with flagellar switch protein, Che protein could determine the rotation direction of organisms flagella to be clockwise or anticlockwise, thus modulating moving direction to achieve chemotaxis.<sup>517</sup> In eukaryotic cells of vertebrates, external chemical gradient can be converted into a PIP3 gradient within the cells. Resulted polarized polymerization of actin filaments leads to pseudopods formation and directed motion (Figure 47). In this section, we will discuss the bioinspired approaches to design synthetic chemotactic systems to achieve directional control over synthetic nanomotors.

Outside living systems, taxis phenomenon has been demonstrated with particles being directed along local chemical or adhesion gradients.<sup>502,518</sup> Sen's group discovered that

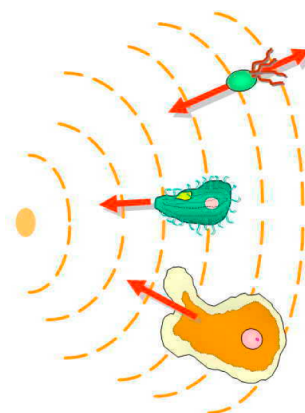


**Figure 47.** Chemotaxis of prokaryotic cells, flagellar carrying eukaryotic cells and eukaryotic cells of vertebrates origin. Reprinted from the Wikipedia (author: Laszlo Kohidai) under the terms of the GNU free documentation license. (<http://en.wikipedia.org/wiki/Chemotaxis#/media/File:Chtxbaseukl1.png>).

platinum-gold microrods (2  $\mu\text{m}$  in length) could exhibit a directed motion up the hydrogen peroxide gradient generated by a 30% aqueous  $\text{H}_2\text{O}_2$  soaked hydrogel.<sup>501</sup> After 110 h, 70% of the microrods were shown to be attracted to the vicinity of the gel. This mechanism for the chemotaxis behavior was attributed to the higher active diffusion coefficient at higher hydrogen peroxide level. As the microrods moved further when they moved up the gradient, a net movement of the microrods ensemble toward the high concentration of fuel was responsible for the chemotaxis phenomenon. The enhanced diffusion assumption was further supported by the observation of accelerated motion of the microrods when approaching the hydrogen peroxide source. Schimdt and Sanchez et al. demonstrated a similar chemotactic behavior toward  $\text{H}_2\text{O}_2$  in a channel of  $\psi$  geometry for catalytic microjets and Janus motors.<sup>502</sup> Motors deviated toward the  $\text{H}_2\text{O}_2$  containing channel in a  $\text{H}_2\text{O}_2$  concentration dependent manner. They also assumed that catalytic motors could make longer runs as they move up the fuel concentration gradient. Self-assembled stomatocyte nanomotors developed by Wilson and co-workers were also found to demonstrate chemotactic behavior in both a glass channel (similar in shape to a PP chamber, which is commonly used for cell chemotaxis evaluation) and a microfluidic device. The chemotactic behavior was also observed in the presence of hydrogen peroxide gradient generated by model cells. (Figure 48). Several techniques such as cryo-TEM, confocal fluorescence microscopy, and flow-field fractionation technology were used to confirm the assembly of the stomatocytes motors loaded with both fluorescent anticancer drug doxorubicin and catalyst platinum nanoparticles. The presence of the fluorescent drug facilitated also the tracking of nanomotor movement and chemotaxis evaluation. Giving their ability to control their directionality through chemotaxis, such self-assembled motors are promising in actively delivering therapeutic agents precisely to diseased tissues and cells.<sup>519</sup> Furthermore, their soft biointerface, stealth properties, and nanometer dimensions make these motors ideal for drug delivery in blood vessels/interstitial tissues and particularly attractive for biomedical applications. Furthermore, the supramolecular approach for the nanomotor assembly afford also versatility, as choosing different polymers may lead to vesicles of different sizes, biodegradability, even morphologies. Sen's group demonstrated that even enzyme molecules

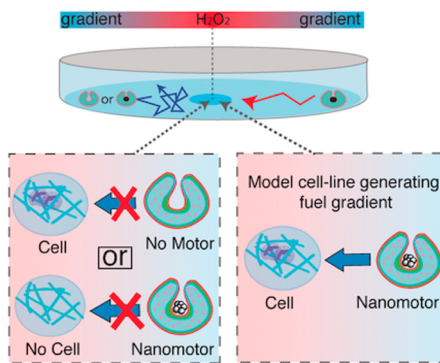


**Figure 48.** Chemotaxis evaluation of PtNPs-loaded stomatocytes toward cells. Reprinted with permission from ref 519. Copyright 2015 Wiley-VCH.

show chemotactic behavior in a substrate gradient generated by a Y-shaped microfluidic device<sup>520,521</sup> (Figure 49). In this case, the diffusion coefficient of catalase showed a substrate concentration dependent increase. When placed in the microfluidic device, the catalase ensembles deviated toward the channel containing the hydrogen peroxide substrate. A similar phenomenon was also observed for urease. Bon and co-workers fabricated match-stick shaped  $\text{SiO}_2-\text{Mn}_x\text{O}_y$  rod motors.<sup>522</sup> In the presence of a gradient of hydrogen peroxide generated by a wax sealed Dunn cell, these motors demonstrated motion toward hydrogen peroxide filled well. Inert polystyrene microspheres were also observed to move away from hydrogen peroxide source due to convection. By tracking the orientation of particles, it was found that the rod motors tend to face toward hydrogen peroxide source against Brownian motion and convection flow. Chattopadhyay's group reported pH taxis with palladium nanoparticles functionalized polymer microspheres.<sup>523</sup> Hydrogen peroxide catalytic activities of Pd microspheres was found to be higher at a higher pH. With an alkali supplying thread in the middle of the hydrogen peroxide bath, acceleration toward the higher pH area was observed. It was assumed that the chemotactic behavior was in this case due to the solute pressure imbalance caused by local solute depletion and asymmetric self-decomposition of the bulk hydrogen peroxide solution. Chattopadhyay and collaborators later replaced the palladium nanoparticles with iron nanoparticles.<sup>524</sup> This design allowed for the resulting iron nanoparticle coated microsphere to show simultaneous chemo- and magneto-taxis. The microsphere motors placed into a hydrogen peroxide bath were able to respond to both pH gradient and external magnetic field generated either by an electromagnet or a permanent magnet. Sen also described an attractive chemotactic phenomenon observed for a polymerization driven motor.<sup>265</sup> In this case, the silica side of a silica-gold Janus particle was modified with the Grubbs's catalyst. This catalyst was then further used in the ring opening metathesis polymerization of norbornene monomer. The monomer/product gradient generated by the asymmetric catalyst and the local thermal effect were suggested to be responsible for the self-propulsion of the structures. An overall increased diffusion of up to 70% was observed for the Janus motors in the presence of a 1 M norbornene solution. Then with a norbornene-containing acrylate gel, a monomer gradient could be created. A slight higher agglomeration was observed at the gel edge for the Janus motors.

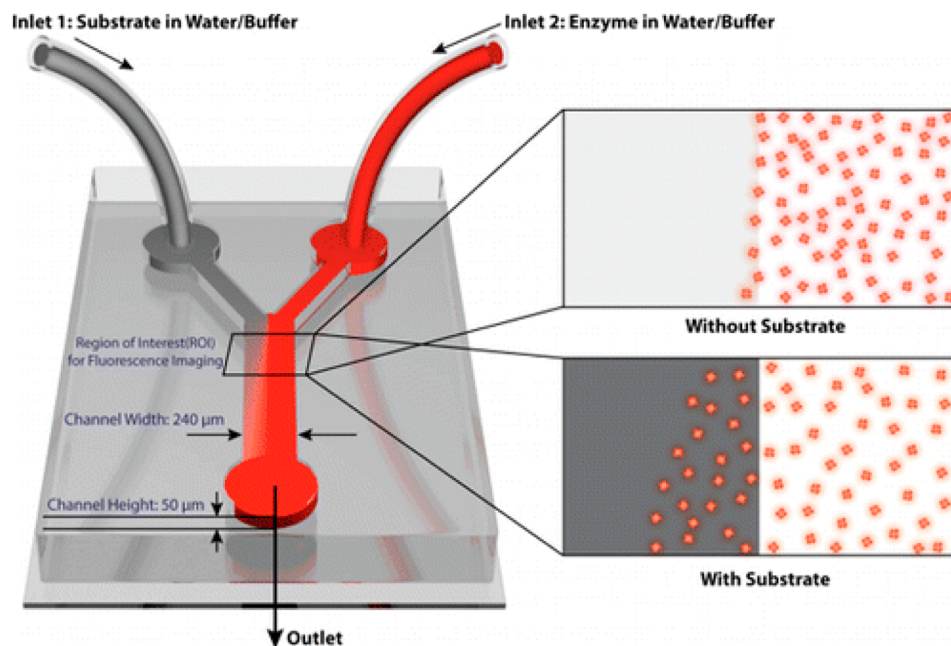


**Figure 49.** Schematic representation of the Y-shaped microfluidic channel used for chemotactic studies of ensembles of enzyme molecules. Reprinted with permission from ref 520. Copyright 2013 American Chemical Society.

**3.4.2. Magnetotaxis.** Magnetotaxis is observed in natural systems in bacteria such as *magnetotacticum gryphiswaldense*. The iron oxide nanoparticles filled vesicles (magnetosomes) in the bacteria allow the bacteria to orient themselves along the magnetic field. Johanson et al. designed paramagnetic and ferromagnetic rod motors and evaluated their navigation in a heterogeneous magnetic field in comparison with magnetotactic bacteria.<sup>525</sup> Navigation was achieved for paramagnetic rod motors with synergy between autonomous motion and magnetic guidance. Sanchez and Schmidt et al. demonstrated with gradients of magnetic field the guiding of microjets toward a targeting position at a velocity of 90  $\mu\text{m/s}$ , while magnetotactic bacterium showed a velocity of 28  $\mu\text{m/s}$ .<sup>526</sup> Another example was provided by Pumera's group who designed magnetic gold-nickel-platinum nanotubes via electrochemical deposition method. The structures were found to behave similarly with magnetotactic bacterium; the nickel-incorporated tubular motor was able to magnetize and align itself with the external field when exposed to a neodymium permanent magnet. When the bubble ejecting jet motor moved away from the magnet, the velocity decreased as magnetic attraction force was against the propulsion force.<sup>527</sup>

**3.4.3. Other Forms of Taxis.** Nature provides other examples of taxis, for instance in adhesion gradients. During inflammation, the formation of intracellular adhesion molecules (ICAM-1) is up-regulated and P selectin is expressed.<sup>528</sup> The catch and slip interaction between antigen bearing leukocytes with P selectin is fast but weak while interaction with ICAM-1 is slower but firmer, therefore, an adhesion gradient is established. This results in a recruitment of leukocytes toward inflamed areas. Balazs et al. theoretically predicted that microspheres could also be directed based also on adhesion gradient. They assumed particles with Brownian motion would deposit more at higher adhesion levels.<sup>529</sup> In mimicking leukocytes, Hammer's group functionalized PEO-*b*-PBD polymersomes with sialyl Lewis X and anti-ICAM-1, which selectively bind to P selectin and ICAM-1. By tuning the antigen functionalization density,

they demonstrated *in vitro* selectivity toward the inflamed endothelium.<sup>499,518</sup> (Figure 50) Bassereau described also a

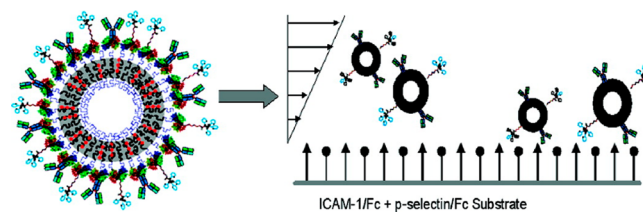


**Figure 50.** Schematic illustrating the avidin-coated polymersome used for all experiments. Anti-ICAM-1 ab and sLex polymer were titrated onto the surface of this vesicle at varied ratios. Use of avidin-coated vesicles ensures a similar particle size distribution of vesicles for all experiments, and supersaturating conditions during association of ligands ensure similar surface site densities for all experiments. Reprinted from ref 518. Copyright 2010 American Chemical Society.

heptotactic behavior of a negatively charged lipid vesicle. When placed on a positively charged bilayer surface, the close contact of oppositely charged membrane led to local neutralization. The induced adhesion gradient would propel the lipid vesicles along the self-generated gradient.<sup>530</sup>

**3.4.4. Conclusion.** Since T. W. Engelmann brought up the chemotaxis concept in 1881, it was not until 1950s and 1960s that various qualitatively evaluation methods were proposed and in-depth understanding was obtained. Almost half century later, synthetic chemotactic systems were developed, yet most of them via a top-down approach. Nevertheless, for applications in drug delivery, sensing, and machinery,<sup>20</sup> soft bottom-up self-assembled chemotactic motors that allow a better interface with biological systems are required. In addition, most assessing techniques for artificial chemotaxis are adapted from available techniques of organism chemotaxis. As differences in scale, response time, and response gradient exist between organisms and synthetic systems with chemotactic behavior, techniques have to be carefully selected to facilitate accurate qualitative/

quantitative evaluation. Bacteria such as *E. coli* with temporal sensing abilities could differentiate small chemokines concentration difference and maintain high temporal sensing efficiency without a steep gradient. Therefore, artificial systems with high chemotactic efficiency as well as other chemical attractant besides hydrogen peroxide based systems are needed for future application. This is an exciting field of research, and new breakthroughs are expected in the future.

### 3.5. Self-Replication of Supramolecular Assemblies

Cells are basic structural and functional units of life that can grow, metabolize, replicate, synthesize proteins, and move. Inspired by these tiny cells with complex functions, an increasing number of scientists are focused on mimicking simple living cells to achieve specific functions.<sup>531–533</sup> Until now, supramolecular assemblies that are manufactured in a laboratory batch-wise process are commonly used systems for building artificial cells because of their biomimetic properties such as similar membrane structure and a confined space limited by a membrane.<sup>534</sup> Self-replication is one of the most important properties in living organisms. During the replication process in cells, DNA is replicated and the parent cell divides into two daughter cells. Therefore, to appropriately form artificial cells and close the life cycle loop using supramolecular assemblies, the highly complex function of self-replication must be mimicked.<sup>535,536</sup> The ability to achieve automatic self-replication of highly monodisperse biologically inspired systems would allow for the development of systems that are not limited by either operator or processing factors but instead by the availability of raw material. However, such property of cells is not trivial. Self-replication, key to artificial cells, is indeed a function with a higher level of complexity compared to other functions such as transport, catalysis, or motion and thus is essential for the mimicking of cells. Self-replication in assembled systems have been classified into two main types: genetic replication<sup>537,538</sup> and compartmental replication.<sup>539,540</sup> Genetic replication implies that genome DNA or RNA can be amplified or replicated in the confined compartments of supramolecular assemblies. Compartmental replication however denotes that the membrane of assembled systems grows and then divides into two separated entities, similar to the biological process of cells division. In our review, we mainly focus on the self-replication of self-assembled systems. Polymersomes with their intact and stable bilayer membrane are not suitable for the formation of self-replicating artificial cells. This property indeed requires the implementation of structures that, unlike those used in transport and catalytic reactions, have some degree of instability. Therefore, compartments assembled from phospholipids-(liposomes) can easily grow through (1) the external supplement of their membrane components,<sup>541</sup> (2) the in situ catalytic synthesis of fatty acid<sup>542</sup> and/or lipid,<sup>543</sup> or (3) their fusion with other vesicles or micelles.<sup>544–546</sup> After their growth, their membrane structure becomes unstable and the compartment divides into two or more daughter vesicles. In order to visualize the process of growth and division in real time, fluorescent dye is loaded into the membrane of vesicles as a tracer.<sup>547</sup> In this way, the mechanism by which fatty acid vesicles and liposomes grow and divide is well-monitored. Here we show two examples of self-replicated supramolecular assemblies. A first successful attempt of compartmental self-replication was reported in 2009 by Szostak et al. Multilamellar oleate vesicles loaded with dye 8-hydroxypyrene-1,3,6-trisulfonic acid trisodium salt (HPTS) have been prepared, and their ability to grow

into tubular-like structures by adding fatty acid based micelles due to faster increase of surface area than that of volume was confirmed.<sup>539</sup> These tubules were further shown to divide into multiple daughter vesicles without any leakage of their internal content by shear force. Upon RNA encapsulation, daughter vesicles were found to also encapsulate RNA molecule, and the process of self-replication was repeated over several cycles. However, this system did not achieve the final goal of synthesizing complete protocells with simultaneous self-replication of both genome and the compartment. To succeed both the self-replication of the genetic replication and compartmental replication, Sugawara and his co-workers encapsulated DNA polymerase, DNA, and a polymerase chain reaction (PCR) component in the cavity of giant liposomal vesicles made by zwitterionic phospholipid, positively charged membrane molecule, anionic phospholipid, and amphiphilic acidic catalyst.<sup>536</sup> As depicted in Figure 51, the replication of

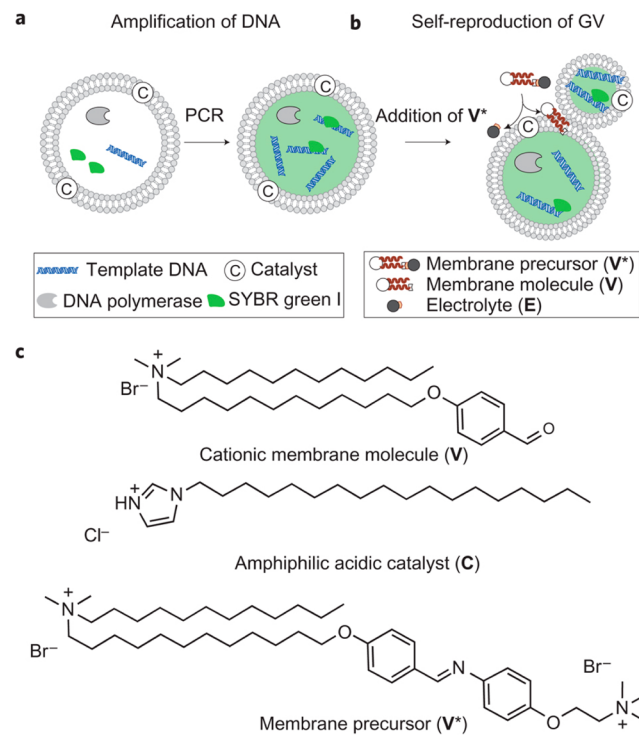


**Figure 51.** Schematic representation of artificial cells that can amplify DNA and self-reproduce compartment. (a) Self-replication of DNA within a giant liposome. Template DNA, DNA polymerase, and SYBR green I were encapsulated in the cavity of liposomes. And membrane precursor catalyst was incorporated into the membrane of liposomes. (b) Compartmental replication of giant liposomes after addition of membrane precursor. Membrane precursors can be transferred to lipids due to the catalysis. (c) Chemical structures of cationic membrane lipid V, precursor catalyst C, and membrane precursor V\*. Reprinted with permission from ref 536. Copyright 2011 Nature Publishing Group.

DNA has been shown to take place in the cavity by PCR. After the addition of lipidic membrane precursors, the acidic catalyst in membrane of liposomes cleaved the terminal moiety of precursors converting them to lipid molecules that was further incorporated into the membrane, leading to the growth of liposomes. Cationic membrane accumulated around the formed DNA because of the electrostatic interaction between polyanionic DNA and cationic membranes, which further induced the compartmental replication of the liposomal

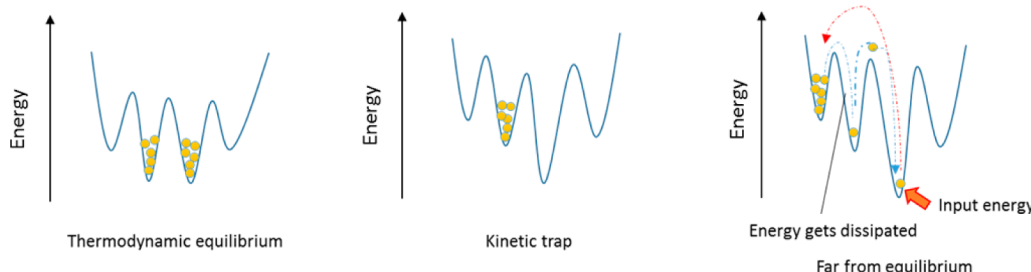


**Figure 52.** Thermodynamic regimes of a chemical system, including thermodynamic equilibrium kinetic trap and far from equilibrium. Adapted with permission from ref 555. Copyright 2015 Nature Publishing Group.

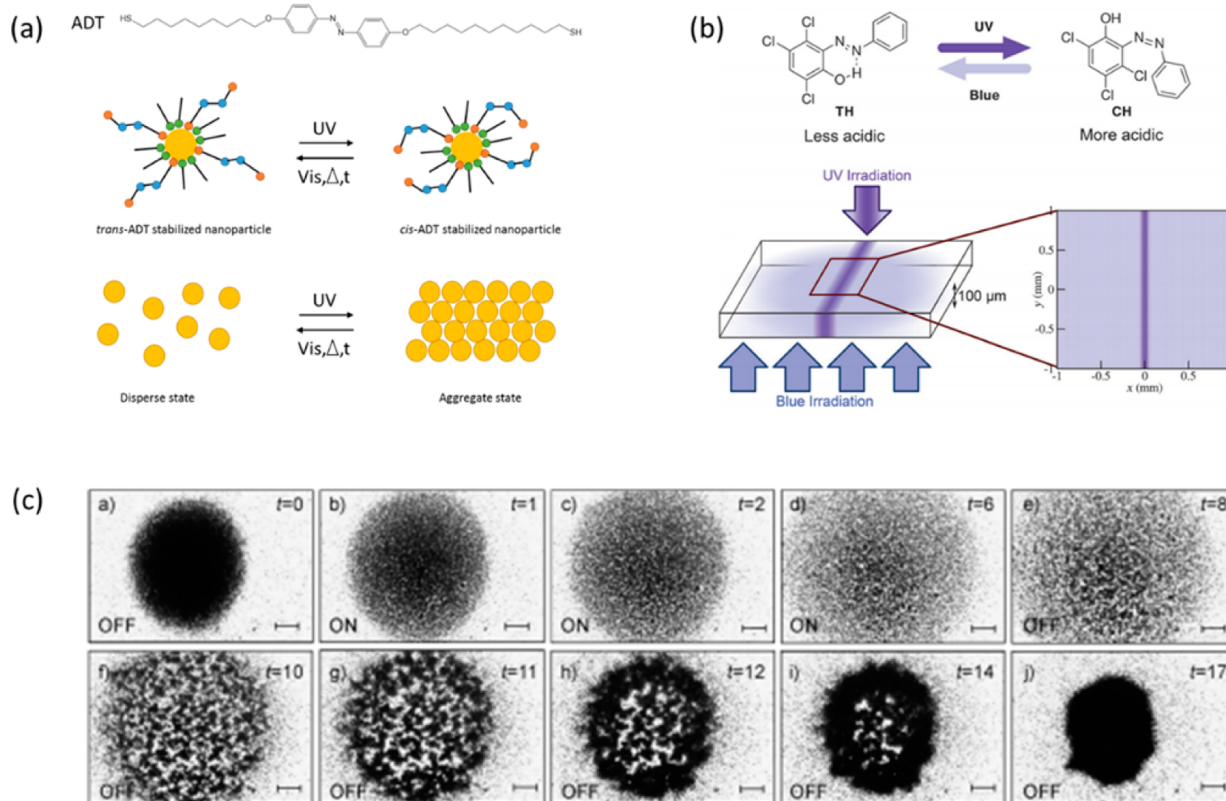


**Figure 53.** Far-from-equilibrium supramolecular systems driven by light irradiation. (a) Gold nanoparticle stabilized with dodecylamine (DDA) and a small amount of azobenzene dithiol ligands (ADT) can transfer from homogeneous suspension state to crystal state via UV light illumination due to cis-trans transition of ADT. In the absence of UV light either by visible light irradiation, heat ( $\Delta$ ), or spontaneously over time ( $t$ ), cis-ADTs relax back to trans conformation and the self-assembled crystals fall apart. (b) Phenol molecule solution presents acidity when exposed to them under UV irradiation due to trans to cis isomerization of the molecules. The acidity will be decreased when cis molecules diffuse to blue light irradiation region, creating a pH gradient. (c) A large school of AgCl particles previously exposed to UV light are observed under visible light with variation of time. Scale bars: 20  $\mu\text{m}$ . Adapted from ref 557. Copyright 2007 National Academy of Science U.S.A. Reprinted with permission from refs 559 and 480. Copyright 2012 and 2009, respectively, Wiley-VCH.

vesicles. This confirmed the synergy between the replication of genomic information and division of liposomes. During the compartmental division, replicated DNA was distributed into the cavity of daughter liposomes by the action of electrostatic interactions. Nevertheless, the catalysts for lipid synthesis and DNA reproduction were not able to replicate in this system. Therefore, self-replication stopped after several cycles due to the effective lower level of the precursor catalyst and polymerase after several divisions of liposomes.<sup>548</sup> It is therefore essential that DNA or RNA molecule can catalyze the synthesis of membrane components so that amplified DNA or RNA in newly formed vesicles can still facilitate the growth and division when sufficient membrane precursors are added. As presented

here, mimicking this fundamental function of cells and designing a real self-replication of bottom-up synthetic supramolecular assemblies is still in its infancy and many challenges are still ahead.

#### 4. DYNAMIC INTERACTION AND SELF-ASSEMBLY

##### 4.1. Far-from-Equilibrium Self-Assembly

Cellular assemblies, such as cell membranes, ribosomes, and nucleic acid transcription machineries, are formed and carry out their complex functions by relying on energy input.<sup>549–552</sup> Continuous free-energy consumption maintains the activities of complex biological supramolecular machineries and thus enables cells to function properly.<sup>553</sup> Inspired from the

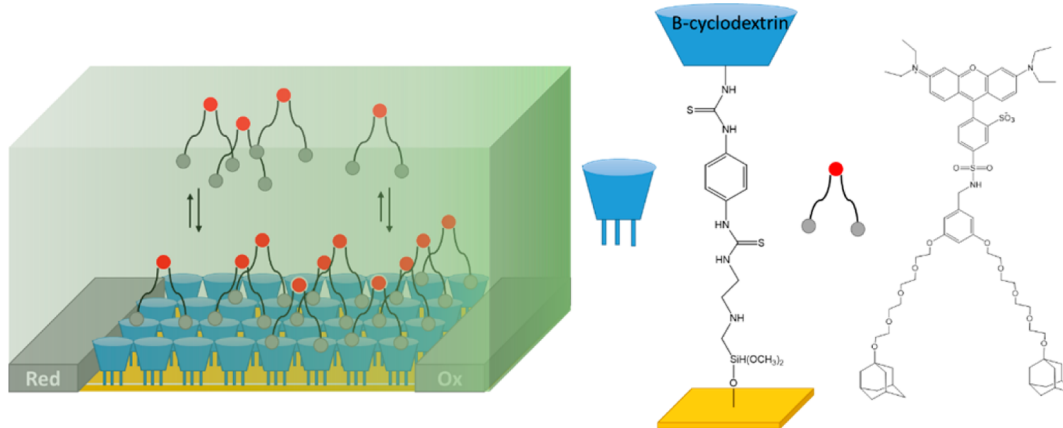


**Figure 54.** Schematic of the dynamic self-assembly system out of equilibrium.  $\text{Ad}_2$ -rhodamine molecules dynamically coordinate with  $\beta$ -cyclodextrins with a tunable efficiency along the electrical gradient. Adapted from ref 560. University of Twente.

organization process and energy flow in the cell system, scientists extended their interests from mimicking the functions obtained via static assembly processes to a more unpredictable dynamic system that develops structures and functions only when dissipating energy, which is of particular interest for studying complex behavior.

**4.1.1. Definition of Self-Assembly Far-from-Equilibrium.** The difficulty in indicating that a certain structure has been assembled far-from-equilibrium can be shown by the number of structures that have been reported in the literature as thermodynamically stable. It is clear that the frame of reference used by each research group or discipline to define far-from-equilibrium systems is not unified. Critically the definition of dynamic self-assembly depends on the selected frame, as the definition of motion that is observed by attaching a frame of reference to a body and measuring its change in position relative to that frame. At the intra molecular level, dynamic interaction/motion exists between various noncovalent bonds such as hydrogen bonds and coordinative bonds. However, in most cases, the selected frame for the definition of a dynamic process is the whole system based on energy flow, as reported by Whitesides.<sup>554</sup> In this context, here the whole system is chosen as the observing reference frame to define dynamic self-assembly. In a recent review paper, Otto et al. distinguished three thermodynamic states of a chemical system, as (1) equilibrium assemblies, (2) kinetically trapped assemblies, and (3) far-from-equilibrium self-assembly, as shown in Figure S2.<sup>555</sup> Dynamic systems that are far-from-equilibrium need continuous energy input to maintain the system function without disruption. The trapped state in dynamic system is largely undeterminable and depends on the balance between the rates of material formation and degradation, whereas thermodynamic equilibrium and most kinetically trapped systems are easily predictable and reach their final states. However, it is important to mention here that some kinetic trapped systems in a relative stable transition state are also able to be designed as a dynamic system.<sup>556</sup> From an experimental design point of view, the crucial challenge is the selection of a suitable energy source for maintaining the system far from equilibrium. Herein, we classify the selected examples from energy sources point of view, including light, electricity, magnetic field, and chemical fuel.

**4.1.2. Light as Energy Source.** One of the most famous examples for assemblies far-from-equilibrium was given by Grzybowski et al. and is composed of gold nanoparticles (NP,

5.6 nm in diameter) decorated with azobenzene dithiol ligands [4,4'-bis(11-mercaptopoundecanoxy)azobenzene (ADT)] and stabilizer [dodecylamine (DDA)].<sup>557,558</sup> At certain conditions, gold NPs with a low number of adsorbed ADT ( $\sim 20$  per NP) organize into three-dimensional crystals and stay stable under continuous UV-irradiation. Interestingly, when the UV light is turned off, the formed crystals disassemble and disperse again in the solution. The whole cycle takes a short time ( $\sim 10$  min) with good repeatability (Figure 53a). The authors believe that the binding energy of stabilized NPs is slightly greater than the thermal energy disrupting the aggregate. Therefore, when the UV light induced the cis-trans transition of ADT, the NP binding energy was weakened, leading to the disintegration of the crystals. In this system, UV light provides continuous energy support that keeps the crystal structure and dissipates the energy during the aggregate state, which can be seen as a far-from-equilibrium state. Without this continuous transformation, the assembly falls apart to a disperse state.

In another example provided by Jullien et al.,<sup>559</sup> a tunable proton gradient was designed via switching UV and blue light on a thin solution layer containing photoacid [(2-hydroxy-3,5,6-trichlorozaobenzene ( $\text{THCl}_3$ ))] and fluorescent pH indicator.  $\text{THCl}_3$  changed its structure from a trans-stereoisomer (less acidic,  $pK_a = 9.4$ ) to a cis-stereoisomer (more acidic,  $pK_a = 6.6$ ) via UV light induction. In a UV illuminated area, cis-stereoisomer  $\text{THCl}_3$  is the main product generating an acidic region. The acidic fluorescent pH indicator can be excited at a low pH to result in a fluorescent line. In contrast, other places under blue light illumination do not fluoresce because high proton concentration prevents the excitation of the pH indicator. In this designed system (Figure 53b), no conventional non-covalent supramolecular assemblies are formed; however, a long-range supramolecular structure is built-up based on the acid–base reactions and the diffusion process due to the pH gradient. Continuous supplement of UV energy maintains the existence of the proton gradient until reaching saturation of the most stable isomer. This can also be deemed as an energy storage process. A proton-consuming reaction is built up as another energy-transfer chain in this system, which releases the energy through chemical reaction. The chemical gradient is crucial for biological systems, maintaining the energy exchange and creating new units. This model provides a tool for understanding simple energy transfer in a complex system, such as cells.

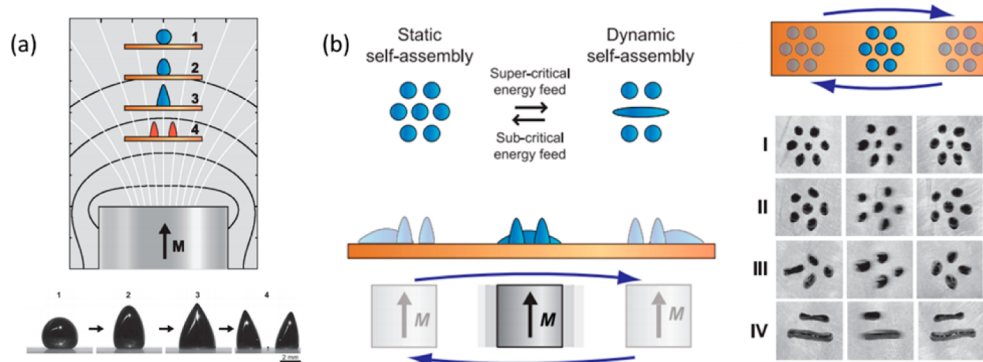


**Figure 55.** (a) Schematic side-view of the magnetic field geometry of a cylindrical permanent magnet and photographs of ferrofluid droplet separation. (b) Scheme of the switching, and photographs of dynamic patterns with the change of driving field. Reprinted with permission from ref 567. Copyright 2013 American Association for the Advancement of Science.

Dynamic schooling behavior of AgCl particles in water induced by UV light was reported by Sen et al.<sup>480</sup> Tight-packed AgCl particles were found to disperse automatically with large interparticle spacing under exposure to UV light. The dispersed particles school together again to reform an even tighter aggregate, when UV light is turned off. This phenomenon can be repeated over many cycles, when switching between the UV and visible light while the magnitude of the gradient is dependent on the concentration of the ions in the bulk solution (Figure 53c). The suggested mechanism is the formation under UV exposure of local ion gradients surrounding the individual particles leading to phoretic repulsive forces between individual particles. When visible light is switched on, the ion gradients decrease, allowing the AgCl NPs to pack tighter. In this dynamic assembly system, UV light provided continuous energy input, causing an ion gradient surrounding AgCl NPs to expand the interparticle spacing. At this far-from-equilibrium state, switching UV light to visible light, the NPs school again with weak energy consumption.

Considering the extreme unpredictability and complexity of self-assembly far-from-equilibrium system, the real applications of these systems have been underinvestigated so far. However, biological systems have operated in a dynamic far from equilibrium state for billions of years utilizing energy in the form of sun light to drive them, we believe this is one of the most promising systems for understanding the origin of life and creating new functional materials, like light-sensitive ink.

**4.1.3. Electricity as Energy Source.** Electric energy is commonly used in chemical reactions. A chemical concentration gradient can be created between two electrodes, providing thus the possibility to create a far-from-equilibrium system. One designed system (Figure 54) consists of  $\beta$ -cyclodextrins as a multivalent receptor interface, placed between two electrodes of an electric device, and Ad2-rhodamine (a fluorescently modified adamantane guest), as a multivalent guest competing for coordination with a competitor ferrocene carboxylic acid. Ferrocene carboxylic acid can be oxidized to its corresponding cation at the anode, losing its coordination property.<sup>560</sup> On the contrary, at cathode ferrocene carboxylic cation is reduced to acid, which can compete with Ad2-rhodamine to coordinate with  $\beta$ -cyclodextrins. When electric current is switched on, a chemical gradient is generated, leading to a host–guest dynamic interaction. The system turns back to equilibrium when the current is switched off. From the whole system perspective, long-range supramolecular order in the form of concentration gradients is far-from equilibrium. Due to

the high degree of control over electricity powered devices, systems built up with electricity as energy source might give a chance for accurate study of the dynamics of self-assembled processes and fabricate advanced materials at the micro/nanometer level, such as ion-gradient-controlled microgel.

**4.1.4. Magnetic Field as Energy Source.** Magnetic field is regularly used to design dynamic self-assembled and self-organized systems in magnetic materials.<sup>561–563</sup> Millimeter-sized disks floating at the liquid–air interface were shown to assemble into various patterns by tuning the rotating rate of the external magnetic field.<sup>564</sup> Similar phenomenon was also observed by tuning the interface forces with different organic solvents and surfactants.<sup>565,566</sup>

An important work from Timonen et al. has succeeded in bridging the gap between static and dynamic self-assembly. In this case, the magnetic field is applied on a model system containing ferrofluid droplets and superhydrophobic surfaces making sure the droplets are not physically connected.<sup>567</sup> One droplet from the aqueous ferrofluid placed on the superhydrophobic surface deforms and divides into smaller daughter droplets when the droplet is subjected to confining critical field strength from a cylindrical permanent magnet placed underneath the substrate (Figure 55). This division process only occurs when the droplet is exposed in both high magnetic field and high vertical magnetic field gradient. The droplets do not coalesce back after switching off the static magnetic field. Dynamic self-assembly occurs when the continuous energy feed is provided to keep the system away from the energy minimum and relies on low friction and energy dissipation. At low-energy feed rates, the droplets pattern move with the oscillating magnet as a whole, rendering the energy at a minimum state. When the energy feed rates are, however, increased above a certain level, the droplets start to coalesce to form elongated droplets and/or regular circular droplets due to the short distances between the droplets. Thus, in this system, the external trigger is the dynamic magnetic force. Once the magnetic field is switched on, it is impossible to determine the exact state (e.g., the shape of the pattern) of the system. Switching off the magnetic field, the patterns decay back to the predictable static pattern. Potential applications of magnetic systems lie not only on the fundamental understanding of the dynamic self-assembled process, but also on functional pattern design. Moreover, in this system, magnetic molecules might assemble to unexpected structures with diverse morphologies.

**4.1.5. Catalytic and Fuel Consuming System.** Catalysts are usually used to change the reaction route and to decrease

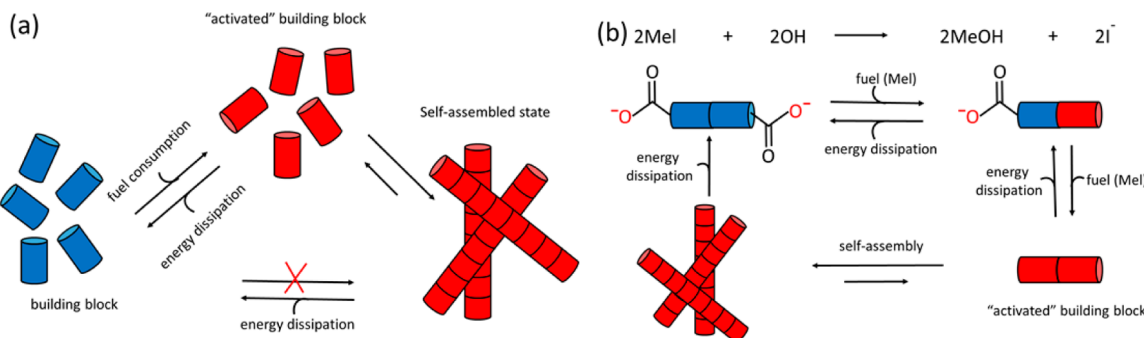


**Figure 56.** (a) The strategy of building dissipative self-assembly gel system. Building blocks (blue) are activated by fuel consumption and are able to assemble into fibers (red). The assembled fibers can dissipate its energy and revert to its monomeric state (blue). Once provided with sufficient fuel to start the reaction, fibers will be built and disassembled simultaneously, depending on the energy dissipation rate. (b) Reaction cycle of the dissipative system. MeI as a fuel reacts with DBC dicarboxylate (blue) to get activated DBC-OMe, which can dissipate its energy through hydrolysis to form DBC or continuously react with MeI to form diester DBC-OMe<sub>2</sub> (red). The diester can assemble into fibers, which is dynamically stable until all the MeI has consumed. Adapted with permission from ref 570. Copyright 2010 Wiley-VCH.

the activation energy of the reactions. The catalyst properties and features of a catalytic system facilitate the prospect of designing out-of-equilibrium systems with kinetic control.<sup>568</sup> A low-molecular-weight gel has been synthesized with kinetically controllable structure and mechanical properties by means of catalytic reaction.<sup>569</sup>

The design of chemically consuming self-assembly fibrous hydrogel is based on the fact that the rate of energy dissipation is lower than the consumption of fuel to form self-assembled architectures (Figure 56). Esch et al. reported a dynamic self-assembled fibrous network obtained by continuous methylation of a carboxylate acid gelator precursor by reaction with a chemical fuel methyl iodide.<sup>570</sup> The acid precursor (dibenzoyl-(l)-cystine, DBC) is a nonactivated building block due to the electrostatic repulsion. After being activated by methylation, the obtained monomer DBC-OMe can either be hydrolyzed back to DBC or react with fuel again to form diester DBC-OMe<sub>2</sub>, which has the ability to self-assemble into fibrous structures. These fibers are not stable and in equilibrium between fiber formation and hydrolysis of diester. When all the fuel is consumed, the fibers fall apart. In this system, gel state and solution state can be cycled by controlling the amount of methyl iodide, without which the formed gel will disassemble.

Therefore, the whole system is considered as a far-from-equilibrium system. Recently, the same group designed a spatially and directionally controlled supramolecular hydrogel system though catalytic micropatterned surfaces.<sup>570</sup> The surface-bounded catalyst locally enhances the concentration of the activated building block, which leads to the continuous assembly of fibers near the surface, as long as the self-assembly process is faster than diffusion. The assembled fibers networks can entrap solvent around them to form hydrogels when they are above their critical gelation concentration. The gel property (stiffness) and sol–gel transition can be tuned *in situ* by acidic or nucleophilic catalysis, and it is impossible to stop the gel formation reaction at a specific energy state. Thus, this gel system can be defined as a far-from-equilibrium system.

Another similar hydrogel system based on peptide nanofibers displaying dynamic instability and far-from-equilibrium features has been designed by Ulijn et al.<sup>571</sup> This system is built on naphthalene-dipeptide structures as an activated building block obtained from the transacylation reactions via biocatalyst, meanwhile thermolysin catalyzes a reversible hydrolysis reaction of the peptide. These transacylation and hydrolysis reactions

formed a competitive system making it difficult to stop the reaction at a desired state. The lifetime of the gel can be tuned by parameters such as the enzyme concentrations.

By mimicking the reversible self-assembly from nature, Bhatia et al. designed a nanoparticle system containing two types of nanoparticles and enzymes.<sup>572</sup> One type of nanoparticles was modified with peptide substrates that can be phosphorylated by tyrosine kinase and dephosphorylated by a phosphatase. The other type of nanoparticles with Src Homology 2 (SH<sub>2</sub>) domains can recognize and bind the phosphorylated kinase substrate in a sequence-specific fashion. The self-assembly is dynamically coupled to the balance between these antagonism enzymes: tyrosine kinase and phosphatase. In this system, ATP is a fuel that support phosphate groups to substrate nanoparticles by kinase transferring, which in turn triggers the assembly of the nanoparticles via phosphopeptide-SH<sub>2</sub> binding. The aggregates then disassemble when running out of fuel or with a high concentration of phosphatase-removing phosphates. Another biorelated example from Dambenieks and Fyles is a mimetic membrane transport system via dissipative assembly, which is kinetically controlled though the provision of a chemical fuel (Figure 57).<sup>573</sup> Briefly, two oligoesters, one highly active as a membrane transporter and one inactive in the self-assembly of the pore have been used for the design of the dynamic out-of-equilibrium system. A fast intermolecular thiol-thioester exchange reaction allows the transition between the two forms in the presence of fuel, followed by a slow intramolecular degradation of the active ester to release the inactive thiol form and a side cyclic lactam or lactone. As in other examples, designing such dynamic self-assembled systems proved to be challenging, especially in terms of prediction of their function.

Catalytic and fuel consuming systems may be the most promising systems to design and fabricate real usable materials via dynamic self-assembly. For example, hydrogels assembled from fibers built up by small molecules are expected to perform self-healing and shape switchable behaviors, which are stimuli responsive with chemicals as well. This might be the closest way to fabricate a totally artificial intelligent material.

## 5. CONCLUSION AND PERSPECTIVE

The complex structure of biological systems fascinated scientists and led to many efforts in mimicking their architectures. However, the crucial outcome of the self-assembly in nature is

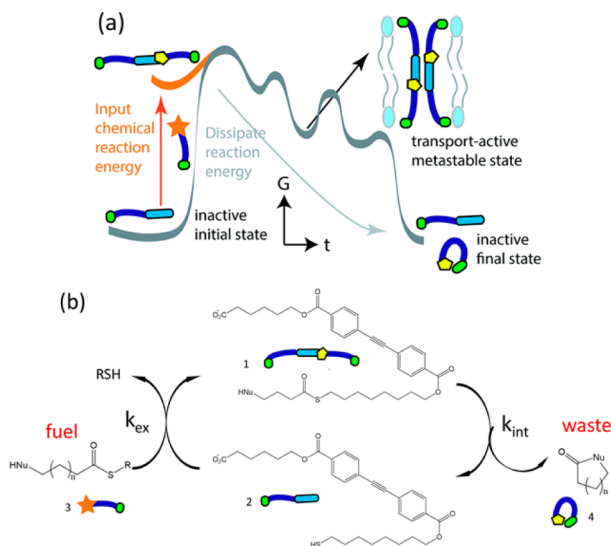


**Figure 57.** Design of dissipative assembly of a membrane transport system. (a) The schematic energy profile and (b) the implementation design. Reprinted with permission from ref 573. Copyright 2014 Royal Society of Chemistry.

not so much the structure but more importantly the function. These structures are complex systems that cannot be analyzed in isolation and they rely on interaction and communication with their environment. Biological systems adapt, self-control, and self-heal and are continuously evolving. They are “more than the sum of their parts”.

This review attempted to look at functions of supramolecular assemblies from a biomimetic/bioinspired point of view taking inspiration from one of the basic building blocks of life: the eukaryotic cell.

### 5.1. Toward Artificial Cell

In previous sections, major achievements on natural functions with inspiration and similarity to bioinspired structures has been summarized. Among the progress made, mimicking morphologies and properties of cell with artificial building blocks is a hot topic in the field of bioinspired self-assembled structures and represents a future direction concerning biorelated application. Following is a brief description of the efforts made for the construction of artificial cells. Different approaches are described and compared. Artificial cells/synthetic cells are engineered to mimic structures or functions of the natural cells. In general, these approaches involve constructing cell-like compartments with enclosing enzymes/genes to mimic certain functions of natural cell such as metabolism, growth, and reproduction, the three characters of living system. With reengineered genetic sequence and materials, the functions are not necessarily limited to current existent functionality of biological cells. With possibilities envisaged by synthetic materials, artificial cells with designed structure and properties could be created. While most current constructs are still distant from a fully operational cell, these represent watermarks on the roadmap toward fully operational cells.

A great step toward artificial cells is constructing a complete DNA gene sequence and incorporating the genome into a recipient vesicle. By redesigning a DNA sequence, which contains complete information for biological maintenance and reproduction, Venter and co-workers achieved construction of minimal cells. With digital genetic information, they kicked out genes of a living species *M. mycoides* bacteria to 1.08-mega-base pair genome, which was considered to be the minimal required for life and transplanted the genome into a gene empty *M. mycoides* cell. Through this approach they created a new strain of Mycoplasma mycoides (**Figure 58**). This system was expected to lead to the creation of a strain with desirable cell

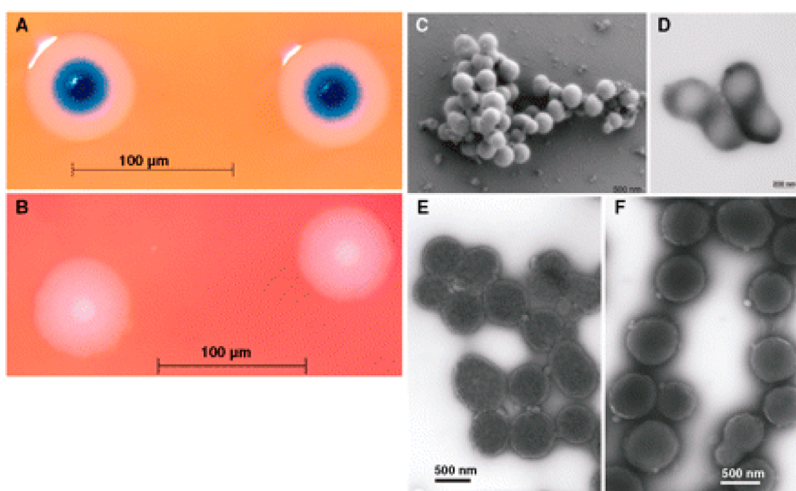


**Figure 58.** Images of *M. mycoides* JCVI-syn1.0 and WT *M. mycoides*. To compare the phenotype of the JCVI-syn1.0 and non-YCp WT strains, colony morphology was examined by plating cells on SP4 agar plates containing X-gal. Three days after plating, the JCVI-syn1.0 colonies are blue because the cells contain the lacZ gene and express  $\beta$ -galactosidase, which converts the X-gal to (A) a blue compound. (B) The WT cells do not contain lacZ and remain white. Both cell types have the fried egg colony morphology characteristic of most mycoplasmas. EMs were made of the JCVI-syn1.0 isolate using two methods. (C) For scanning EM, samples were postfixed in osmium tetroxide, dehydrated and critical point dried with CO<sub>2</sub> and visualized with a Hitachi SU6600 SEM at 2.0 keV. (D) Negatively stained transmission EMs of dividing cells with 1% uranyl acetate on pure carbon substrate visualized using JEOL 1200EX CTEM at 80 keV. To examine cell morphology, we compared (E) uranyl acetate-stained EMs of *M. mycoides* JCVI-syn1.0 cells with EMs of WT cells made in 2006 that were stained with (F) ammonium molybdate. Both cell types show the same ovoid morphology and general appearance. Reprinted with permission from ref 574. Copyright 2010 American Association for the Advancement of Science.

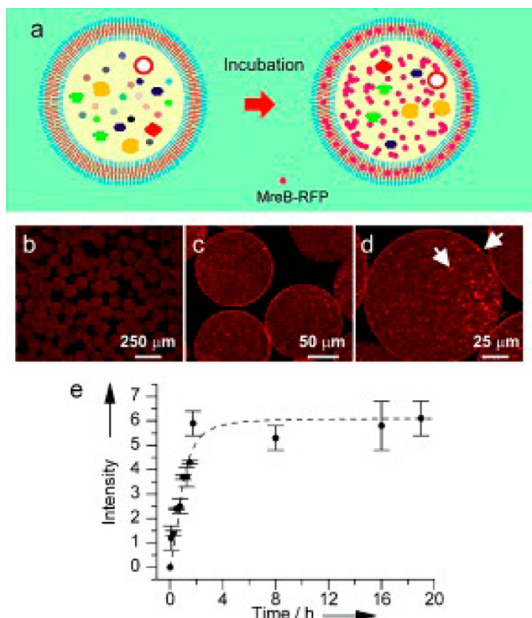


**Figure 59.** MreB-RFP expression in polymersomes. (a) Schematic illustration of a polymersome containing the cell-free protein expression solution. After 2 h of incubation at 32 °C, the MreB-RFP protein is produced (red spots). (b–d) Confocal microscope images at different magnifications of reinforced PEG-b-PLA polymersomes after 3 h of incubation. Arrows indicate the formation of polymerized MreB-RFP patches dispersed in the inner phase and the adhesion of the protein on the membrane. (e) Fluorescence signal over time owing to protein expression in polymersomes. Reprinted with permission from ref 579. Copyright 2012 Wiley-VCH.

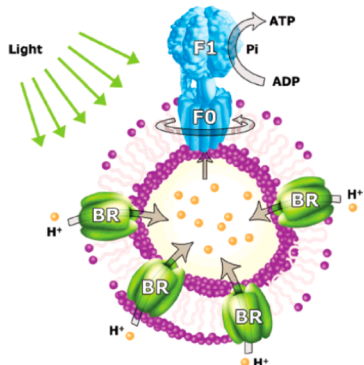


**Figure 60.** Schematic representation of proteopolymersomes reconstituted with both BR and F0F1-ATP synthase. ATP synthase uses an electrochemical proton gradient generated by BR to synthesize ATP from ADP and inorganic phosphate (Pi). Reprinted from ref 581. Copyright 2005 American Chemical Society.

functions.<sup>574</sup> Although not fully synthetic, this approach is of great significance as a first step toward artificial cells. Furthermore, since it is a top-down approach, the complicated signaling and cascade network is not well-understood. The methodology is also not completely synthetic as both cytoplasm and the cell membrane were from a host cell. From this aspect, the correlation between minimal genome and minimal cell is not that direct. Therefore, further reduction of genome complexity and cellular content is required. The distance of this type of artificial cell from fully operational cells also gives rise to concerns about potential harm to human species with unlimited duplication. However, as the timescale of genetic

materials and vesicle materials duplication may not be the same, or replicating with exactly the same genetic materials and lipid shells is not ensured with most current artificial cells, the fate of “death by dilution” is anyway unavoidable. In this scenario, the self-replication for several generations followed by death by dilution brings up both ethical issues and the concerns about hazards of species/strains with uncontrollable reproduction.

A similar type of artificial cell, corresponding to evolution, is the RNA-containing artificial cell. By incorporating Q $\beta$  replicase, which could replicate RNA template in liposome, Luisi et al. developed a system capable of achieving self-reproduction for several generations. Notably, the outside vesicle shell also underwent replication if not synchronously. The system, however, could not replenish the Q $\beta$  replicase, leading to the absence of Q $\beta$  replicase in new generation, thus death by dilution.<sup>537</sup>

Another proposed approach was to build up the system entirely from nonliving building blocks (bottom-up approach). Such synthetic cells contain a fully synthetic membrane in comparison to the other systems where a natural lipid bilayer is present. Synthetic liposomes, polymersomes, micelles, and proteinosomes containing either a single layer or double layer membrane are able to encapsulate bioactive molecules. By tuning the membrane composition or by incorporating biological molecules, membrane permeability is varied, allowing for macromolecules, ions, and energy exchange between the enclosed entity and the environment.

As the closest analogues of natural cell membranes, vesicles made of phospholipid, fatty acid, and synthetic lipids could allow for dynamic component exchange; however, they are less robust compared to polymeric vesicles. Difficulty in functionalizing them remains a hurdle for this type of membrane. Polymer-based membranes are, however, more tough and resistant as polymer molecules are typically entangled and of higher molecular weight. This brings, however, disadvantages such as low permeability, which could inhibit the exchange between the inner “water reservoir” and the outer environment. The relatively low membrane permeability requires the addition of all the components to be encapsulated at the formation of vesicles step, while natural cells allow the continuous entrance of nutrients and outflux of waste. Functional transmembrane protein such as Na/K-ATPase ion channels incorporated into the polymer membranes offers a solution. Meier’s group inserted a channel protein OmpF into the polymer membrane and showed that  $\beta$ -lactamase enclosed in the membrane could catalyze the hydrolysis of the substrate that was able to pass through the protein channel.<sup>575</sup> Noireaux et al. demonstrated another biomimetic system by coexpressing  $\alpha$ -hemolysin along with GFP.<sup>576</sup> The water-soluble hemolysin was shown to self-assemble into the heptamer in the vesicle membrane followed by the formation of a 1.4 nm pore. In this way, the increased membrane permeability ensured long-term expression of GFP for up to 4 days. Naturally occurring protein or recombinant proteins were also part of the membrane composition of the artificial cells. The recombinant protein was expected to ensure monodisperse self-assembly systems as well as offering the possibility of readily functionalization. Hammer et al. demonstrated the formation of vesicles with recombined protein oleosin. Superstructures of the recombined protein could be tuned by varying the ionic strength and pH.<sup>577</sup> The usage of protein in the membrane composition is of great interest as the incorporation of gene expression and protein

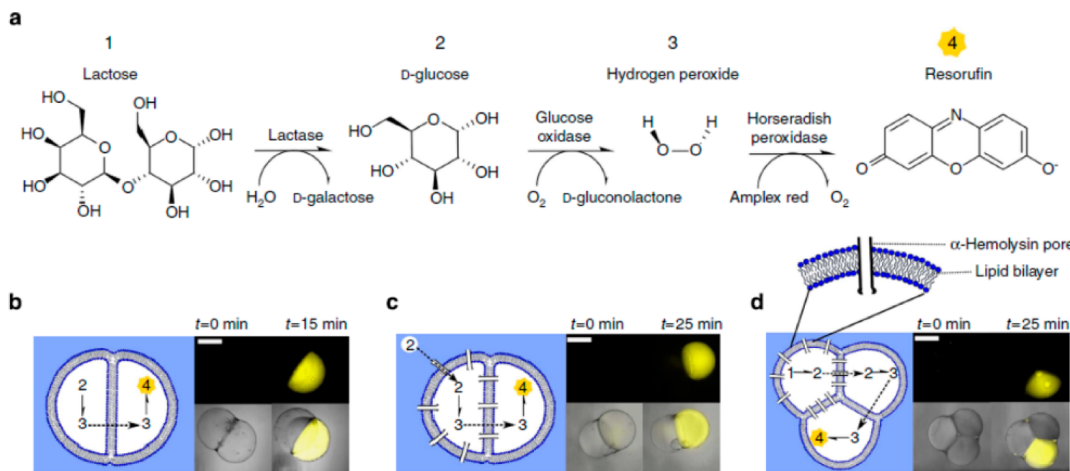


**Figure 61.** Spatially segregated reaction sequences in multicompartiment vesicles. (a) Multistep enzymatic pathway scheme. (b–d) Schematic of the three vesicle systems that were generated, together with fluorescence and composite images of representative vesicles at the start and at the end of the reaction. Brightness and contrasts enhanced equally across all images. Scale bar, 250 nm. Graphs showing fluorescence intensity of the Amplex Red containing compartment show the dye being oxidized to fluorescent resorufin as the reaction proceeds. (b) Glucose is oxidized, producing hydrogen peroxide, which translocates through the bilayer to initiate the oxidation of Amplex Red. (c) Glucose diffuses in from the exterior, through α-HL pores, to initiate subsequent reaction steps. This represents a simple sense/response network. (d) The full three-step reaction cascade where each step is isolated in a single compartment. Lactose is first hydrolyzed to glucose, which then translocates through the bilayer to initiate subsequent steps as before. Reprinted from ref 582 under a Creative Commons Attribution 4.0 International License.

production inside would possibly give rise to membrane regeneration, crucial to artificial cell reproduction.

Bioactive molecules can also be incorporated within the synthetic membrane. Detailed discussion has been covered in the previous compartmentalization and transport section of this review. By encapsulating hormones, enzymes, proteins, and genes, the particles could be used for replacement or supplementary therapy. This is particularly important for metabolic diseases, caused by underexpression, overexpression, or malfunction of enzymes; the artificial cell is promising by locating enzymes and genes inside the vesicles and delivering them. By encapsulating hemoglobins into lipid vesicles, the structure could also act as artificial red blood cells and perform oxygen delivery. Furthermore, the usage of artificial cells for gene therapy could circumvent the danger of inducing immune response with viral vectors.<sup>578</sup>

From delivering a single enzyme/gene, advances have been made toward exploring the function and signaling/coupling between synthetic cells. Weitz's group incorporated *E. coli* ribosomal extract and MreB DNA plasmid into a biodegradable PEG–PLA polymersomes.<sup>579</sup> By expressing a MreB-RFP fluorescent fusion protein, it was demonstrated that the MreB cytoskeletal protein was expressed within a few hours and its adherence to the membrane was observed (Figure 59). It was hoped this would lead to the formation of a functional cytoskeleton network inside the synthetic vesicle and achieve possible vesicle polarization and motion. Importantly, in this attempt, the PEG–PLA vesicles were fabricated with a microfluidic approach, allowing the production of vesicles with highly homogeneous content.

It is the chemical cascades that made possible autonomous motion, communication, and replication of cells. A network of constantly interplayed reactions also enables the maintenance of the cell equilibrium. Thus, cooperation between artificial cells and interplays of cascades inside artificial cells are explored. It was reported that GFP expression could be accomplished by fusion of different component-containing vesicles or solute exchange.<sup>580</sup> Driven by protons generated via light activated

bacteriorhodopsin, ATP synthase incorporated into polymer vesicles could produce high-energy phosphates<sup>581</sup> (Figure 60). This not only provided an example of sophisticated signaling networks achievable within artificial cells but also represents a leap toward a self-sustaining artificial cell.

Constructing artificial cells via a bottom-up approach using the toolbox provided by supramolecular chemistry sheds light on the essence of the origin of life<sup>582–584</sup> (Figure 61).

While compartmentalization, catalysis, transport, motion, and collective movement are bioinspired functions that have been extensively mimicked, endogenous synthesis of membrane materials and replication of nongenetic materials remains challenging. Luisi et al. reported the production of lethicin within lethicin liposomes.<sup>585</sup> Sugawara et al. discovered that amplification of anionic DNA could induce the division of cationic vesicles.<sup>586</sup> However, self-synthesis and replication of polymer membranes in general are a complicated task, and new approaches are required to achieve these goals.

## 5.2. Outlook

Cellular structures are one of the basic building blocks of life: a collection of complex systems that have inspired many scientific disciplines to design synthetic structures that can mimic both their structures and functions. In this review, recent accomplishments in bioinspired self-assembly research have been highlighted with emphases on bioinspired functions from the cell. Significant progress in the field of self-assembled micelles and vesicles with bioinspired functions such as compartmentalization, transport, catalysis, motion, and self-replication has been made. We predict these fields will continue to be vivid in the coming years. Mimicking complex structures was however more successful over the years; while less progress has been made in mimicking complex functions arising from combining multiple functions into a single machine and even more challenging to mimic both the structure and the function in unison. This is because biological systems are complex systems that are continuously moving, evolving, and very dynamic and, therefore, out-of-equilibrium, while the traditional approach in

supramolecular chemistry was to study the self-assembled systems in equilibrium. Therefore, one of the greatest unresolved grand challenges of supramolecular chemistry is creation of artificial life and complex biological systems that can mimic the complexity of life, in both structure and function. This review tried to convey this message and limit itself in showing examples of bioinspired functions of supramolecular assemblies starting with simple concepts such as compartmentalization to more complex functions, which involve transfer of information, communication, and self-replication.

Furthermore, in mimicking organelles, self-assembled structures provide ideal platforms for retaining cargoes in confined structures for applications on transport/catalysis, as they are more robust and versatile. Research on selective transport with stimuli-responsive systems and ligand/receptor-modified structures will lead to more investigation on how self-assembled structures communicate with its environment as well as how they communicate and interact with each other under out-of-equilibrium conditions. Furthermore, combined research on interactive/communicative structures via catalysis may benefit in the development of bioinspired system colonies. In mimicking motile cells, self-assembled structures demonstrated self-propelled motion by consuming fuel from its environment. Environment change induced by fuel consumption of motor may however influence the behaviors of other motors. This can potentially lead to research on communicative particles. Development of polymer chemistry and biochemistry provides researchers with an increasingly growing toolbox of building blocks, which could potentially meet different demands of mimicking natural prototypes. The list of resulting bioinspired self-assembled structures would be ongoing and exciting. Besides a relatively mature research field, the new branches of supramolecular chemistry such as dynamic and far-from-equilibrium self-assembly and systems chemistry are expected to potentially lead to other emerging properties and eventually to mimic the function of the eukaryotic cell in a minimal life system. While still in an infant stage, examples covered in this review show great promise for application and commercialization of such structures. It is an exciting time in supramolecular chemistry!

## AUTHOR INFORMATION

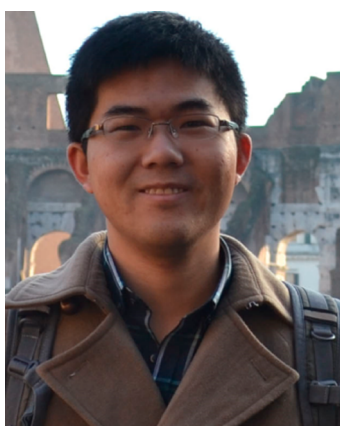
### Corresponding Author

\*E-mail: [D.Wilson@science.ru.nl](mailto:D.Wilson@science.ru.nl).

### Notes

The authors declare no competing financial interest.

### Biographies



Yingfeng Tu received his BSc Degree in Pharmacy from Wenzhou Medical University, China, in 2010 and a Master Degree in Pharmaceutical Science from Peking University in 2013. During the master's program, he focused on drug delivery systems targeting brain tumors using multifunctional liposomal formulations. Currently he is a Ph.D. candidate in the Department of Bio-organic Chemistry at Radboud University, The Netherlands. His research is focused on self-propelled supramolecular motors with stimuli responsive valves for movement control and novel drug delivery.



Fei Peng obtained her Master's degree from Health Science Center, Peking University, China, in 2013. During her Master's program (2010-2013), she carried out research on poly(amidoamine) dendrimers as a multifunctional drug delivery system. She is now a Ph.D. candidate at the Department of Bio-organic Chemistry, Radboud University, and a recipient of a scholarship from the China Scholarship Council. Her research interests concerns self-guided supramolecular polymeric nanomotors for drug delivery.



Alaa Adawy obtained her Bachelor Degree in Biophysics with honours (top of the class) from Faculty of Science, Ain Shams University, Cairo, Egypt. After a first appointment as academic assistant at the Physics Department in the same faculty, with 28 h/week teaching tasks, and completion of her Medical Biophysics Master's program in Biomaterials she was promoted to Assistant lecturer. In 2009, she relocated to Nijmegen, The Netherlands, and conducted her Ph.D. research on crystallization of biological macromolecules at the Institute for Molecules and Materials, Radboud University, under the supervision of Prof. Dr. Elias Vlieg, Prof. Dr. Willem de Grip, and Dr. Willem van Enckevort. Since 2014, she has been a postdoctoral fellow at the same institute. Alaa is interested in conducting research on interdisciplinary topics, and her current research focuses on crystallization in nanoconfined compartments.



Yongjun Men received his Bachelor's Degree in Chemistry in Zhengzhou University, China, in 2007, and his Master's degree in Polymer Chemistry in Beijing Normal University, China, in 2011. Then, he moved to Max Planck Institute of Colloids and Interfaces, Germany, and completed his Ph.D. degree on a topic of poly(ionic liquid)-based thermoresponsive polymers and porous carbon materials under the supervision of Prof. Markus Antonietti and Dr Jiayin Yuan. At present, he is a postdoctoral researcher in the Department of Bio-organic Chemistry at Radboud University, The Netherlands. His current research focuses on the design of intelligent, self-propelled supramolecular assemblies as nanoengineered delivery systems.



Loai K. Abdelmohsen received his B. Sc. Degree in Chemistry and Microbiology from Alexandria University, Egypt. He completed his Master's degree at Radboud University, The Netherlands, in the Departments of Bio-organic and Physical Organic Chemistry. He is currently a Ph.D. student in the department of Bio-organic Chemistry at Radboud University. His current research focuses on designing new biocompatible nanomotor systems that utilize natural substrates for their propulsion.



Daniela A. Wilson (born Apreutesei) received her B.Sc. degree (Hon) in chemistry from "A. I. Cuza" University of Iasi, Romania, in 2001, and an M.S. degree (Hon) in environmental chemistry from the same university in 2003. In 2006, she received her Ph.D. with distinction "summa cum laude" from "Gh. Asachi" Technical University of Iasi, Romania. During her Ph.D. she obtained two fellowships in Japan and the U.K. as an exchange Ph.D. student and Marie Curie fellow. She then worked as a postdoctoral researcher at University of Pennsylvania, Philadelphia, USA, and Radboud University Nijmegen, Netherlands, in the groups of Prof. Virgil Percec and Prof. Roeland Nolte on several topics in synthetic organic chemistry, organometallic chemistry, and supramolecular and polymer chemistry. In 2012, she was awarded an ERC starting grant to investigate nanomotors with autonomous propulsion in biological systems. She is currently assistant professor at the Institute for Molecules and Materials, Radboud University. Her research interests span a broad range of topics at the interface of supramolecular chemistry, macromolecular chemistry, and nanotechnology.

## ACKNOWLEDGMENTS

This work was supported by the European Research Council under the European Union's Seventh Framework Programme (FP7/2007-20012)/ERC-StG 307679 "StomaMotors". We acknowledge support from the Ministry of Education, Culture and Science (Gravity program 024.001.035). F.P. acknowledges funding from China Scholarship Council.

## REFERENCES

- (1) Lehn, J.-M. *Supramolecular Chemistry: Concepts and Perspectives*; Wiley-VCH: Weinheim, Germany, 2006.
- (2) Ruben, M.; Ziener, U.; Lehn, J. M.; Ksenofontov, V.; Gütlich, P.; Vaughan, G. Hierarchical Self-Assembly of Supramolecular Spintronic Modules into 1D- and 2D-Architectures with Emergence of Magnetic Properties. *Chem. - Eur. J.* **2005**, *11*, 94–100.
- (3) Vriezema, D. M.; Comellas Aragón, M.; Elemans, J. A.; Cornelissen, J. J.; Rowan, A. E.; Nolte, R. J. Self-assembled nanoreactors. *Chem. Rev.* **2005**, *105*, 1445–1490.
- (4) Lehn, J. M. Perspectives in Supramolecular Chemistry—From Molecular Recognition towards Molecular Information Processing and Self-Organization. *Angew. Chem., Int. Ed. Engl.* **1990**, *29*, 1304–1319.
- (5) Kataoka, K.; Harada, A.; Nagasaki, Y. Block copolymer micelles for drug delivery: design, characterization and biological significance. *Adv. Drug Delivery Rev.* **2001**, *47*, 113–131.
- (6) Lorenzo, M. O.; Baddeley, C.; Muryn, C.; Raval, R. Extended surface chirality from supramolecular assemblies of adsorbed chiral molecules. *Nature* **2000**, *404*, 376–379.
- (7) Sun, H.-J.; Zhang, S.; Percec, V. From structure to function via complex supramolecular dendrimer systems. *Chem. Soc. Rev.* **2015**, *44*, 3900.
- (8) Busseron, E.; Ruff, Y.; Moulin, E.; Giuseppone, N. Supramolecular self-assemblies as functional nanomaterials. *Nanoscale* **2013**, *5*, 7098–7140.
- (9) Schwille, P. Bottom-up synthetic biology: engineering in a tinkerer's world. *Science* **2011**, *333*, 1252–1254.
- (10) The Honeybee Genome Sequencing Consortium. Insights into social insects from the genome of the honeybee *Apis mellifera*. *Nature* **2006**, *443*, 931–949.
- (11) Ban, N.; Nissen, P.; Hansen, J.; Moore, P. B.; Steitz, T. A. The complete atomic structure of the large ribosomal subunit at 2.4 Å resolution. *Science* **2000**, *289*, 905–920.
- (12) Israelachvili, J. N.; Mitchell, D. J.; Ninham, B. W. Theory of self-assembly of hydrocarbon amphiphiles into micelles and bilayers. *J. Chem. Soc., Faraday Trans. 2* **1976**, *72*, 1525–1568.
- (13) Bangham, A.; Standish, M. M.; Watkins, J. Diffusion of univalent ions across the lamellae of swollen phospholipids. *J. Mol. Biol.* **1965**, *13*, 238–252.

- (14) Hanczyc, M. M.; Szostak, J. W. Replicating vesicles as models of primitive cell growth and division. *Curr. Opin. Chem. Biol.* **2004**, *8*, 660–664.
- (15) Discher, B. M.; Won, Y.-Y.; Ege, D. S.; Lee, J. C.; Bates, F. S.; Discher, D. E.; Hammer, D. A. Polymersomes: Tough vesicles made from diblock copolymers. *Science* **1999**, *284*, 1143–1146.
- (16) Percec, V.; Wilson, D. A.; Leowanawat, P.; Wilson, C. J.; Hughes, A. D.; Kaucher, M. S.; Hammer, D. A.; Levine, D. H.; Kim, A. J.; Bates, F. S.; et al. Self-assembly of Janus dendrimers into uniform dendrimersomes and other complex architectures. *Science* **2010**, *328*, 1009–1014.
- (17) Aida, T.; Meijer, E.; Stupp, S. Functional supramolecular polymers. *Science* **2012**, *335*, 813–817.
- (18) Henry, L. *Ann. Soc. Sci. Brux.* **1878**, *3*, 267.
- (19) Fouquey, C.; Lehn, J. M.; Levelut, A. M. Molecular recognition directed self-assembly of supramolecular liquid crystalline polymers from complementary chiral components. *Adv. Mater.* **1990**, *2*, 254–257.
- (20) Deutman, A. B.; Monnereau, C.; Elemans, J. A.; Ercolani, G.; Nolte, R. J.; Rowan, A. E. Mechanism of threading a polymer through a macrocyclic ring. *Science* **2008**, *322*, 1668–1671.
- (21) Thordarson, P.; Bijsterveld, E. J.; Rowan, A. E.; Nolte, R. J. Epoxidation of polybutadiene by a topologically linked catalyst. *Nature* **2003**, *424*, 915–918.
- (22) Zhang, S.; Altman, M. Peptide self-assembly in functional polymer science and engineering. *React. Funct. Polym.* **1999**, *41*, 91–102.
- (23) Lindoy, L. F.; Atkinson, I. M. *Self-Assembly in Supramolecular Systems*; Royal Society of Chemistry: London, 2000.
- (24) Rosen, B. M.; Wilson, C. J.; Wilson, D. A.; Peterca, M.; Imam, M. R.; Percec, V. Dendron-mediated self-assembly, disassembly, and self-organization of complex systems. *Chem. Rev.* **2009**, *109*, 6275–6540.
- (25) Rosen, B. M.; Wilson, D. A.; Wilson, C. J.; Peterca, M.; Won, B. C.; Huang, C.; Lipski, L. R.; Zeng, X.; Ungar, G.; Heiney, P. A.; et al. Predicting the structure of supramolecular dendrimers via the analysis of libraries of AB<sub>3</sub> and constitutional isomeric AB<sub>2</sub> biphenylpropyl ether self-assembling dendrons. *J. Am. Chem. Soc.* **2009**, *131*, 17500–17521.
- (26) Whitesides, G. M.; Mathias, J. P.; Seto, C. T. Molecular self-assembly and nanochemistry: a chemical strategy for the synthesis of nanostructures. *Science* **1991**, *254*, 1312–1319.
- (27) Whitesides, G. M.; Boncheva, M. Beyond molecules: Self-assembly of mesoscopic and macroscopic components. *Proc. Natl. Acad. Sci. U. S. A.* **2002**, *99*, 4769–4774.
- (28) Halley, J.; Winkler, D. A. Consistent concepts of self-organization and self-assembly. *Complexity* **2008**, *14*, 10–17.
- (29) Ashby, W. R. Principles of the self-organizing dynamic system. *J. Gen. Psychol.* **1947**, *37*, 125–128.
- (30) Ottino, J. M. Complex systems. *AIChE J.* **2003**, *49*, 292–299.
- (31) Vandermeulen, G. W.; Klok, H. A. Peptide/protein hybrid materials: enhanced control of structure and improved performance through conjugation of biological and synthetic polymers. *Macromol. Biosci.* **2004**, *4*, 383–398.
- (32) Löwik, D. W.; Ayres, L.; Smeenk, J. M.; Van Hest, J. C. In *Peptide Hybrid Polymers*; Springer: New York City, 2006.
- (33) van Dongen, S. F.; de Hoog, H.-P. M.; Peters, R. J.; Nallani, M.; Nolte, R. J.; van Hest, J. C. Biohybrid polymer capsules. *Chem. Rev.* **2009**, *109*, 6212–6274.
- (34) Zhang, S. Fabrication of novel biomaterials through molecular self-assembly. *Nat. Biotechnol.* **2003**, *21*, 1171–1178.
- (35) Hoeben, F. J.; Jonkheijm, P.; Meijer, E.; Schenning, A. P. About supramolecular assemblies of  $\pi$ -conjugated systems. *Chem. Rev.* **2005**, *105*, 1491–1546.
- (36) Chakrabarty, R.; Mukherjee, P. S.; Stang, P. J. Supramolecular coordination: self-assembly of finite two-and three-dimensional ensembles. *Chem. Rev.* **2011**, *111*, 6810–6918.
- (37) Adawy, A. *The ceiling Method for the Growth of High Resolution Protein Crystals*; Radboud University: Nijmegen, The Netherlands, 2014.
- (38) Yeates, T. O.; Padilla, J. E. Designing supramolecular protein assemblies. *Curr. Opin. Struct. Biol.* **2002**, *12*, 464–470.
- (39) Berman, H. M.; Westbrook, J.; Feng, Z.; Gilliland, G.; Bhat, T.; Weissig, H.; Shindyalov, I. N.; Bourne, P. E. The protein data bank. *Nucleic Acids Res.* **2000**, *28*, 235–242.
- (40) Percec, V.; Dulcey, A. E.; Balagurusamy, V. S.; Miura, Y.; Smidrkal, J.; Peterca, M.; Nummelin, S.; Edlund, U.; Hudson, S. D.; Heiney, P. A.; et al. Self-assembly of amphiphilic dendritic dipeptides into helical pores. *Nature* **2004**, *430*, 764–768.
- (41) Peterca, M.; Imam, M. R.; Leowanawat, P.; Rosen, B. M.; Wilson, D. A.; Wilson, C. J.; Zeng, X.; Ungar, G.; Heiney, P. A.; Percec, V. Self-assembly of hybrid dendrons into doubly segregated supramolecular polyhedral columns and vesicles. *J. Am. Chem. Soc.* **2010**, *132*, 11288–11305.
- (42) Percec, V.; Imam, M. R.; Peterca, M.; Wilson, D. A.; Graf, R.; Spiess, H. W.; Balagurusamy, V. S.; Heiney, P. A. Self-assembly of dendronized triphenylenes into helical pyramidal columns and chiral spheres. *J. Am. Chem. Soc.* **2009**, *131*, 7662–7677.
- (43) Percec, V.; Mitchell, C. M.; Cho, W.-D.; Uchida, S.; Glodde, M.; Ungar, G.; Zeng, X.; Liu, Y.; Balagurusamy, V. S.; Heiney, P. A. Designing libraries of first generation AB<sub>3</sub> and AB<sub>2</sub> self-assembling dendrons via the primary structure generated from combinations of (AB)<sub>y</sub>-AB<sub>3</sub> and (AB)<sub>y</sub>-AB<sub>2</sub> building blocks. *J. Am. Chem. Soc.* **2004**, *126*, 6078–6094.
- (44) Kang, H. J.; Lee, C.; Drew, D. Breaking the barriers in membrane protein crystallography. *Int. J. Biochem. Cell Biol.* **2013**, *45*, 636–644.
- (45) Moraes, I.; Evans, G.; Sanchez-Weatherby, J.; Newstead, S.; Stewart, P. D. S. Membrane protein structure determination—the next generation. *Biochim. Biophys. Acta, Biomembr.* **2014**, *1838*, 78–87.
- (46) Bill, R. M.; Henderson, P. J.; Iwata, S.; Kunji, E. R.; Michel, H.; Neutze, R.; Newstead, S.; Poolman, B.; Tate, C. G.; Vogel, H. Overcoming barriers to membrane protein structure determination. *Nat. Biotechnol.* **2011**, *29*, 335–340.
- (47) Michel, H.; Oesterhelt, D. Three-dimensional crystals of membrane proteins: bacteriorhodopsin. *Proc. Natl. Acad. Sci. U. S. A.* **1980**, *77*, 1283–1285.
- (48) Garavito, R. M.; Rosenbusch, J. P. Three-dimensional crystals of an integral membrane protein: an initial x-ray analysis. *J. Cell Biol.* **1980**, *86*, 327–329.
- (49) Deisenhofer, J.; Epp, O.; Miki, K.; Huber, R.; Michel, H. Structure of the protein subunits in the photosynthetic reaction center of *Nature* **1985**, *318*, 618–624.
- (50) Giegé, R. A historical perspective on protein crystallization from 1840 to the present day. *FEBS J.* **2013**, *280*, 6456–6497.
- (51) Vincentelli, R.; Bignon, C.; Gruez, A.; Canaan, S.; Sulzenbacher, G.; Tegoni, M.; Campanacci, V.; Cambillau, C. Medium-scale structural genomics: strategies for protein expression and crystallization. *Acc. Chem. Res.* **2003**, *36*, 165–172.
- (52) Walter, T. S.; Meier, C.; Assenberg, R.; Au, K.-F.; Ren, J.; Verma, A.; Nettleship, J. E.; Owens, R. J.; Stuart, D. I.; Grimes, J. M. Lysine methylation as a routine rescue strategy for protein crystallization. *Structure* **2006**, *14*, 1617–1622.
- (53) Dong, A.; Xu, X.; Edwards, A. M.; Chang, C.; Chruszcz, M.; Cuff, M.; Cymborowski, M.; Di Leo, R.; Egorova, O.; Evdokimova, E.; et al. In situ proteolysis for protein crystallization and structure determination. *Nat. Methods* **2007**, *4*, 1019–1021.
- (54) Hiller, S.; Garces, R. G.; Malia, T. J.; Orekhov, V. Y.; Colombini, M.; Wagner, G. Solution structure of the integral human membrane protein VDAC-1 in detergent micelles. *Science* **2008**, *321*, 1206–1210.
- (55) Privé, G. G. Detergents for the stabilization and crystallization of membrane proteins. *Methods* **2007**, *41*, 388–397.
- (56) le Maire, M.; Champel, P.; Møller, J. V. Interaction of membrane proteins and lipids with solubilizing detergents. *Biochim. Biophys. Acta, Biomembr.* **2000**, *1508*, 86–111.

- (57) Seddon, A. M.; Curnow, P.; Booth, P. J. Membrane proteins, lipids and detergents: not just a soap opera. *Biochim. Biophys. Acta, Biomembr.* **2004**, *1666*, 105–117.
- (58) Yeagle, P. L. Non-covalent binding of membrane lipids to membrane proteins. *Biochim. Biophys. Acta, Biomembr.* **2014**, *1838*, 1548–1559.
- (59) Pebay-Peyroula, E.; Garavito, R.; Rosenbusch, J.; Zulauf, M.; Timmins, P. Detergent structure in tetragonal crystals of OmpF porin. *Structure* **1995**, *3*, 1051–1059.
- (60) Rigaud, J.-L.; Chami, M.; Lambert, O.; Levy, D.; Ranck, J.-L. Use of detergents in two-dimensional crystallization of membrane proteins. *Biochim. Biophys. Acta, Biomembr.* **2000**, *1508*, 112–128.
- (61) Wiener, M. C. A pedestrian guide to membrane protein crystallization. *Methods* **2004**, *34*, 364–372.
- (62) Möller, J.; Le Maire, M. Detergent binding as a measure of hydrophobic surface area of integral membrane proteins. *J. Biol. Chem.* **1993**, *268*, 18659–18672.
- (63) Matar-Merheb, R.; Rhimi, M.; Leydier, A.; Huché, F.; Galián, C.; Desuzinges-Mandon, E.; Ficheux, D.; Flot, D.; Aghajari, N.; Kahn, R.; et al. Structuring detergents for extracting and stabilizing functional membrane proteins. *PLoS One* **2011**, *6*, e18036.
- (64) Patchornik, G.; Danino, D.; Kesselman, E.; Wachtel, E.; Friedman, N.; Sheves, M. Purification of a Membrane protein with conjugated engineered micelles. *Bioconjugate Chem.* **2013**, *24*, 1270–1275.
- (65) Zorman, S.; Botte, M.; Jiang, Q.; Collinson, I.; Schaffitzel, C. Advances and challenges of membrane–protein complex production. *Curr. Opin. Struct. Biol.* **2015**, *32*, 123–130.
- (66) Popot, J.-L. Amphipols, nanodiscs, and fluorinated surfactants: three nonconventional approaches to studying membrane proteins in aqueous solutions. *Annu. Rev. Biochem.* **2010**, *79*, 737–775.
- (67) Jap, B.; Zulauf, M.; Scheybani, T.; Hefti, A.; Baumeister, W.; Aebi, U.; Engel, A. 2D crystallization: from art to science. *Ultramicroscopy* **1992**, *46*, 45–84.
- (68) Dürr, U. H.; Soong, R.; Ramamoorthy, A. When detergent meets bilayer: birth and coming of age of lipid bicolles. *Prog. Nucl. Magn. Reson. Spectrosc.* **2013**, *69*, 1–22.
- (69) Tribet, C.; Audebert, R.; Popot, J.-L. Stabilization of hydrophobic colloidal dispersions in water with amphiphilic polymers: application to integral membrane proteins. *Langmuir* **1997**, *13*, 5570–5576.
- (70) Tribet, C.; Audebert, R.; Popot, J.-L. Amphipols: polymers that keep membrane proteins soluble in aqueous solutions. *Proc. Natl. Acad. Sci. U. S. A.* **1996**, *93*, 15047–15050.
- (71) Tribet, C.; Mills, D.; Haider, M.; Popot, J. Scanning transmission electron microscopy study of the molecular mass of amphipol/cytochrome b 6 f complexes. *Biochimie* **1998**, *80*, 475–482.
- (72) Popot, J.-L.; Berry, E.; Charvolin, D.; Creuzenet, C.; Ebel, C.; Engelmann, D.; Flötenmeyer, M.; Giusti, F.; Gohon, Y.; Hervé, P.; et al. Amphipols: polymeric surfactants for membrane biology research. *Cell. Mol. Life Sci.* **2003**, *60*, 1559–1574.
- (73) Kleinschmidt, J. H.; Popot, J.-L. Folding and stability of integral membrane proteins in amphipols. *Arch. Biochem. Biophys.* **2014**, *564*, 327–343.
- (74) Pocanschi, C. L.; Dahmane, T.; Gohon, Y.; Rappaport, F.; Apell, H.-J.; Kleinschmidt, J. H.; Popot, J.-L. Amphiphilic polymers: tools to fold integral membrane proteins to their active form. *Biochemistry* **2006**, *45*, 13954–13961.
- (75) Della Pia, E. A.; Hansen, R. W.; Zoonens, M.; Martinez, K. L. Functionalized amphipols: a versatile toolbox suitable for applications of membrane proteins in synthetic biology. *J. Membr. Biol.* **2014**, *247*, 815–826.
- (76) Planchard, N.; Point, E.; Dahmane, T.; Giusti, F.; Renault, M.; Le Bon, C.; Durand, G.; Milon, A.; Guittet, E.; Zoonens, M. The use of amphipols for solution NMR studies of membrane proteins: advantages and constraints as compared to other solubilizing media. *J. Membr. Biol.* **2014**, *247*, 827–842.
- (77) Nagy, J. K.; Kuhn Hoffmann, A.; Keyes, M. H.; Gray, D. N.; Oxenoid, K.; Sanders, C. R. Use of amphiphilic polymers to deliver a membrane protein to lipid bilayers. *FEBS Lett.* **2001**, *501*, 115–120.
- (78) Polovinkin, V.; Gushchin, I.; Sintsov, M.; Round, E.; Balandin, T.; Chervakov, P.; Schevchenko, V.; Utrobin, P.; Popov, A.; Borshchevskiy, V.; et al. High-resolution structure of a membrane protein transferred from amphipol to a lipidic mesophase. *J. Membr. Biol.* **2014**, *247*, 997–1004.
- (79) Borch, J.; Hamann, T. The nanodisc: a novel tool for membrane protein studies. *Biol. Chem.* **2009**, *390*, 805–814.
- (80) Jonas A. Reconstitution of high-density lipoproteins. *Methods in Enzymology*; Elsevier: Amsterdam, 1986; Vol. 128, pp 553–582.
- (81) Bayburt, T. H.; Grinkova, Y. V.; Sligar, S. G. Self-assembly of discoidal phospholipid bilayer nanoparticles with membrane scaffold proteins. *Nano Lett.* **2002**, *2*, 853–856.
- (82) Bayburt, T. H.; Sligar, S. G. Membrane protein assembly into Nanodiscs. *FEBS Lett.* **2010**, *584*, 1721–1727.
- (83) Carlson, J. W.; Jonas, A.; Sligar, S. G. Imaging and manipulation of high-density lipoproteins. *Biophys. J.* **1997**, *73*, 1184–1189.
- (84) Bayburt, T. H.; Carlson, J. W.; Sligar, S. G. Reconstitution and imaging of a membrane protein in a nanometer-size phospholipid bilayer. *J. Struct. Biol.* **1998**, *123*, 37–44.
- (85) Bayburt, T. H.; Carlson, J. W.; Sligar, S. G. Single molecule height measurements on a membrane protein in nanometer-scale phospholipid bilayer disks. *Langmuir* **2000**, *16*, 5993–5997.
- (86) Bayburt, T. H.; Sligar, S. G. Single-molecule height measurements on microsomal cytochrome P450 in nanometer-scale phospholipid bilayer disks. *Proc. Natl. Acad. Sci. U. S. A.* **2002**, *99*, 6725–6730.
- (87) Blanchette, C. D.; Cappuccio, J. A.; Kuhn, E. A.; Segelke, B. W.; Benner, W. H.; Chromy, B. A.; Coleman, M. A.; Bench, G.; Hoeprich, P. D.; Sulcik, T. A. Atomic force microscopy differentiates discrete size distributions between membrane protein containing and empty nanolipoprotein particles. *Biochim. Biophys. Acta, Biomembr.* **2009**, *1788*, 724–731.
- (88) Goluch, E. D.; Shaw, A. W.; Sligar, S. G.; Liu, C. Microfluidic patterning of nanodisc lipid bilayers and multiplexed analysis of protein interaction. *Lab Chip* **2008**, *8*, 1723–1728.
- (89) Akkaladevi, N.; Mukherjee, S.; Katayama, H.; Janowiak, B.; Patel, D.; Gogoi, E. P.; Pentelute, B. L.; Collier, R. J.; Fisher, M. T. Following Natures Lead: On the Construction of Membrane-Inserted Toxins in Lipid Bilayer Nanodiscs. *J. Membr. Biol.* **2015**, *248*, 595–607.
- (90) Kijac, A. Z.; Li, Y.; Sligar, S. G.; Rienstra, C. M. Magic-angle spinning solid-state NMR spectroscopy of nanodisc-embedded human CYP3A4. *Biochemistry* **2007**, *46*, 13696–13703.
- (91) Lyukmanova, E. N.; Shenkarev, Z. O.; Paramonov, A. S.; Sobol, A. G.; Ovchinnikova, T. V.; Chupin, V. V.; Kirpichnikov, M. P.; Blommers, M. J.; Arseniev, A. S. Lipid-protein nanoscale bilayers: a versatile medium for NMR investigations of membrane proteins and membrane-active peptides. *J. Am. Chem. Soc.* **2008**, *130*, 2140–2141.
- (92) Glück, J. M.; Wittlich, M.; Feuerstein, S.; Hoffmann, S.; Willbold, D.; Koenig, B. W. Integral membrane proteins in nanodiscs can be studied by solution NMR spectroscopy. *J. Am. Chem. Soc.* **2009**, *131*, 12060–12061.
- (93) Park, S. H.; Berkamp, S.; Cook, G. A.; Chan, M. K.; Viadiu, H.; Opella, S. J. Nanodiscs versus macrodiscs for NMR of membrane proteins. *Biochemistry* **2011**, *50*, 8983–8985.
- (94) Shirzad-Wasei, N.; van Oostrum, J.; Bovee-Geurts, P.; Kusters, L.; Bosman, G.; DeGrip, W. J. Rapid transfer of overexpressed integral membrane protein from the host membrane into soluble lipid nanodiscs without previous purification. *Biol. Chem.* **2015**, *396*, 903–915.
- (95) Wallace, E.; Dranow, D.; Laible, P. D.; Christensen, J.; Nollert, P. Monoolein lipid phases as incorporation and enrichment materials for membrane protein crystallization. *PLoS One* **2011**, *6*, e24488.
- (96) Landau, E. M.; Rosenbusch, J. P. Lipidic cubic phases: a novel concept for the crystallization of membrane proteins. *Proc. Natl. Acad. Sci. U. S. A.* **1996**, *93*, 14532–14535.

- (97) Cherezov, V. Lipidic cubic phase technologies for membrane protein structural studies. *Curr. Opin. Struct. Biol.* **2011**, *21*, 559–566.
- (98) Caffrey, M. A comprehensive review of the lipid cubic phase or in meso method for crystallizing membrane and soluble proteins and complexes. *Acta Crystallogr., Sect. F: Struct. Biol. Commun.* **2015**, *71*, 3–18.
- (99) Caffrey, M.; Cherezov, V. Crystallizing membrane proteins using lipidic mesophases. *Nat. Protoc.* **2009**, *4*, 706–731.
- (100) Wadsten, P.; Wöhri, A. B.; Snijder, A.; Katona, G.; Gardiner, A. T.; Cogdell, R. J.; Neutze, R.; Engström, S. Lipidic sponge phase crystallization of membrane proteins. *J. Mol. Biol.* **2006**, *364*, 44–53.
- (101) Wöhri, A. B.; Johansson, L. C.; Wadsten-Hindrichsen, P.; Wahlgren, W. Y.; Fischer, G.; Horsefield, R.; Katona, G.; Nyblom, M.; Öberg, F.; Young, G.; et al. A lipidic-sponge phase screen for membrane protein crystallization. *Structure* **2008**, *16*, 1003–1009.
- (102) Faham, S.; Ujwal, R.; Abramson, J.; Bowie, J. U. Practical aspects of membrane proteins crystallization in bicelles. *Curr. Top. Membr.* **2009**, *63*, 109–125.
- (103) Faham, S.; Bowie, J. U. Bicelle crystallization: a new method for crystallizing membrane proteins yields a monomeric bacteriorhodopsin structure. *J. Mol. Biol.* **2002**, *316*, 1–6.
- (104) Dürr, U. H.; Gildenberg, M.; Ramamoorthy, A. The magic of bicelles lights up membrane protein structure. *Chem. Rev.* **2012**, *112*, 6054–6074.
- (105) Gourdon, P.; Andersen, J. L.; Hein, K. L.; Bublitz, M.; Pedersen, B. P.; Liu, X.-Y.; Yatime, L.; Nyblom, M.; Nielsen, T. T.; Olesen, C.; et al. HiLiDe-Systematic Approach to Membrane Protein Crystallization in Lipid and Detergent. *Cryst. Growth Des.* **2011**, *11*, 2098–2106.
- (106) Tan, A.; Rajadas, J.; Seifalian, A. M. Exosomes as nanotheranostic delivery platforms for gene therapy. *Adv. Drug Delivery Rev.* **2013**, *65*, 357–367.
- (107) O'Loughlin, A.; Woffindale, C.; Wood, M. Exosomes and the emerging field of exosome-based gene therapy. *Curr. Gene Ther.* **2012**, *12*, 262–274.
- (108) Théry, C.; Zitvogel, L.; Amigorena, S. Exosomes: composition, biogenesis and function. *Nat. Rev. Immunol.* **2002**, *2*, 569–579.
- (109) Bangham, A.; Horne, R.; Glauert, A.; Dingle, J.; Lucy, J. Action of saponin on biological cell membranes. *Nature* **1962**, *196*, 952–955.
- (110) Bangham, A. Physical structure and behavior of lipids and lipid enzymes. *Adv. Lipid Res.* **1963**, *1*, 65–104.
- (111) Torchilin, V. P. Recent advances with liposomes as pharmaceutical carriers. *Nat. Rev. Drug Discovery* **2005**, *4*, 145–160.
- (112) Bader, H.; Ringsdorf, H.; Schmidt, B. Watersoluble polymers in medicine. *Angew. Makromol. Chem.* **1984**, *123*, 457–485.
- (113) Torchilin, V. P. Micellar nanocarriers: pharmaceutical perspectives. *Pharm. Res.* **2006**, *24*, 1–16.
- (114) Dubertret, B.; Skourides, P.; Norris, D. J.; Noireaux, V.; Brivanlou, A. H.; Libchaber, A. In vivo imaging of quantum dots encapsulated in phospholipid micelles. *Science* **2002**, *298*, 1759–1762.
- (115) Discher, D. M.; Hammer, D. A.; Bates, F. S.; Discher, D. E. Polymer vesicles in various media. *Curr. Opin. Colloid Interface Sci.* **2000**, *5*, 125–131.
- (116) Brinkhuis, R. P.; Visser, T. R.; Rutjes, F. P.; van Hest, J. C. Polymeric vesicles in biomedical applications. *Polym. Chem.* **2011**, *2*, 1449–1462.
- (117) Discher, D. E.; Ortiz, V.; Srinivas, G.; Klein, M. L.; Kim, Y.; Christian, D.; Cai, S.; Photos, P.; Ahmed, F. Emerging applications of polymersomes in delivery: from molecular dynamics to shrinkage of tumors. *Prog. Polym. Sci.* **2007**, *32*, 838–857.
- (118) Huang, X.; Li, M.; Green, D. C.; Williams, D. S.; Patil, A. J.; Mann, S. Interfacial assembly of protein–polymer nano-conjugates into stimulus-responsive biomimetic protocells. *Nat. Commun.* **2013**, DOI: [10.1038/ncomms3239](https://doi.org/10.1038/ncomms3239).
- (119) Huang, X.; Patil, A. J.; Li, M.; Mann, S. Design and construction of higher-order structure and function in proteinosome-based protocells. *J. Am. Chem. Soc.* **2014**, *136*, 9225–9234.
- (120) Nazemi, A.; Gillies, E. R. Dendrimersomes with photo-degradable membranes for triggered release of hydrophilic and hydrophobic cargo. *Chem. Commun.* **2014**, *50*, 11122–11125.
- (121) Allen, T. M.; Cullis, P. R. Drug delivery systems: entering the mainstream. *Science* **2004**, *303*, 1818–1822.
- (122) Brannon-Peppas, L.; Blanchette, J. O. Nanoparticle and targeted systems for cancer therapy. *Adv. Drug Delivery Rev.* **2012**, *64*, 206–212.
- (123) Couvreur, P. Nanoparticles in drug delivery: past, present and future. *Adv. Drug Delivery Rev.* **2013**, *65*, 21–23.
- (124) Mitragotri, S.; Burke, P. A.; Langer, R. Overcoming the challenges in administering biopharmaceuticals: formulation and delivery strategies. *Nat. Rev. Drug Discovery* **2014**, *13*, 655–672.
- (125) Torchilin, V. P. In *Drug Delivery*; Springer: New York City, 2010.
- (126) Matsumura, Y.; Maeda, H. A new concept for macromolecular therapeutics in cancer chemotherapy: mechanism of tumorotropic accumulation of proteins and the antitumor agent smancs. *Cancer Res.* **1986**, *46*, 6387–6392.
- (127) Mura, S.; Nicolas, J.; Couvreur, P. Stimuli-responsive nanocarriers for drug delivery. *Nat. Mater.* **2013**, *12*, 991–1003.
- (128) Zhuang, J.; Gordon, M. R.; Ventura, J.; Li, L.; Thayumanavan, S. Multi-stimuli responsive macromolecules and their assemblies. *Chem. Soc. Rev.* **2013**, *42*, 7421–7435.
- (129) Basile, L.; Pignatello, R.; Passirani, C. Active targeting strategies for anticancer drug nanocarriers. *Curr. Drug Delivery* **2012**, *9*, 255–268.
- (130) Muro, S. Challenges in design and characterization of ligand-targeted drug delivery systems. *J. Controlled Release* **2012**, *164*, 125–137.
- (131) Nicolas, J.; Mura, S.; Brambilla, D.; Mackiewicz, N.; Couvreur, P. Design, functionalization strategies and biomedical applications of targeted biodegradable/biocompatible polymer-based nanocarriers for drug delivery. *Chem. Soc. Rev.* **2013**, *42*, 1147–1235.
- (132) Jeong, B.; Gutowska, A. Lessons from nature: stimuli-responsive polymers and their biomedical applications. *Trends Biotechnol.* **2002**, *20*, 305–311.
- (133) Allen, T. M. Ligand-targeted therapeutics in anticancer therapy. *Nat. Rev. Cancer* **2002**, *2*, 750–763.
- (134) Sudimack, J.; Lee, R. J. Targeted drug delivery via the folate receptor. *Adv. Drug Delivery Rev.* **2000**, *41*, 147–162.
- (135) Discher, D. E.; Eisenberg, A. Polymer vesicles. *Science* **2002**, *297*, 967–973.
- (136) Peer, D.; Karp, J. M.; Hong, S.; Farokhzad, O. C.; Margalit, R.; Langer, R. Nanocarriers as an emerging platform for cancer therapy. *Nat. Nanotechnol.* **2007**, *2*, 751–760.
- (137) Laurent, S.; Forge, D.; Port, M.; Roch, A.; Robic, C.; Vander Elst, L.; Muller, R. N. Magnetic iron oxide nanoparticles: synthesis, stabilization, vectorization, physicochemical characterizations, and biological applications. *Chem. Rev.* **2008**, *108*, 2064–2110.
- (138) Maeda, H. The enhanced permeability and retention (EPR) effect in tumor vasculature: the key role of tumor-selective macromolecular drug targeting. *Adv. Enzyme Regul.* **2001**, *41*, 189–207.
- (139) Fang, J.; Nakamura, H.; Maeda, H. The EPR effect: unique features of tumor blood vessels for drug delivery, factors involved, and limitations and augmentation of the effect. *Adv. Drug Delivery Rev.* **2011**, *63*, 136–151.
- (140) Maeda, H.; Wu, J.; Sawa, T.; Matsumura, Y.; Hori, K. Tumor vascular permeability and the EPR effect in macromolecular therapeutics: a review. *J. Controlled Release* **2000**, *65*, 271–284.
- (141) Schiffelers, R. M.; Storm, G.; Bakker-Woudenberg, I. A. Host factors influencing the preferential localization of sterically stabilized liposomes in Klebsiella pneumoniae-infected rat lung tissue. *Pharm. Res.* **2001**, *18*, 780–787.
- (142) Edens, H. A.; Levi, B. P.; Jaye, D. L.; Walsh, S.; Reaves, T. A.; Turner, J. R.; Nusrat, A.; Parkos, C. A. Neutrophil Transepithelial Migration: Evidence for Sequential, Contact-Dependent Signaling Events and Enhanced Paracellular Permeability Independent of Transjunctional Migration. *J. Immunol.* **2002**, *169*, 476–486.

- (143) Jhaveri, A. M.; Torchilin, V. P. Multifunctional polymeric micelles for delivery of drugs and siRNA. *Front. Pharmacol.* **2014**, DOI: 10.3389/fphar.2014.00077.
- (144) Klibanov, A. L.; Maruyama, K.; Torchilin, V. P.; Huang, L. Amphiphatic polyethyleneglycols effectively prolong the circulation time of liposomes. *FEBS Lett.* **1990**, 268, 235–237.
- (145) Barenholz, Y. Doxil(R)—the first FDA-approved nano-drug: lessons learned. *J. Controlled Release* **2012**, 160, 117–134.
- (146) Borman, S. Dendrimersomes debut. *Chem. Eng. News* **2010**, 88, 7.
- (147) Petros, R. A.; DeSimone, J. M. Strategies in the design of nanoparticles for therapeutic applications. *Nat. Rev. Drug Discovery* **2010**, 9, 615–627.
- (148) Ganta, S.; Devalapally, H.; Shahiwala, A.; Amiji, M. A review of stimuli-responsive nanocarriers for drug and gene delivery. *J. Controlled Release* **2008**, 126, 187–204.
- (149) Rapoport, N. Physical stimuli-responsive polymeric micelles for anti-cancer drug delivery. *Prog. Polym. Sci.* **2007**, 32, 962–990.
- (150) Needham, D.; Anyarambhatla, G.; Kong, G.; Dewhirst, M. W. A new temperature-sensitive liposome for use with mild hyperthermia: characterization and testing in a human tumor xenograft model. *Cancer Res.* **2000**, 60, 1197–1201.
- (151) Preiss, M. R.; Bothun, G. D. Stimuli-responsive liposome-nanoparticle assemblies. *Expert Opin. Drug Delivery* **2011**, 8, 1025–1040.
- (152) Stuart, M. A. C.; Huck, W. T.; Genzer, J.; Müller, M.; Ober, C.; Stamm, M.; Sukhorukov, G. B.; Szleifer, I.; Tsukruk, V. V.; Urban, M.; et al. Emerging applications of stimuli-responsive polymer materials. *Nat. Mater.* **2010**, 9, 101–113.
- (153) Kojima, C. Design of stimuli-responsive dendrimers. *Expert Opin. Drug Delivery* **2010**, 7, 307–319.
- (154) Cheng, R.; Meng, F.; Deng, C.; Klok, H.-A.; Zhong, Z. Dual and multi-stimuli responsive polymeric nanoparticles for programmed site-specific drug delivery. *Biomaterials* **2013**, 34, 3647–3657.
- (155) Mountrichas, G.; Pispas, S. Synthesis and pH responsive self-assembly of new double hydrophilic block copolymers. *Macromolecules* **2006**, 39, 4767–4774.
- (156) Du, J.; Tang, Y.; Lewis, A. L.; Armes, S. P. pH-sensitive vesicles based on a biocompatible zwitterionic diblock copolymer. *J. Am. Chem. Soc.* **2005**, 127, 17982–17983.
- (157) Torchilin, V. P. Multifunctional, stimuli-sensitive nanoparticulate systems for drug delivery. *Nat. Rev. Drug Discovery* **2014**, 13, 813–827.
- (158) Maxfield, F. R.; McGraw, T. E. Endocytic recycling. *Nat. Rev. Mol. Cell Biol.* **2004**, 5, 121–132.
- (159) Huotari, J.; Helenius, A. Endosome maturation. *EMBO J.* **2011**, 30, 3481–3500.
- (160) Tscherne, D. M.; Jones, C. T.; Evans, M. J.; Lindenbach, B. D.; McKeating, J. A.; Rice, C. M. Time-and temperature-dependent activation of hepatitis C virus for low-pH-triggered entry. *J. Virol.* **2006**, 80, 1734–1741.
- (161) Bartenschlager, R.; Vogt, P. K. *Hepatitis C Virus: From Molecular Virology to Antiviral Therapy*; Springer: New York City, 2013.
- (162) Cuesta-Geijo, M. A.; Galindo, I.; Hernández, B.; Quetglas, J. I.; Dalmau-Mena, I.; Alonso, C. Endosomal maturation, Rab7 GTPase and phosphoinositides in African swine fever virus entry. *PLoS One* **2012**, 7, e48853.
- (163) Gruber, P.; Longer, M. A.; Robinson, J. R. Some biological issues in oral, controlled drug delivery. *Adv. Drug Delivery Rev.* **1987**, 1, 1–18.
- (164) Kararli, T. T. Comparison of the gastrointestinal anatomy, physiology, and biochemistry of humans and commonly used laboratory animals. *Biopharm. Drug Dispos.* **1995**, 16, 351–380.
- (165) Steen, K. H.; Steen, A. E.; Reeh, P. W. A dominant role of acid pH in inflammatory excitation and sensitization of nociceptors in rat skin, in vitro. *J. Neurosci.* **1995**, 15, 3982–3989.
- (166) Gethin, G. The significance of surface pH in chronic wounds. *Wounds UK* **2007**, 3, 52–56.
- (167) Nagoba, B. S.; Suryawanshi, N. M.; Wadher, B.; Selkar, S. Acidic Environment and Wound Healing: A Review. *Wounds* **2015**, 27, 5–11.
- (168) Vaupel, P.; Kallinowski, F.; Okunieff, P. Blood flow, oxygen and nutrient supply, and metabolic microenvironment of human tumors: a review. *Cancer Res.* **1989**, 49, 6449–6465.
- (169) Danhier, F.; Feron, O.; Prétat, V. To exploit the tumor microenvironment: passive and active tumor targeting of nanocarriers for anti-cancer drug delivery. *J. Controlled Release* **2010**, 148, 135–146.
- (170) Mo, R.; Sun, Q.; Xue, J.; Li, N.; Li, W.; Zhang, C.; Ping, Q. Multistage pH-Responsive Liposomes for Mitochondrial-Targeted Anticancer Drug Delivery. *Adv. Mater.* **2012**, 24, 3659–3665.
- (171) Miyata, K.; Nishiyama, N.; Kataoka, K. Rational design of smart supramolecular assemblies for gene delivery: chemical challenges in the creation of artificial viruses. *Chem. Soc. Rev.* **2012**, 41, 2562–2574.
- (172) McMahon, B. K.; Pal, R.; Parker, D. A bright and responsive europium probe for determination of pH change within the endoplasmic reticulum of living cells. *Chem. Commun.* **2013**, 49, 5363–5365.
- (173) Ke, C. J.; Su, T. Y.; Chen, H. L.; Liu, H. L.; Chiang, W. L.; Chu, P. C.; Xia, Y.; Sung, H. W. Smart multifunctional hollow microspheres for the quick release of drugs in intracellular lysosomal compartments. *Angew. Chem.* **2011**, 123, 8236–8239.
- (174) Masuda, A.; Oyamada, M.; Nagaoka, T.; Tateishi, N.; Takamatsu, T. Regulation of cytosol–nucleus pH gradients by K<sup>+</sup>/H<sup>+</sup> exchange mechanism in the nuclear envelope of neonatal rat astrocytes. *Brain Res.* **1998**, 807, 70–77.
- (175) Yatin, M. B.; Kreutz, W.; Horwitz, B. A.; Shinitzky, M. pH-sensitive liposomes: possible clinical implications. *Science* **1980**, 210, 1253–1255.
- (176) Lee, E. S.; Oh, K. T.; Kim, D.; Youn, Y. S.; Bae, Y. H. Tumor pH-responsive flower-like micelles of poly (L-lactic acid)-b-poly (ethylene glycol)-b-poly (L-histidine). *J. Controlled Release* **2007**, 123, 19–26.
- (177) Rao N, V.; Mane, S.; Kishore, A.; Das Sarma, J.; Shunmugam, R. Norbornene derived doxorubicin copolymers as drug carriers with pH responsive hydrazone linker. *Biomacromolecules* **2012**, 13, 221–230.
- (178) Bae, Y.; Fukushima, S.; Harada, A.; Kataoka, K. Design of environment-sensitive supramolecular assemblies for intracellular drug delivery: Polymeric micelles that are responsive to intracellular pH change. *Angew. Chem., Int. Ed.* **2003**, 42, 4640–4643.
- (179) Kim, K. S.; Park, W.; Hu, J.; Bae, Y. H.; Na, K. A cancer-recognizable MRI contrast agents using pH-responsive polymeric micelle. *Biomaterials* **2014**, 35, 337–343.
- (180) Lee, E. S.; Shin, H. J.; Na, K.; Bae, Y. H. Poly(L-histidine)-PEG block copolymer micelles and pH-induced destabilization. *J. Controlled Release* **2003**, 90, 363–374.
- (181) Bo, Q.; Zhao, Y. Double-hydrophilic block copolymer for encapsulation and two-way pH change-induced release of metalloporphyrins. *J. Polym. Sci., Part A: Polym. Chem.* **2006**, 44, 1734–1744.
- (182) Liu, F.; Eisenberg, A. Preparation and pH triggered inversion of vesicles from poly(acrylic acid)-block-polystyrene-block-poly(4-vinyl pyridine). *J. Am. Chem. Soc.* **2003**, 125, 15059–15064.
- (183) Rodriguez-Hernandez, J.; Lecommandoux, S. Reversible inside-out micellization of pH-responsive and water-soluble vesicles based on polypeptide diblock copolymers. *J. Am. Chem. Soc.* **2005**, 127, 2026–2027.
- (184) Wu, Y.; Chen, W.; Meng, F.; Wang, Z.; Cheng, R.; Deng, C.; Liu, H.; Zhong, Z. Core-crosslinked pH-sensitive degradable micelles: A promising approach to resolve the extracellular stability versus intracellular drug release dilemma. *J. Controlled Release* **2012**, 164, 338–345.
- (185) Brinkhuis, R. P.; Visser, T. R.; Rutjes, F. P.; van Hest, J. C. Shedding the hydrophilic mantle of polymersomes. *Polym. Chem.* **2011**, 2, 550–552.
- (186) He, L.; Jiang, Y.; Tu, C.; Li, G.; Zhu, B.; Jin, C.; Zhu, Q.; Yan, D.; Zhu, X. Self-assembled encapsulation systems with pH tunable

- release property based on reversible covalent bond. *Chem. Commun.* **2010**, *46*, 7569–7571.
- (187) Minkenberg, C. B.; Florusse, L.; Eelkema, R.; Koper, G. J.; van Esch, J. H. Triggered self-assembly of simple dynamic covalent surfactants. *J. Am. Chem. Soc.* **2009**, *131*, 11274–11275.
- (188) Wang, C.; Wang, G.; Wang, Z.; Zhang, X. A pH-responsive superamphiphile based on dynamic covalent bonds. *Chem. - Eur. J.* **2011**, *17*, 3322–3325.
- (189) Yoo, H. S.; Lee, E. A.; Park, T. G. Doxorubicin-conjugated biodegradable polymeric micelles having acid-cleavable linkages. *J. Controlled Release* **2002**, *82*, 17–27.
- (190) MacKay, J. A.; Chen, M.; McDaniel, J. R.; Liu, W.; Simnick, A. J.; Chilkoti, A. Self-assembling chimeric polypeptide-doxorubicin conjugate nanoparticles that abolish tumours after a single injection. *Nat. Mater.* **2009**, *8*, 993–999.
- (191) Versluis, F.; Tomatsu, I.; Kehr, S.; Fregonese, C.; Tepper, A. W.; Stuart, M. C.; Ravoo, B. J.; Koning, R. I.; Kros, A. Shape and release control of a peptide decorated vesicle through pH sensitive orthogonal supramolecular interactions. *J. Am. Chem. Soc.* **2009**, *131*, 13186–13187.
- (192) Yu, G.; Zhou, X.; Zhang, Z.; Han, C.; Mao, Z.; Gao, C.; Huang, F. Pillar[6]arene/paraquat molecular recognition in water: high binding strength, pH-responsiveness, and application in controllable self-assembly, controlled release, and treatment of paraquat poisoning. *J. Am. Chem. Soc.* **2012**, *134*, 19489–19497.
- (193) Ghosh, A.; Haverick, M.; Stump, K.; Yang, X.; Tweedle, M. F.; Goldberger, J. E. Fine-tuning the pH trigger of self-assembly. *J. Am. Chem. Soc.* **2012**, *134*, 3647–3650.
- (194) Verghese, J.; Abrams, J.; Wang, Y.; Morano, K. A. Biology of the heat shock response and protein chaperones: budding yeast (*Saccharomyces cerevisiae*) as a model system. *Microbiol. Mol. Biol. Rev.* **2012**, *76*, 115–158.
- (195) Wilkop, T. E.; Sanborn, J.; Oliver, A. E.; Hanson, J. M.; Parikh, A. N. On-Demand Self-Assembly of Supported Membranes Using Sacrificial, Anhydrobiotic Sugar Coats. *J. Am. Chem. Soc.* **2014**, *136*, 60–63.
- (196) Haslbeck, M.; Franzmann, T.; Weinfurtner, D.; Buchner, J. Some like it hot: the structure and function of small heat-shock proteins. *Nat. Struct. Mol. Biol.* **2005**, *12*, 842–846.
- (197) Haslbeck, M.; Vierling, E. A First Line of Stress Defense: Small Heat Shock Proteins and Their Function in Protein Homeostasis. *J. Mol. Biol.* **2015**, *427*, 1537–1548.
- (198) Steim, J. M.; Tourtellotte, M. E.; Reinert, J. C.; McElhaney, R. N.; Rader, R. L. Calorimetric evidence for the liquid-crystalline state of lipids in a biomembrane. *Proc. Natl. Acad. Sci. U. S. A.* **1969**, *63*, 104–109.
- (199) Melchior, D. L. Lipid phase transitions and regulation of membrane fluidity in prokaryotes. *Curr. Top. Membr. Transp.* **1982**, *17*, 263–316.
- (200) Redondo-Morata, L.; Giannotti, M. I.; Sanz, F. Influence of cholesterol on the phase transition of lipid bilayers: a temperature-controlled force spectroscopy study. *Langmuir* **2012**, *28*, 12851–12860.
- (201) Mendoza, D. d. Temperature sensing by membranes. *Annu. Rev. Microbiol.* **2014**, *68*, 101–116.
- (202) Mittler, R.; Finka, A.; Goloubinoff, P. How do plants feel the heat? *Trends Biochem. Sci.* **2012**, *37*, 118–125.
- (203) Saidi, Y.; Finka, A.; Muriset, M.; Bromberg, Z.; Weiss, Y. G.; Maathuis, F. J.; Goloubinoff, P. The heat shock response in moss plants is regulated by specific calcium-permeable channels in the plasma membrane. *Plant Cell* **2009**, *21*, 2829–2843.
- (204) Chintalapati, S.; Kiran, M. D.; Shivaji, S. Role of membrane lipid fatty acids in cold adaptation. *Cell. Mol. Biol. (Noisy-le-Grand, France)* **2004**, *50*, 631–642.
- (205) Dewhirst, M. W.; Vujaskovic, Z.; Jones, E.; Thrall, D. Re-setting the biologic rationale for thermal therapy. *Int. J. Hyperthermia* **2005**, *21*, 779–790.
- (206) Hill, C.; Ter Haar, G. High intensity focused ultrasound—potential for cancer treatment. *Br. J. Radiol.* **1995**, *68*, 1296–1303.
- (207) O'Neal, D. P.; Hirsch, L. R.; Halas, N. J.; Payne, J. D.; West, J. L. Photo-thermal tumor ablation in mice using near infrared-absorbing nanoparticles. *Cancer Lett.* **2004**, *209*, 171–176.
- (208) Cherukuri, P.; Glazer, E. S.; Curley, S. A. Targeted hyperthermia using metal nanoparticles. *Adv. Drug Delivery Rev.* **2010**, *62*, 339–345.
- (209) Arthur, R.; Straube, W.; Trobaugh, J.; Moros, E. Non-invasive estimation of hyperthermia temperatures with ultrasound. *Int. J. Hyperthermia* **2005**, *21*, 589–600.
- (210) Jordan, A.; Scholz, R.; Wust, P.; Fähling, H.; Felix, R. Magnetic fluid hyperthermia (MFH): Cancer treatment with AC magnetic field induced excitation of biocompatible superparamagnetic nanoparticles. *J. Magn. Magn. Mater.* **1999**, *201*, 413–419.
- (211) Schmaljohann, D. Thermo-and pH-responsive polymers in drug delivery. *Adv. Drug Delivery Rev.* **2006**, *58*, 1655–1670.
- (212) Bromberg, L. E.; Ron, E. S. Temperature-responsive gels and thermogelling polymer matrices for protein and peptide delivery. *Adv. Drug Delivery Rev.* **1998**, *31*, 197–221.
- (213) Moon, H. J.; Park, M. H.; Joo, M. K.; Jeong, B.; Ko, D. Y. Temperature-responsive compounds as *in situ* gelling biomedical materials. *Chem. Soc. Rev.* **2012**, *41*, 4860–4883.
- (214) Zhang, W.; Shi, L.; Wu, K.; An, Y. Thermoresponsive micellization of poly (ethylene glycol)-b-poly (N-isopropylacrylamide) in water. *Macromolecules* **2005**, *38*, 5743–5747.
- (215) Nakayama, M.; Okano, T.; Miyazaki, T.; Kohori, F.; Sakai, K.; Yokoyama, M. Molecular design of biodegradable polymeric micelles for temperature-responsive drug release. *J. Controlled Release* **2006**, *115*, 46–56.
- (216) Guo, B.; Sun, X.; Zhou, Y.; Yan, D. Supramolecular self-assembly and controllable drug release of thermosensitive hyperbranched multiarm copolymers. *Sci. China: Chem.* **2010**, *53*, 487–494.
- (217) Aoki, T.; Kawashima, M.; Katono, H.; Sanui, K.; Ogata, N.; Okano, T.; Sakurai, Y. Temperature-responsive interpenetrating polymer networks constructed with poly (acrylic acid) and poly (N, N-dimethylacrylamide). *Macromolecules* **1994**, *27*, 947–952.
- (218) Huang, G.; Li, H.; Feng, S. T.; Li, X.; Tong, G.; Liu, J.; Quan, C.; Jiang, Q.; Zhang, C.; Li, Z. Self-assembled UCST-Type Micelles as Potential Drug Carriers for Cancer Therapeutics. *Macromol. Chem. Phys.* **2015**, *216*, 1014–1023.
- (219) Yatin, M. B.; Weinstein, J. N.; Dennis, W. H.; Blumenthal, R. Design of liposomes for enhanced local release of drugs by hyperthermia. *Science* **1978**, *202*, 1290–1293.
- (220) Ellens, H.; Bentz, J.; Szoka, F. C. Destabilization of phosphatidylethanolamine liposomes at the hexagonal phase transition temperature. *Biochemistry* **1986**, *25*, 285–294.
- (221) Van Elk, M.; Deckers, R.; Oerlemans, C.; Shi, Y.; Storm, G.; Vermonden, T.; Hennink, W. E. Triggered release of doxorubicin from temperature-sensitive poly (N-(2-hydroxypropyl)-methacrylamide mono/dilactate) grafted liposomes. *Biomacromolecules* **2014**, *15*, 1002–1009.
- (222) Al-Ahmady, Z. S.; Al-Jamal, W. T.; Bossche, J. V.; Bui, T. T.; Drake, A. F.; Mason, A. J.; Kostarelos, K. Lipid-peptide vesicle nanoscale hybrids for triggered drug release by mild hyperthermia *in vitro* and *in vivo*. *ACS Nano* **2012**, *6*, 9335–9346.
- (223) Al-Ahmady, Z. S.; Scudamore, C. L.; Kostarelos, K. Triggered doxorubicin release in solid tumors from thermosensitive liposome-peptide hybrids: Critical parameters and therapeutic efficacy. *Int. J. Cancer* **2015**, *137*, 731–743.
- (224) Chen, K. J.; Liang, H. F.; Chen, H. L.; Wang, Y.; Cheng, P. Y.; Liu, H. L.; Xia, Y.; Sung, H. W. A thermoresponsive bubble-generating liposomal system for triggering localized extracellular drug delivery. *ACS Nano* **2013**, *7*, 438–446.
- (225) Chen, K. J.; Chaung, E. Y.; Wey, S. P.; Lin, K. J.; Cheng, F.; Lin, C. C.; Liu, H. L.; Tseng, H. W.; Liu, C. P.; Wei, M. C.; et al. Hyperthermia-mediated local drug delivery by a bubble-generating liposomal system for tumor-specific chemotherapy. *ACS Nano* **2014**, *8*, 5105–5115.
- (226) Kavic, M. Three-dimensional ultrasound. *Surg. Endosc.* **1996**, *10*, 74–76.

- (227) Speed, C. Therapeutic ultrasound in soft tissue lesions. *Rheumatology* **2001**, *40*, 1331–1336.
- (228) Li, G.; Fei, G.; Xia, H.; Han, J.; Zhao, Y. Spatial and temporal control of shape memory polymers and simultaneous drug release using high intensity focused ultrasound. *J. Mater. Chem.* **2012**, *22*, 7692–7696.
- (229) Ranjan, A.; Jacobs, G. C.; Woods, D. L.; Negussie, A. H.; Partanen, A.; Yarmolenko, P. S.; Gacchina, C. E.; Sharma, K. V.; Frenkel, V.; Wood, B. J.; et al. Image-guided drug delivery with magnetic resonance guided high intensity focused ultrasound and temperature sensitive liposomes in a rabbit Vx2 tumor model. *J. Controlled Release* **2012**, *158*, 487–494.
- (230) Awad, T.; Moharram, H.; Shaltout, O.; Asker, D.; Youssef, M. Applications of ultrasound in analysis, processing and quality control of food: A review. *Food Res. Int.* **2012**, *48*, 410–427.
- (231) Ninomiya, K.; Kawabata, S.; Tashita, H.; Shimizu, N. Ultrasound-mediated drug delivery using liposomes modified with a thermosensitive polymer. *Ultron. Sonochem.* **2014**, *21*, 310–316.
- (232) Grüll, H.; Langereis, S. Hyperthermia-triggered drug delivery from temperature-sensitive liposomes using MRI-guided high intensity focused ultrasound. *J. Controlled Release* **2012**, *161*, 317–327.
- (233) Nakatsuka, M. A.; Mattrey, R. F.; Esener, S. C.; Cha, J. N.; Goodwin, A. P. Aptamer-Crosslinked Microbubbles: Smart Contrast Agents for Thrombin-Activated Ultrasound Imaging. *Adv. Mater.* **2012**, *24*, 6010–6016.
- (234) Song, S.; Guo, H.; Jiang, Z.; Jin, Y.; Zhang, Z.; Sun, K.; Dou, H. Self-Assembled Fe<sub>3</sub>O<sub>4</sub>/Polymer Hybrid Microbubble with MRI/Ultrasound Dual-Imaging Enhancement. *Langmuir* **2014**, *30*, 10557–10561.
- (235) Sirsi, S. R.; Borden, M. A. State-of-the-art materials for ultrasound-triggered drug delivery. *Adv. Drug Delivery Rev.* **2014**, *72*, 3–14.
- (236) Yan, F.; Li, L.; Deng, Z.; Jin, Q.; Chen, J.; Yang, W.; Yeh, C.-K.; Wu, J.; Shandas, R.; Liu, X.; et al. Paclitaxel-liposome–microbubble complexes as ultrasound-triggered therapeutic drug delivery carriers. *J. Controlled Release* **2013**, *166*, 246–255.
- (237) Husseini, G. A.; Kherbeck, L.; Pitt, W. G.; Hubbell, J. A.; Christensen, D. A.; Velluto, D. Kinetics of Ultrasonic Drug Delivery from Targeted Micelles. *J. Nanosci. Nanotechnol.* **2015**, *15*, 2099–2104.
- (238) Chung, M. F.; Chen, K. J.; Liang, H. F.; Liao, Z. X.; Chia, W. T.; Xia, Y.; Sung, H. W. A liposomal system capable of generating CO<sub>2</sub> bubbles to induce transient cavitation, lysosomal rupturing, and cell necrosis. *Angew. Chem.* **2012**, *124*, 10236–10240.
- (239) Guo, G.; Ma, Q.; Zhao, B.; Zhang, D. Ultrasound-assisted permeability improvement and acoustic characterization for solid-state fabricated PLA foams. *Ultron. Sonochem.* **2013**, *20*, 137–143.
- (240) Hagisawa, K.; Nishioka, T.; Suzuki, R.; Maruyama, K.; Takase, B.; Ishihara, M.; Kurita, A.; Yoshimoto, N.; Nishida, Y.; Iida, K.; et al. Thrombus-targeted perfluorocarbon-containing liposomal bubbles for enhancement of ultrasonic thrombolysis: in vitro and in vivo study. *J. Thromb. Haemostasis* **2013**, *11*, 1565–1573.
- (241) Rapoport, N.; Nam, K.-H.; Gupta, R.; Gao, Z.; Mohan, P.; Payne, A.; Todd, N.; Liu, X.; Kim, T.; Shea, J.; et al. Ultrasound-mediated tumor imaging and nanotherapy using drug loaded, block copolymer stabilized perfluorocarbon nanoemulsions. *J. Controlled Release* **2011**, *153*, 4–15.
- (242) Kennedy, J.; Ter Haar, G.; Cranston, D. High intensity focused ultrasound: surgery of the future? *Br. J. Radiol.* **2003**, *76*, 590–599.
- (243) de Smet, M.; Heijman, E.; Langereis, S.; Huijnen, N. M.; Grüll, H. Magnetic resonance imaging of high intensity focused ultrasound mediated drug delivery from temperature-sensitive liposomes: an in vivo proof-of-concept study. *J. Controlled Release* **2011**, *150*, 102–110.
- (244) Ta, T.; Bartolak-Suki, E.; Park, E. J.; Karrobi, K.; McDannold, N. J.; Porter, T. M. Localized delivery of doxorubicin in vivo from polymer-modified thermosensitive liposomes with MR-guided focused ultrasound-mediated heating. *J. Controlled Release* **2014**, *194*, 71–81.
- (245) Schroeder, A.; Kost, J.; Barenholz, Y. Ultrasound, liposomes, and drug delivery: principles for using ultrasound to control the release of drugs from liposomes. *Chem. Phys. Lipids* **2009**, *162*, 1–16.
- (246) Rizzitelli, S.; Giustetto, P.; Boffa, C.; Delli Castelli, D.; Cutrin, J. C.; Aime, S.; Terreno, E. In vivo MRI visualization of release from liposomes triggered by local application of pulsed low-intensity non-focused ultrasound. *Nanomedicine* **2014**, *10*, e901–e904.
- (247) de Smet, M.; Langereis, S.; van den Bosch, S.; Bitter, K.; Huijnen, N. M.; Heijman, E.; Grull, H. SPECT/CT imaging of temperature-sensitive liposomes for MR-image guided drug delivery with high intensity focused ultrasound. *J. Controlled Release* **2013**, *169*, 82–90.
- (248) Rizzitelli, S.; Giustetto, P.; Cutrin, J.; Delli Castelli, D.; Boffa, C.; Ruzza, M.; Menchise, V.; Molinari, F.; Aime, S.; Terreno, E. Sonosensitive theranostic liposomes for preclinical in vivo MRI-guided visualization of doxorubicin release stimulated by pulsed low intensity non-focused ultrasound. *J. Controlled Release* **2015**, *202*, 21–30.
- (249) Yin, T.; Wang, P.; Li, J.; Wang, Y.; Zheng, B.; Zheng, R.; Cheng, D.; Shuai, X. Tumor-penetrating codelivery of siRNA and paclitaxel with ultrasound-responsive nanobubbles hetero-assembled from polymeric micelles and liposomes. *Biomaterials* **2014**, *35*, 5932–5943.
- (250) Liang, X.; Gao, J.; Jiang, L.; Luo, J.; Jing, L.; Li, X.; Jin, Y.; Dai, Z. Nano-hybrid Liposomal Cerasomes with Good Physiological Stability and Rapid Temperature Responsiveness for High Intensity Focused Ultrasound Triggered Local Chemotherapy of Cancer. *ACS Nano* **2015**, *9*, 1280–1293.
- (251) Zhang, H. t.; Fan, X. d.; Tian, W.; Suo, R. t.; Yang, Z.; Bai, Y.; Zhang, W. b. Ultrasound-Driven Secondary Self-Assembly of Amphiphilic β-Cyclodextrin Dimers. *Chem. - Eur. J.* **2015**, *21*, 5256.
- (252) Griepenburg, J. C.; Sood, N.; Vargo, K. B.; Williams, D.; Rawson, J.; Therien, M. J.; Hammer, D. A.; Dmochowski, I. J. Caging metal ions with visible light-responsive nano-polymersomes. *Langmuir* **2015**, *31*, 799–807.
- (253) Yan, Q.; Hu, J.; Zhou, R.; Ju, Y.; Yin, Y.; Yuan, J. Visible light-responsive micelles formed from dialkoxanthracene-containing block copolymers. *Chem. Commun.* **2012**, *48*, 1913–1915.
- (254) Hansen, M. B.; van Gaal, E.; Minten, I.; Storm, G.; van Hest, J. C.; Löwik, D. W. Constrained and UV-activatable cell-penetrating peptides for intracellular delivery of liposomes. *J. Controlled Release* **2012**, *164*, 87–94.
- (255) Fomina, N.; McFearin, C.; Sermsakdi, M.; Edigin, O.; Almutairi, A. UV and near-IR triggered release from polymeric nanoparticles. *J. Am. Chem. Soc.* **2010**, *132*, 9540–9542.
- (256) Feng, Z.; Lin, L.; Yan, Z.; Yu, Y. Dual responsive block copolymer micelles functionalized by NIPAM and azobenzene. *Macromol. Rapid Commun.* **2010**, *31*, 640–644.
- (257) Yan, B.; Boyer, J.-C.; Branda, N. R.; Zhao, Y. Near-infrared light-triggered dissociation of block copolymer micelles using upconverting nanoparticles. *J. Am. Chem. Soc.* **2011**, *133*, 19714–19717.
- (258) Cao, J.; Huang, S.; Chen, Y.; Li, S.; Li, X.; Deng, D.; Qian, Z.; Tang, L.; Gu, Y. Near-infrared light-triggered micelles for fast controlled drug release in deep tissue. *Biomaterials* **2013**, *34*, 6272–6283.
- (259) Nomoto, T.; Fukushima, S.; Kumagai, M.; Machitani, K.; Matsumoto, Y.; Oba, M.; Miyata, K.; Osada, K.; Nishiyama, N.; Kataoka, K.; et al. Three-layered polyplex micelle as a multifunctional nanocarrier platform for light-induced systemic gene transfer. *Nat. Commun.* **2014**, *5*, 354510.1038/ncomms4545.
- (260) Sun, L.; Zhu, B.; Su, Y.; Dong, C.-M. Light-responsive linear-dendritic amphiphiles and their nanomedicines for NIR-triggered drug release. *Polym. Chem.* **2014**, *5*, 1605–1613.
- (261) Jiang, J.; Tong, X.; Zhao, Y. A new design for light-breakable polymer micelles. *J. Am. Chem. Soc.* **2005**, *127*, 8290–8291.
- (262) Babin, J.; Pelletier, M.; Lepage, M.; Allard, J. F.; Morris, D.; Zhao, Y. A New Two-Photon-Sensitive Block Copolymer Nanocarrier. *Angew. Chem., Int. Ed.* **2009**, *48*, 3329–3332.
- (263) Ding, J.; Liu, G. Hairy, Semi-shaved, and Fully Shaved Hollow Nanospheres from Polyisoprene-b lock-poly (2-cinnamoylethyl methacrylate). *Chem. Mater.* **1998**, *10*, 537–542.

- (264) Jiang, J.; Qi, B.; Lepage, M.; Zhao, Y. Polymer micelles stabilization on demand through reversible photo-cross-linking. *Macromolecules* **2007**, *40*, 790–792.
- (265) Pavlick, R. A.; Sengupta, S.; McFadden, T.; Zhang, H.; Sen, A. A Polymerization-Powered Motor. *Angew. Chem.* **2011**, *123*, 9546–9549.
- (266) Zhao, Y.; Ikeda, T. *Smart Light-Responsive Materials: Azobenzene-Containing Polymers and Liquid Crystals*; John Wiley & Sons: New York City, 2009.
- (267) Zhao, Y. Light-responsive block copolymer micelles. *Macromolecules* **2012**, *45*, 3647–3657.
- (268) Zhao, H.; Sterner, E. S.; Coughlin, E. B.; Theato, P. O-nitrobenzyl alcohol derivatives: Opportunities in polymer and materials science. *Macromolecules* **2012**, *45*, 1723–1736.
- (269) Xiao, W.; Chen, W. H.; Xu, X. D.; Li, C.; Zhang, J.; Zhuo, R. X.; Zhang, X. Z. Design of a Cellular-Uptake-Shielding “Plug and Play” Template for Photo Controllable Drug Release. *Adv. Mater.* **2011**, *23*, 3526–3530.
- (270) Wang, Y.; Ma, N.; Wang, Z.; Zhang, X. Photocontrolled Reversible Supramolecular Assemblies of an Azobenzene-Containing Surfactant with  $\alpha$ -Cyclodextrin. *Angew. Chem., Int. Ed.* **2007**, *46*, 2823–2826.
- (271) Shanmugam, V.; Selvakumar, S.; Yeh, C.-S. Near-infrared light-responsive nanomaterials in cancer therapeutics. *Chem. Soc. Rev.* **2014**, *43*, 6254–6287.
- (272) Jochum, F. D.; Theato, P. Temperature-and light-responsive smart polymer materials. *Chem. Soc. Rev.* **2013**, *42*, 7468–7483.
- (273) Gohy, J.-F.; Zhao, Y. Photo-responsive block copolymer micelles: design and behavior. *Chem. Soc. Rev.* **2013**, *42*, 7117–7129.
- (274) Fomina, N.; Sankaranarayanan, J.; Almutairi, A. Photochemical mechanisms of light-triggered release from nanocarriers. *Adv. Drug Delivery Rev.* **2012**, *64*, 1005–1020.
- (275) Hu, D.; Peng, H.; Niu, Y.; Li, Y.; Xia, Y.; Li, L.; He, J.; Liu, X.; Xia, X.; Lu, Y.; et al. Reversibly light-responsive biodegradable poly(carbonate) micelles constructed via CuAAC reaction. *J. Polym. Sci., Part A: Polym. Chem.* **2015**, *53*, 750–760.
- (276) Xia, D.; Yu, G.; Li, J.; Huang, F. Photo-responsive self-assembly based on a water-soluble pillar [6] arene and an azobenzene-containing amphiphile in water. *Chem. Commun.* **2014**, *50*, 3606–3608.
- (277) Yu, G.; Han, C.; Zhang, Z.; Chen, J.; Yan, X.; Zheng, B.; Liu, S.; Huang, F. Pillar [6] arene-based photoresponsive host-guest complexation. *J. Am. Chem. Soc.* **2012**, *134*, 8711–8717.
- (278) Xiao, Z.; Ji, C.; Shi, J.; Pridgen, E. M.; Frieder, J.; Wu, J.; Farokhzad, O. C. DNA Self-Assembly of Targeted Near-Infrared-Responsive Gold Nanoparticles for Cancer Thermo-Chemotherapy. *Angew. Chem.* **2012**, *124*, 12023–12027.
- (279) Deng, H.; Zhong, Y.; Du, M.; Liu, Q.; Fan, Z.; Dai, F.; Zhang, X. Theranostic self-assembly structure of gold nanoparticles for NIR photothermal therapy and X-Ray computed tomography imaging. *Theranostics* **2014**, *4*, 904–918.
- (280) Kim, D.; Park, S.; Lee, J. H.; Jeong, Y. Y.; Jon, S. Antibiofouling polymer-coated gold nanoparticles as a contrast agent for in vivo X-ray computed tomography imaging. *J. Am. Chem. Soc.* **2007**, *129*, 7661–7665.
- (281) Chen, J.; Saeki, F.; Wiley, B. J.; Cang, H.; Cobb, M. J.; Li, Z.-Y.; Au, L.; Zhang, H.; Kimmey, M. B.; Li, X.; et al. Gold nanocages: bioconjugation and their potential use as optical imaging contrast agents. *Nano Lett.* **2005**, *5*, 473–477.
- (282) Wang, Y.-C.; Wang, F.; Sun, T.-M.; Wang, J. Redox-responsive nanoparticles from the single disulfide bond-bridged block copolymer as drug carriers for overcoming multidrug resistance in cancer cells. *Bioconjugate Chem.* **2011**, *22*, 1939–1945.
- (283) Zhao, M.; Biswas, A.; Hu, B.; Joo, K.-I.; Wang, P.; Gu, Z.; Tang, Y. Redox-responsive nanocapsules for intracellular protein delivery. *Biomaterials* **2011**, *32*, 5223–5230.
- (284) Cheng, R.; Feng, F.; Meng, F.; Deng, C.; Feijen, J.; Zhong, Z. Glutathione-responsive nano-vehicles as a promising platform for targeted intracellular drug and gene delivery. *J. Controlled Release* **2011**, *152*, 2–12.
- (285) Wang, K.; Liu, Y.; Yi, W.-J.; Li, C.; Li, Y.-Y.; Zhuo, R.-X.; Zhang, X.-Z. Novel shell-cross-linked micelles with detachable PEG corona for glutathione-mediated intracellular drug delivery. *Soft Matter* **2013**, *9*, 692–699.
- (286) Machlin, L. J.; Bendich, A. Free radical tissue damage: protective role of antioxidant nutrients. *FASEB J.* **1987**, *1*, 441–445.
- (287) Fang, Y.-Z.; Yang, S.; Wu, G. Free radicals, antioxidants, and nutrition. *Nutrition* **2002**, *18*, 872–879.
- (288) Couto, N.; Malys, N.; Gaskell, S. J.; Barber, J. Partition and turnover of glutathione reductase from *Saccharomyces cerevisiae*: a proteomic approach. *J. Proteome Res.* **2013**, *12*, 2885–2894.
- (289) Schafer, F. Q.; Buettner, G. R. Redox environment of the cell as viewed through the redox state of the glutathione disulfide/glutathione couple. *Free Radical Biol. Med.* **2001**, *30*, 1191–1212.
- (290) Saito, G.; Swanson, J. A.; Lee, K.-D. Drug delivery strategy utilizing conjugation via reversible disulfide linkages: role and site of cellular reducing activities. *Adv. Drug Delivery Rev.* **2003**, *55*, 199–215.
- (291) Kim, J.; Baek, K.; Shetty, D.; Selvapalam, N.; Yun, G.; Kim, N. H.; Ko, Y. H.; Park, K. M.; Hwang, I.; Kim, K. Reversible Morphological Transformation between Polymer Nanocapsules and Thin Films through Dynamic Covalent Self-Assembly. *Angew. Chem.* **2015**, *127*, 2731–2735.
- (292) Wen, Y.; Zhang, Z.; Li, J. Highly Efficient Multifunctional Supramolecular Gene Carrier System Self-Assembled from Redox-Sensitive and Zwitterionic Polymer Blocks. *Adv. Funct. Mater.* **2014**, *24*, 3874–3884.
- (293) Yang, Q.; Tan, L.; He, C.; Liu, B.; Xu, Y.; Zhu, Z.; Shao, Z.; Gong, B.; Shen, Y.-M. Redox-responsive micelles self-assembled from dynamic covalent block copolymers for intracellular drug delivery. *Acta Biomater.* **2015**, *17*, 193–200.
- (294) Chang, Y.; Yang, K.; Wei, P.; Huang, S.; Pei, Y.; Zhao, W.; Pei, Z. Cationic Vesicles Based on Amphiphilic Pillar [5] arene Capped with Ferrocenium: A Redox-Responsive System for Drug/siRNA Co-Delivery. *Angew. Chem., Int. Ed.* **2014**, *53*, 13126–13130.
- (295) Liang, Z.-P.; Lauterbur, P. C. *Principles of magnetic resonance imaging*; SPIE Optical Engineering Press: Bellingham, WA, 2000.
- (296) Villringer, A.; Chance, B. Non-invasive optical spectroscopy and imaging of human brain function. *Trends Neurosci.* **1997**, *20*, 435–442.
- (297) Ai, H.; Flask, C.; Weinberg, B.; Shuai, X. T.; Pagel, M. D.; Farrell, D.; Duerk, J.; Gao, J. Magnetite-Loaded Polymeric Micelles as Ultrasensitive Magnetic-Resonance Probes. *Adv. Mater.* **2005**, *17*, 1949–1952.
- (298) McCarthy, J. R.; Weissleder, R. Multifunctional magnetic nanoparticles for targeted imaging and therapy. *Adv. Drug Delivery Rev.* **2008**, *60*, 1241–1251.
- (299) Dai, Q.; Nelson, A. Magnetically-responsive self assembled composites. *Chem. Soc. Rev.* **2010**, *39*, 4057–4066.
- (300) Wang, H.; Zhang, S.; Liao, Z.; Wang, C.; Liu, Y.; Feng, S.; Jiang, X.; Chang, J. PEGlated magnetic polymeric liposome anchored with TAT for delivery of drugs across the blood-spinal cord barrier. *Biomaterials* **2010**, *31*, 6589–6596.
- (301) Lesieur, S.; Gazeau, F.; Luciani, N.; Ménager, C.; Wilhelm, C. Multifunctional nanovectors based on magnetic nanoparticles coupled with biological vesicles or synthetic liposomes. *J. Mater. Chem.* **2011**, *21*, 14387–14393.
- (302) Mamiya, H.; Jeyadevan, B. Hyperthermic Effects of Dissipative Structures of Magnetic Nanoparticles in Large Alternating Magnetic Fields. *Sci. Rep.* **2011**, *1*, 15710.1038/srep00157.
- (303) Katagiri, K.; Imai, Y.; Koumoto, K.; Kaiden, T.; Kono, K.; Aoshima, S. Magneto-responsive On-Demand Release of Hybrid Liposomes Formed from Fe<sub>3</sub>O<sub>4</sub> Nanoparticles and Thermosensitive Block Copolymers. *Small* **2011**, *7*, 1683–1689.
- (304) Huang, H.-Y.; Hu, S.-H.; Chian, C.-S.; Chen, S.-Y.; Lai, H.-Y.; Chen, Y.-Y. Self-assembling PVA-F127 thermosensitive nanocarriers with highly sensitive magnetically-triggered drug release for epilepsy therapy in vivo. *J. Mater. Chem.* **2012**, *22*, 8566–8573.

- (305) Kumar, C. S.; Mohammad, F. Magnetic nanomaterials for hyperthermia-based therapy and controlled drug delivery. *Adv. Drug Delivery Rev.* **2011**, *63*, 789–808.
- (306) Reinert, M.; Widmer, H. R.; Bregy, A.; Lönnfors-Weitzel, T.; Vajtai, I.; Corazza, N.; Bernau, V. J.; Weitzel, T.; Mordasini, P.; Schlachter, E. K.; et al. Metabolic pathway and distribution of superparamagnetic iron oxide nanoparticles: in vivo study. *Int. J. Nanomed.* **2011**, *6*, 1793.
- (307) Jiang, S.; Eltoukhy, A. A.; Love, K. T.; Langer, R.; Anderson, D. G. Lipidoid-coated iron oxide nanoparticles for efficient DNA and siRNA delivery. *Nano Lett.* **2013**, *13*, 1059–1064.
- (308) Love, K. T.; Mahon, K. P.; Levins, C. G.; Whitehead, K. A.; Querbes, W.; Dorkin, J. R.; Qin, J.; Cantley, W.; Qin, L. L.; Racie, T.; et al. Lipid-like materials for low-dose, in vivo gene silencing. *Proc. Natl. Acad. Sci. U. S. A.* **2010**, *107*, 1864–1869.
- (309) Kong, S. D.; Sartor, M.; Hu, C.-M. J.; Zhang, W.; Zhang, L.; Jin, S. Magnetic field activated lipid–polymer hybrid nanoparticles for stimuli-responsive drug release. *Acta Biomater.* **2013**, *9*, 5447–5452.
- (310) Lee, J. H.; Chen, K. J.; Noh, S. H.; Garcia, M. A.; Wang, H.; Lin, W. Y.; Jeong, H.; Kong, B. J.; Stout, D. B.; Cheon, J.; et al. On-demand drug release system for in vivo cancer treatment through self-assembled magnetic nanoparticles. *Angew. Chem.* **2013**, *125*, 4480–4484.
- (311) van Rhee, P. G.; Rikken, R. S. M.; Abdelmohsen, L. K. E. A.; Maan, J. C.; Nolte, R. J. M.; van Hest, J. C. M.; Christianen, P. C. M.; Wilson, D. A. Polymersome magneto-valves for reversible capture and release of nanoparticles. *Nat. Commun.* **2014**, *5*, 501010.1038/ncomms6010.
- (312) Kim, K. T.; Zhu, J.; Meeuwissen, S. A.; Cornelissen, J. J.; Pochan, D. J.; Nolte, R. J.; van Hest, J. C. Polymersome stomatocytes: controlled shape transformation in polymer vesicles. *J. Am. Chem. Soc.* **2010**, *132*, 12522–12524.
- (313) Meeuwissen, S. A.; Kim, K. T.; Chen, Y.; Pochan, D. J.; van Hest, J. Controlled shape transformation of polymersome stomatocytes. *Angew. Chem.* **2011**, *123*, 7208–7211.
- (314) Wilson, D. A.; Nolte, R. J.; van Hest, J. C. Autonomous movement of platinum-loaded stomatocytes. *Nat. Chem.* **2012**, *4*, 268–274.
- (315) Rikken, R. S.; Nolte, R. J.; Maan, J. C.; van Hest, J. C.; Wilson, D. A.; Christianen, P. C. Manipulation of micro-and nanostructure motion with magnetic fields. *Soft Matter* **2014**, *10*, 1295–1308.
- (316) Rikken, R. S.; Kerkenaar, H. H.; Nolte, R. J.; Maan, J. C.; van Hest, J. C.; Christianen, P. C.; Wilson, D. A. Probing morphological changes in polymersomes with magnetic birefringence. *Chem. Commun.* **2014**, *50*, 5394–5396.
- (317) Ge, J.; Neofytou, E.; Cahill, T. J., III; Beygui, R. E.; Zare, R. N. Drug release from electric-field-responsive nanoparticles. *ACS Nano* **2012**, *6*, 227–233.
- (318) Yan, Q.; Yuan, J.; Cai, Z.; Xin, Y.; Kang, Y.; Yin, Y. Voltage-responsive vesicles based on orthogonal assembly of two homopolymers. *J. Am. Chem. Soc.* **2010**, *132*, 9268–9270.
- (319) Schmidt, D. J.; Moskowitz, J. S.; Hammond, P. T. Electrically triggered release of a small molecule drug from a polyelectrolyte multilayer coating. *Chem. Mater.* **2010**, *22*, 6416–6425.
- (320) Peng, L.; Feng, A.; Zhang, H.; Wang, H.; Jian, C.; Liu, B.; Gao, W.; Yuan, J. Voltage-responsive micelles based on the assembly of two biocompatible homopolymers. *Polym. Chem.* **2014**, *5*, 1751–1759.
- (321) Feng, A.; Yan, Q.; Zhang, H.; Peng, L.; Yuan, J. Electrochemical redox responsive polymeric micelles formed from amphiphilic supramolecular brushes. *Chem. Commun.* **2014**, *50*, 4740–4742.
- (322) Yang, J. M.; Xu, Z.; Wu, H.; Zhu, H.; Wu, X.; Hait, W. N. Overexpression of Extracellular Matrix Metalloproteinase Inducer in Multidrug Resistant Cancer Cells 1 US Public Health Service National Cancer Institute CA 66077 and CA 72720. Note: JM. Yang and Z. Xu contributed equally to this study. *Mol. Cancer Res.* **2003**, *1*, 420–427.
- (323) Kessenbrock, K.; Plaks, V.; Werb, Z. Matrix metalloproteinases: regulators of the tumor microenvironment. *Cell* **2010**, *141*, 52–67.
- (324) McFadyen, M. C.; Melvin, W. T.; Murray, G. I. Cytochrome P450 enzymes: novel options for cancer therapeutics. *Mol. Cancer Ther.* **2004**, *3*, 363–371.
- (325) Zelzer, M.; Todd, S. J.; Hirst, A. R.; McDonald, T. O.; Ulijn, R. V. Enzyme responsive materials: design strategies and future developments. *Biomater. Sci.* **2013**, *1*, 11–39.
- (326) Banerjee, A.; Chatterjee, K.; Madras, G. Enzymatic degradation of polymers: a brief review. *Mater. Sci. Technol.* **2014**, *30*, 567–573.
- (327) Toledano, S.; Williams, R. J.; Jayawarna, V.; Ulijn, R. V. Enzyme-triggered self-assembly of peptide hydrogels via reversed hydrolysis. *J. Am. Chem. Soc.* **2006**, *128*, 1070–1071.
- (328) Vemula, P. K.; Cruikshank, G. A.; Karp, J. M.; John, G. Self-assembled prodrugs: an enzymatically triggered drug-delivery platform. *Biomaterials* **2009**, *30*, 383–393.
- (329) Rosenbaum, I.; Harnoy, A. J.; Tirosh, E.; Buzhor, M.; Segal, M.; Frid, L.; Shaharabani, R.; Avinery, R.; Beck, R.; Amir, R. J. Encapsulation and covalent binding of molecular payload in enzymatically activated micellar nanocarriers. *J. Am. Chem. Soc.* **2015**, *137*, 2276–2284.
- (330) Hu, J.; Zhang, G.; Liu, S. Enzyme-responsive polymeric assemblies, nanoparticles and hydrogels. *Chem. Soc. Rev.* **2012**, *41*, 5933–5949.
- (331) Harnoy, A. J.; Rosenbaum, I.; Tirosh, E.; Ebenstein, Y.; Shaharabani, R.; Beck, R.; Amir, R. J. Enzyme-Responsive Amphiphilic PEG-Dendron Hybrids and Their Assembly into Smart Micellar Nanocarriers. *J. Am. Chem. Soc.* **2014**, *136*, 7531–7534.
- (332) Zhang, H.; Fei, J.; Yan, X.; Wang, A.; Li, J. Enzyme-Responsive Release of Doxorubicin from Monodisperse Dipeptide-Based Nanocarriers for Highly Efficient Cancer Treatment In Vitro. *Adv. Funct. Mater.* **2015**, *25*, 1193–1204.
- (333) Amir, R. J.; Zhong, S.; Pochan, D. J.; Hawker, C. J. Enzymatically triggered self-assembly of block copolymers. *J. Am. Chem. Soc.* **2009**, *131*, 13949–13951.
- (334) Rao, J.; Hottinger, C.; Khan, A. Enzyme-Triggered Cascade Reactions and Assembly of Abiotic Block Copolymers into Micellar Nanostructures. *J. Am. Chem. Soc.* **2014**, *136*, 5872–5875.
- (335) Seshasai, S. R. K.; Kaptoge, S.; Thompson, A.; Di Angelantonio, E.; Gao, P.; Sarwar, N.; Whincup, P. H.; Mukamal, K. J.; Gillum, R. F.; Holme, I.; et al. Diabetes mellitus, fasting glucose, and risk of cause-specific death. *N. Engl. J. Med.* **2011**, *364*, 829–841.
- (336) American Diabetes Association. Standards of medical care in diabetes-2014. *Diabetes Care* **2014**, *37*, S14–S80.
- (337) Forbes, J. M.; Cooper, M. E. Mechanisms of diabetic complications. *Physiol. Rev.* **2013**, *93*, 137–188.
- (338) Breton, M.; Farret, A.; Bruttomesso, D.; Anderson, S.; Magni, L.; Patek, S.; Dalla Man, C.; Place, J.; Demartini, S.; Del Favero, S.; et al. Fully integrated artificial pancreas in type 1 diabetes modular closed-loop glucose control maintains near normoglycemia. *Diabetes* **2012**, *61*, 2230–2237.
- (339) Kim, H.; Kang, Y. J.; Kang, S.; Kim, K. T. Monosaccharide-responsive release of insulin from polymersomes of polyboroxole block copolymers at neutral pH. *J. Am. Chem. Soc.* **2012**, *134*, 4030–4033.
- (340) Liu, G.; Ma, R.; Ren, J.; Li, Z.; Zhang, H.; Zhang, Z.; An, Y.; Shi, L. A glucose-responsive complex polymeric micelle enabling repeated on-off release and insulin protection. *Soft Matter* **2013**, *9*, 1636–1644.
- (341) Wu, Q.; Wang, L.; Yu, H.; Wang, J.; Chen, Z. Organization of glucose-responsive systems and their properties. *Chem. Rev.* **2011**, *111*, 7855–7875.
- (342) Zhao, L.; Ding, J.; Xiao, C.; He, P.; Tang, Z.; Pang, X.; Zhuang, X.; Chen, X. Glucose-sensitive polypeptide micelles for self-regulated insulin release at physiological pH. *J. Mater. Chem.* **2012**, *22*, 12319–12328.
- (343) Chou, D. H.-C.; Webber, M. J.; Tang, B. C.; Lin, A. B.; Thapa, L. S.; Deng, D.; Truong, J. V.; Cortinas, A. B.; Langer, R.; Anderson, D. G. Glucose-responsive insulin activity by covalent modification with aliphatic phenylboronic acid conjugates. *Proc. Natl. Acad. Sci. U. S. A.* **2015**, *112*, 2401–2406.
- (344) Kim, H.; Kang, Y. J.; Jeong, E. S.; Kang, S.; Kim, K. T. Glucose-responsive disassembly of polymersomes of sequence-specific borox-

- ole-containing block copolymers under physiologically relevant conditions. *ACS Macro Lett.* **2012**, *1*, 1194–1198.
- (345) Tai, W.; Mo, R.; Di, J.; Subramanian, V.; Gu, X.; Buse, J. B.; Gu, Z. Bio-inspired synthetic nanovesicles for glucose-responsive release of insulin. *Biomacromolecules* **2014**, *15*, 3495–3502.
- (346) Chen, X.; Wu, W.; Guo, Z.; Xin, J.; Li, J. Controlled insulin release from glucose-sensitive self-assembled multilayer films based on 21-arm star polymer. *Biomaterials* **2011**, *32*, 1759–1766.
- (347) Gu, Z.; Aimetti, A. A.; Wang, Q.; Dang, T. T.; Zhang, Y.; Veiseh, O.; Cheng, H.; Langer, R. S.; Anderson, D. G. Injectable nano-network for glucose-mediated insulin delivery. *ACS Nano* **2013**, *7*, 4194–4201.
- (348) Schattling, P.; Jochum, F. D.; Theato, P. Multi-stimuli responsive polymers—the all-in-one talents. *Polym. Chem.* **2014**, *5*, 25–36.
- (349) Stoffelen, C.; Voskuhl, J.; Jonkheijm, P.; Huskens, J. Dual Stimuli-Responsive Self-Assembled Supramolecular Nanoparticles. *Angew. Chem.* **2014**, *126*, 3468–3472.
- (350) Das, S.; Ranjan, P.; Maiti, P. S.; Singh, G.; Leitus, G.; Klajn, R. Dual-Responsive Nanoparticles and their Self-Assembly. *Adv. Mater.* **2013**, *25*, 422–426.
- (351) Schilli, C. M.; Zhang, M.; Rizzato, E.; Thang, S. H.; Chong, Y.; Edwards, K.; Karlsson, G.; Müller, A. H. A New Double-Responsive Block Copolymer Synthesized via RAFT Polymerization: Poly (N-isopropylacrylamide)-b lock-poly (acrylic acid). *Macromolecules* **2004**, *37*, 7861–7866.
- (352) Chen, D.; Yu, H.; Sun, K.; Liu, W.; Wang, H. Dual thermoresponsive and pH-responsive self-assembled micellar nanogel for anticancer drug delivery. *Drug Delivery* **2014**, *21*, 258–264.
- (353) André, X.; Zhang, M.; Müller, A. H. Thermo- and pH-Responsive Micelles of Poly (acrylic acid)-block-Poly (N, N-diethylacrylamide). *Macromol. Rapid Commun.* **2005**, *26*, 558–563.
- (354) Tong, R.; Lu, X.; Xia, H. A facile mechanophore functionalization of an amphiphilic block copolymer towards remote ultrasound and redox dual stimulus responsiveness. *Chem. Commun.* **2014**, *50*, 3575–3578.
- (355) Chi, X.; Ji, X.; Xia, D.; Huang, F. A Dual-Responsive Supra-Amphiphilic Polypseudorotaxane Constructed from A Water-Soluble Pillar [7] arene and An Azobenzene-Containing Random Copolymer. *J. Am. Chem. Soc.* **2015**, *137*, 1440–1443.
- (356) Xiao, W.; Zeng, X.; Lin, H.; Han, K.; Jia, H.-Z.; Zhang, X.-Z. Dual stimuli-responsive multi-drug delivery system for the individually controlled release of anti-cancer drugs. *Chem. Commun.* **2015**, *51*, 1475–1478.
- (357) Zhu, G.; Zheng, J.; Song, E.; Donovan, M.; Zhang, K.; Liu, C.; Tan, W. Self-assembled, aptamer-tethered DNA nanotrains for targeted transport of molecular drugs in cancer theranostics. *Proc. Natl. Acad. Sci. U. S. A.* **2013**, *110*, 7998–8003.
- (358) Shi, J.; Xiao, Z.; Kamaly, N.; Farokhzad, O. C. Self-assembled targeted nanoparticles: evolution of technologies and bench to bedside translation. *Acc. Chem. Res.* **2011**, *44*, 1123–1134.
- (359) Cemazar, M.; Sersa, G.; Wilson, J.; Tozer, G. M.; Hart, S. L.; Grosel, A.; Dachs, G. U. Effective gene transfer to solid tumors using different nonviral gene delivery techniques: electroporation, liposomes, and integrin-targeted vector. *Cancer Gene Ther.* **2002**, *9*, 399–406.
- (360) Kibria, G.; Hatakeyama, H.; Ohga, N.; Hida, K.; Harashima, H. The effect of liposomal size on the targeted delivery of doxorubicin to Integrin  $\alpha v\beta 3$ -expressing tumor endothelial cells. *Biomaterials* **2013**, *34*, S617–S627.
- (361) Polyák, A.; Hajdu, I.; Bodnár, M.; Dabasi, G.; Jóbá, R. P.; Borbély, J.; Balogh, L. Folate receptor targeted self-assembled chitosan-based nanoparticles for SPECT/CT imaging: Demonstrating a preclinical proof of concept. *Int. J. Pharm.* **2014**, *474*, 91–94.
- (362) Li, J.; Qu, X.; Payne, G. F.; Zhang, C.; Zhang, Y.; Li, J.; Ren, J.; Hong, H.; Liu, C. Biospecific Self-Assembly of a Nanoparticle Coating for Targeted and Stimuli-Responsive Drug Delivery. *Adv. Funct. Mater.* **2015**, *25*, 1404–1417.
- (363) Ishida, O.; Maruyama, K.; Tanahashi, H.; Iwatsuru, M.; Sasaki, K.; Eriguchi, M.; Yanagie, H. Liposomes bearing polyethyleneglycol-coupled transferrin with intracellular targeting property to the solid tumors in vivo. *Pharm. Res.* **2001**, *18*, 1042–1048.
- (364) Mamot, C.; Drummond, D. C.; Greiser, U.; Hong, K.; Kirpotin, D. B.; Marks, J. D.; Park, J. W. Epidermal growth factor receptor (EGFR)-targeted immunoliposomes mediate specific and efficient drug delivery to EGFR-and EGFRvIII-overexpressing tumor cells. *Cancer Res.* **2003**, *63*, 3154–3161.
- (365) Mamot, C.; Drummond, D. C.; Noble, C. O.; Kallab, V.; Guo, Z.; Hong, K.; Kirpotin, D. B.; Park, J. W. Epidermal growth factor receptor-targeted immunoliposomes significantly enhance the efficacy of multiple anticancer drugs in vivo. *Cancer Res.* **2005**, *65*, 11631–11638.
- (366) Miura, Y.; Takenaka, T.; Toh, K.; Wu, S.; Nishihara, H.; Kano, M. R.; Ino, Y.; Nomoto, T.; Matsumoto, Y.; Koyama, H.; et al. Cyclic RGD-linked polymeric micelles for targeted delivery of platinum anticancer drugs to glioblastoma through the blood-brain tumor barrier. *ACS Nano* **2013**, *7*, 8583–8592.
- (367) Wang, W.; Cheng, D.; Gong, F.; Miao, X.; Shuai, X. Design of multifunctional micelle for tumor-targeted intracellular drug release and fluorescent imaging. *Adv. Mater.* **2012**, *24*, 115–120.
- (368) Sun, W.; Jiang, T.; Lu, Y.; Reiff, M.; Mo, R.; Gu, Z. Cocoon-like self-degradable DNA nanoclew for anticancer drug delivery. *J. Am. Chem. Soc.* **2014**, *136*, 14722–14725.
- (369) Braakman, I.; Bulleid, N. J. Protein folding and modification in the mammalian endoplasmic reticulum. *Annu. Rev. Biochem.* **2011**, *80*, 71–99.
- (370) Hsu, V. W.; Lee, S. Y.; Yang, J.-S. The evolving understanding of COPI vesicle formation. *Nat. Rev. Mol. Cell Biol.* **2009**, *10*, 360–364.
- (371) Lee, M. C.; Miller, E. A.; Goldberg, J.; Orci, L.; Schekman, R. Bi-directional protein transport between the ER and Golgi. *Annu. Rev. Cell Dev. Biol.* **2004**, *20*, 87–123.
- (372) Bonifacino, J. S.; Glick, B. S. The mechanisms of vesicle budding and fusion. *Cell* **2004**, *116*, 153–166.
- (373) Lodish, H.; Berk, A.; Zipursky, S. L.; Matsudaira, P.; Baltimore, D.; Darnell, J. In *Molecular Cell Biology*, 4th ed.; W. H. Freeman: New York, 2000; Section 17.3.
- (374) Lodish, H.; Berk, A.; Zipursky, S. L.; Matsudaira, P.; Baltimore, D.; Darnell, J. In *Molecular Cell Biology*, 4th ed.; W. H. Freeman: New York, 2000; Section 17.4.
- (375) Helenius, A.; Aeby, M. Intracellular functions of N-linked glycans. *Science* **2001**, *291*, 2364–2369.
- (376) Lodish, H.; Berk, A.; Zipursky, S. L.; Matsudaira, P.; Baltimore, D.; Darnell, J. In *Molecular Cell Biology*, 4th ed.; W. H. Freeman: New York, 2000; Section 17.7.
- (377) Alberts, B.; Johnson, A.; Lewis, J.; Raff, M.; Roberts, K.; Walter, P. In *Molecular Biology of the Cell*; 4th ed.; Garland Science: New York, 2002.
- (378) Ding, K.; Uozumi, Y. *Handbook of Asymmetric Heterogeneous Catalysis*; Wiley Online Library: Hoboken, NJ, 2008.
- (379) Burguete, M. I.; Fraile, J. M.; García, J. I.; García-Verdugo, E.; Herreras, C. I.; Luis, S. V.; Mayoral, J. A. Bis (oxazoline) copper complexes covalently bonded to insoluble support as catalysts in cyclopropanation reactions. *J. Org. Chem.* **2001**, *66*, 8893–8901.
- (380) Morandi, B.; Carreira, E. M. Iron-catalyzed cyclopropanation in 6 M KOH with in situ generation of diazomethane. *Science* **2012**, *335*, 1471–1474.
- (381) La Sorella, G.; Strukul, G.; Scarso, A. Recent advances in catalysis in micellar media. *Green Chem.* **2015**, *17*, 644–683.
- (382) Narayan, S.; Muldoon, J.; Finn, M.; Fokin, V. V.; Kolb, H. C.; Sharpless, K. B. On water": Unique reactivity of organic compounds in aqueous suspension. *Angew. Chem., Int. Ed.* **2005**, *44*, 3275–3279.
- (383) Li, C. J. Organic reactions in aqueous media—with a focus on carbon–carbon bond formation. *Chem. Rev.* **1993**, *93*, 2023–2035.
- (384) Li, C.-J. Organic reactions in aqueous media with a focus on carbon–carbon bond formations: a decade update. *Chem. Rev.* **2005**, *105*, 3095–3166.
- (385) Raynal, M.; Ballester, P.; Vidal-Ferran, A.; van Leeuwen, P. W. Supramolecular catalysis. Part 1: non-covalent interactions as a tool for

- building and modifying homogeneous catalysts. *Chem. Soc. Rev.* **2014**, *43*, 1660–1733.
- (386) Raynal, M.; Ballester, P.; Vidal-Ferran, A.; van Leeuwen, P. W. Supramolecular catalysis. Part 2: Artificial enzyme mimics. *Chem. Soc. Rev.* **2014**, *43*, 1734–1787.
- (387) Akagawa, K.; Akabane, H.; Sakamoto, S.; Kudo, K. Organocatalytic asymmetric transfer hydrogenation in aqueous media using resin-supported peptide having a polyleucine tether. *Org. Lett.* **2008**, *10*, 2035–2037.
- (388) Douglas, T.; Young, M. Host-guest encapsulation of materials by assembled virus protein cages. *Nature* **1998**, *393*, 152–155.
- (389) Kuiper, S. M.; Nallani, M.; Vriezema, D. M.; Cornelissen, J. J.; van Hest, J. C.; Nolte, R. J.; Rowan, A. E. Enzymes containing porous polymersomes as nano reaction vessels for cascade reactions. *Org. Biomol. Chem.* **2008**, *6*, 4315–4318.
- (390) van Oers, M. C.; Abdelmohsen, L. K.; Rutjes, F. P.; van Hest, J. C. Aqueous asymmetric cyclopropanation reactions in polymersome membranes. *Chem. Commun.* **2014**, *50*, 4040–4043.
- (391) Breslow, R.; Dong, S. D. Biomimetic reactions catalyzed by cyclodextrins and their derivatives. *Chem. Rev.* **1998**, *98*, 1997–2012.
- (392) Lu, J.; Zhao, X.; Yaseen, M. Biomimetic amphiphiles: biosurfactants. *Curr. Opin. Colloid Interface Sci.* **2007**, *12*, 60–67.
- (393) Leenders, S. H. A. M.; Gramage-Doria, R.; de Bruin, B.; Reek, J. N. H. Transition metal catalysis in confined spaces. *Chem. Soc. Rev.* **2015**, *44*, 433–448.
- (394) Minten, I. J.; Claessen, V. I.; Blank, K.; Rowan, A. E.; Nolte, R. J.; Cornelissen, J. J. Catalytic capsids: the art of confinement. *Chem. Sci.* **2011**, *2*, 358–362.
- (395) Wang, Z. J.; Clary, K. N.; Bergman, R. G.; Raymond, K. N.; Toste, F. D. A supramolecular approach to combining enzymatic and transition metal catalysis. *Nat. Chem.* **2013**, *5*, 100–103.
- (396) Helms, B.; Guillaudeu, S. J.; Xie, Y.; McMurdo, M.; Hawker, C. J.; Fréchet, J. M. One-Pot Reaction Cascades Using Star Polymers with Core-Confining Catalysts. *Angew. Chem., Int. Ed.* **2005**, *44*, 6384–6387.
- (397) Dwars, T.; Paetzold, E.; Oehme, G. Reactions in micellar systems. *Angew. Chem., Int. Ed.* **2005**, *44*, 7174–7199.
- (398) Sorrenti, A.; Illa, O.; Ortuño, R. Amphiphiles in aqueous solution: Well beyond a soap bubble. *Chem. Soc. Rev.* **2013**, *42*, 8200–8219.
- (399) Lipshutz, B. H.; Ghorai, S.; Abela, A. R.; Moser, R.; Nishikata, T.; Duplais, C.; Krasovskiy, A.; Gaston, R. D.; Gadwood, R. C. TPGS-750-M: a second-generation amphiphile for metal-catalyzed cross-couplings in water at room temperature. *J. Org. Chem.* **2011**, *76*, 4379–4391.
- (400) Lipshutz, B. H.; Ghorai, S.; Leong, W. W. Y.; Taft, B. R.; Krogstad, D. V. Manipulating micellar environments for enhancing transition metal-catalyzed cross-couplings in water at room temperature. *J. Org. Chem.* **2011**, *76*, 5061–5073.
- (401) Wang, L.-M.; Jiao, N.; Qiu, J.; Yu, J.-J.; Liu, J.-Q.; Guo, F.-L.; Liu, Y. Sodium stearate-catalyzed multicomponent reactions for efficient synthesis of spirooxindoles in aqueous micellar media. *Tetrahedron* **2010**, *66*, 339–343.
- (402) Rosati, F.; Oelerich, J.; Roelfes, G. Dramatic micellar rate enhancement of the Cu<sup>2+</sup> catalyzed vinologous Friedel–Crafts alkylation in water. *Chem. Commun.* **2010**, *46*, 7804–7806.
- (403) Rajendar Reddy, K.; Rajanna, K. C.; Uppalaiah, K. Environmentally benign contemporary Friedel–Crafts acylation of 1-halo-2-methoxynaphthalenes and its related compounds under conventional and nonconventional conditions. *Tetrahedron Lett.* **2013**, *54*, 3431–3436.
- (404) Nairoukh, Z.; Avnir, D.; Blum, J. Acid-Catalyzed Hydration of Alkynes in Aqueous Microemulsions. *ChemSusChem* **2013**, *6*, 430–432.
- (405) Hamasaki, G.; Muto, T.; Uozumi, Y. A novel amphiphilic pincer palladium complex: design, preparation and self-assembling behavior. *Dalton Trans.* **2011**, *40*, 8859–8868.
- (406) Hamasaki, G.; Muto, T.; Uozumi, Y. Molecular-Architecture-Based Administration of Catalysis in Water: Self-Assembly of an Amphiphilic Palladium Pincer Complex. *Angew. Chem.* **2011**, *123*, 4978–4980.
- (407) Patterson, J. P.; Cotanda, P.; Kelley, E. G.; Moughton, A. O.; Lu, A.; Epps, T. H., III; O'Reilly, R. K. Catalytic Y-tailed amphiphilic homopolymers—aqueous nanoreactors for high activity, low loading SCS pincer catalysts. *Polym. Chem.* **2013**, *4*, 2033–2039.
- (408) Lipshutz, B. H.; Abela, A. R. Micellar Catalysis of Suzuki–Miyaura Cross-Couplings with Heteroaromatics in Water. *Org. Lett.* **2008**, *10*, 5329–5332.
- (409) Kim, K. T.; Cornelissen, J. J.; Nolte, R. J.; van Hest, J. A. Polymersome Nanoreactor with Controllable Permeability Induced by Stimuli-Responsive Block Copolymers. *Adv. Mater.* **2009**, *21*, 2787–2791.
- (410) van Dongen, S. F.; Nallani, M.; Cornelissen, J. J.; Nolte, R. J.; van Hest, J. A. Three-Enzyme Cascade Reaction through Positional Assembly of Enzymes in a Polymersome Nanoreactor. *Chem. - Eur. J.* **2009**, *15*, 1107–1114.
- (411) Peters, R. J.; Marguet, M.; Marais, S.; Fraaije, M. W.; van Hest, J.; Lecommandoux, S. Cascade reactions in multicompartimentalized polymersomes. *Angew. Chem.* **2014**, *126*, 150–154.
- (412) Wang, Z.; van Oers, M.; Rutjes, F. P.; van Hest, J. Polymersome colloidosomes for enzyme catalysis in a biphasic system. *Angew. Chem., Int. Ed.* **2012**, *51*, 10746–10750.
- (413) Flenniken, M.; Uchida, M.; Liepold, L.; Kang, S.; Young, M.; Douglas, T. In *Viruses and Nanotechnology*; Springer: Berlin, 2009.
- (414) de la Escosura, A.; Nolte, R. J.; Cornelissen, J. J. Viruses and protein cages as nanocontainers and nanoreactors. *J. Mater. Chem.* **2009**, *19*, 2274–2278.
- (415) Suttle, C. A. Viruses in the sea. *Nature* **2005**, *437*, 356–361.
- (416) Uchida, M.; Klem, M. T.; Allen, M.; Suci, P.; Flenniken, M.; Gillitzer, E.; Varpness, Z.; Liepold, L. O.; Young, M.; Douglas, T. Biological containers: protein cages as multifunctional nanoplateform. *Adv. Mater.* **2007**, *19*, 1025–1042.
- (417) Schoonen, L.; van Hest, J. C. Functionalization of protein-based nanocages for drug delivery applications. *Nanoscale* **2014**, *6*, 7124–7141.
- (418) Minten, I. J.; Hendriks, L. J.; Nolte, R. J.; Cornelissen, J. J. Controlled encapsulation of multiple proteins in virus capsids. *J. Am. Chem. Soc.* **2009**, *131*, 17771–17773.
- (419) Sikkema, F. D.; Comellas-Aragones, M.; Fokkink, R. G.; Verduin, B. J.; Cornelissen, J. J.; Nolte, R. J. Monodisperse polymer-virus hybrid nanoparticles. *Org. Biomol. Chem.* **2007**, *5*, 54–57.
- (420) Minten, I. J.; Ma, Y.; Nolte, R. J. M.; Cornelissen, J. J. L. M.; Hempenius, M. A.; Vancso, G. J. CCMV capsid formation induced by a functional negatively charged polymer. *Org. Biomol. Chem.* **2009**, *7*, 4685–4688.
- (421) Minten, I. J.; Wilke, K. D.; Hendriks, L. J.; van Hest, J.; Nolte, R. J.; Cornelissen, J. J. Metal-Ion-Induced Formation and Stabilization of Protein Cages Based on the Cowpea Chlorotic Mottle Virus. *Small* **2011**, *7*, 911–919.
- (422) Comellas-Aragones, M.; Engelkamp, H.; Claessen, V. I.; Sommerdijk, N. A.; Rowan, A. E.; Christianen, P. C.; Maan, J. C.; Verduin, B. J.; Cornelissen, J. J.; Nolte, R. J. A virus-based single-enzyme nanoreactor. *Nat. Nanotechnol.* **2007**, *2*, 635–639.
- (423) Zhang, W.; Liu, X.; Walsh, D.; Yao, S.; Kou, Y.; Ma, D. Caged-Protein-Confining Bimetallic Structural Assemblies with Mimetic Peroxidase Activity. *Small* **2012**, *8*, 2948–2953.
- (424) Zhen, Z.; Tang, W.; Chen, H.; Lin, X.; Todd, T.; Wang, G.; Cowger, T.; Chen, X.; Xie, J. RGD-modified apoferritin nanoparticles for efficient drug delivery to tumors. *ACS Nano* **2013**, *7*, 4830–4837.
- (425) Zhen, Z.; Tang, W.; Guo, C.; Chen, H.; Lin, X.; Liu, G.; Fei, B.; Chen, X.; Xu, B.; Xie, J. Ferritin nanocages to encapsulate and deliver photosensitizers for efficient photodynamic therapy against cancer. *ACS Nano* **2013**, *7*, 6988–6996.
- (426) Fan, R.; Chew, S. W.; Cheong, V. V.; Orner, B. P. Fabrication of gold nanoparticles inside unmodified horse spleen apoferritin. *Small* **2010**, *6*, 1483–1487.
- (427) Sun, C.; Yang, H.; Yuan, Y.; Tian, X.; Wang, L.; Guo, Y.; Xu, L.; Lei, J.; Gao, N.; Anderson, G. J.; et al. Controlling assembly of paired

- gold clusters within apoferritin nanoreactor for in vivo kidney targeting and biomedical imaging. *J. Am. Chem. Soc.* **2011**, *133*, 8617–8624.
- (428) Fan, J.; Yin, J.-J.; Ning, B.; Wu, X.; Hu, Y.; Ferrari, M.; Anderson, G. J.; Wei, J.; Zhao, Y.; Nie, G. Direct evidence for catalase and peroxidase activities of ferritin–platinum nanoparticles. *Biomaterials* **2011**, *32*, 1611–1618.
- (429) Abe, S.; Niemeyer, J.; Abe, M.; Takezawa, Y.; Ueno, T.; Hikage, T.; Erker, G.; Watanabe, Y. Control of the coordination structure of organometallic palladium complexes in an apo-ferritin cage. *J. Am. Chem. Soc.* **2008**, *130*, 10512–10514.
- (430) Abe, S.; Hirata, K.; Ueno, T.; Morino, K.; Shimizu, N.; Yamamoto, M.; Takata, M.; Yashima, E.; Watanabe, Y. Polymerization of phenylacetylene by rhodium complexes within a discrete space of apo-ferritin. *J. Am. Chem. Soc.* **2009**, *131*, 6958–6960.
- (431) Naylor, A. M.; Goddard, W. A., III; Kiefer, G. E.; Tomalia, D. A. Starburst dendrimers. 5. Molecular shape control. *J. Am. Chem. Soc.* **1989**, *111*, 2339–2341.
- (432) Tomalia, D. A. Dendrimer research. *Science* **1991**, *252*, 1231.
- (433) Smith, D. K.; Diederich, F. Functional dendrimers: unique biological mimics. *Chem. - Eur. J.* **1998**, *4*, 1353–1361.
- (434) Tomalia, D. A.; Naylor, A. M.; Goddard, W. A. Starburst dendrimers: molecular-level control of size, shape, surface chemistry, topology, and flexibility from atoms to macroscopic matter. *Angew. Chem., Int. Ed. Engl.* **1990**, *29*, 138–175.
- (435) Yang, H.-B.; Northrop, B. H.; Zheng, Y.-R.; Ghosh, K.; Stang, P. J. Facile self-assembly of neutral dendritic metallocycles via oxygen-to-platinum coordination. *J. Org. Chem.* **2009**, *74*, 7067–7074.
- (436) Habicher, T.; Diederich, F.; Gramlich, V. Catalytic Dendrophanes as Enzyme Mimics: Synthesis, Binding Properties, Micropolarity Effect, and Catalytic Activity of Dendritic Thiazolocyclophanes. *Helv. Chim. Acta* **1999**, *82*, 1066–1095.
- (437) Delort, E.; Nguyen-Trung, N.-Q.; Darbre, T.; Reymond, J.-L. Synthesis and activity of histidine-containing catalytic peptide dendrimers. *J. Org. Chem.* **2006**, *71*, 4468–4480.
- (438) Darbre, T.; Reymond, J.-L. Peptide dendrimers as artificial enzymes, receptors, and drug-delivery agents. *Acc. Chem. Res.* **2006**, *39*, 925–934.
- (439) Reymond, J.-L.; Darbre, T. Peptide and glycopeptide dendrimer apple trees as enzyme models and for biomedical applications. *Org. Biomol. Chem.* **2012**, *10*, 1483–1492.
- (440) Lee, H.; Son, S. H.; Sharma, R.; Won, Y.-Y. A Discussion of the pH-Dependent Protonation Behaviors of Poly (2-(dimethylamino) ethyl methacrylate) (PDMAEMA) and Poly (ethylenimine-ran-2-ethyl-2-oxazoline)(P (EI-r-EOz)). *J. Phys. Chem. B* **2011**, *115*, 844–860.
- (441) Koplin, S. A.; Lin, S.; Domanski, T. Evaluation of the antimicrobial activity of cationic polyethylenimines on dry surfaces. *Biotechnol. Prog.* **2008**, *24*, 1160–1165.
- (442) Beyth, N.; Yudovin-Farber, I.; Perez-David, M.; Domb, A. J.; Weiss, E. I. Polyethylenimine nanoparticles incorporated into resin composite cause cell death and trigger biofilm stress in vivo. *Proc. Natl. Acad. Sci. U. S. A.* **2010**, *107*, 22038–22043.
- (443) Yudovin-Farber, I.; Golenser, J.; Beyth, N.; Weiss, E. I.; Domb, A. J. Quaternary ammonium polyethylenimine: antibacterial activity. *J. Nanomater.* **2010**, *2010*, 1.
- (444) Poe, S. L.; Kobašija, M.; McQuade, D. T. Microcapsule enabled multicatalyst system. *J. Am. Chem. Soc.* **2006**, *128*, 15586–15587.
- (445) Klotz, I. M.; Royer, G. P.; Scarpa, I. S. Synthetic derivatives of polyethylenimine with enzyme-like catalytic activity (synzymes). *Proc. Natl. Acad. Sci. U. S. A.* **1971**, *68*, 263–264.
- (446) Marchetti, L.; Levine, M. Biomimetic catalysis. *ACS Catal.* **2011**, *1*, 1090–1118.
- (447) Spetnagel, W. J.; Klotz, I. M. Catalysis of decarboxylation of oxalic acid by modified poly (ethylenimines). *J. Am. Chem. Soc.* **1976**, *98*, 8199–8204.
- (448) Zhao, H.; Foss, F. W., Jr; Breslow, R. Artificial enzymes with thiazolium and imidazolium coenzyme mimics. *J. Am. Chem. Soc.* **2008**, *130*, 12590–12591.
- (449) Chruma, J. J.; Liu, L.; Zhou, W.; Breslow, R. Hydrophobic and electronic factors in the design of dialkylglycine decarboxylase mimics. *Bioorg. Med. Chem.* **2005**, *13*, 5873–5883.
- (450) Poe, S. L.; Kobašija, M.; McQuade, D. T. Mechanism and application of a microcapsule enabled multicatalyst reaction. *J. Am. Chem. Soc.* **2007**, *129*, 9216–9221.
- (451) Liu, L.; Etika, K. C.; Liao, K. S.; Hess, L. A.; Bergbreiter, D. E.; Grunlan, J. C. Comparison of covalently and noncovalently functionalized carbon nanotubes in epoxy. *Macromol. Rapid Commun.* **2009**, *30*, 627–632.
- (452) Peng, Q.; Chen, F.; Zhong, Z.; Zhuo, R. Enhanced gene transfection capability of polyethylenimine by incorporating boronic acid groups. *Chem. Commun.* **2010**, *46*, 5888–5890.
- (453) Hashemi, M.; Parhiz, B.; Hatefi, A.; Ramezani, M. Modified polyethylenimine with histidine–lysine short peptides as gene carrier. *Cancer Gene Ther.* **2011**, *18*, 12–19.
- (454) Purse, B. W.; Gissot, A.; Rebek, J. A deep cavitand provides a structured environment for the menschutkin reaction. *J. Am. Chem. Soc.* **2005**, *127*, 11222–11223.
- (455) Purse, B. W.; Rebek, J. Functional cavitands: Chemical reactivity in structured environments. *Proc. Natl. Acad. Sci. U. S. A.* **2005**, *102*, 10777–10782.
- (456) Hooley, R. J.; Rebek, J., Jr A deep cavitand catalyzes the Diels–Alder reaction of bound maleimides. *Org. Biomol. Chem.* **2007**, *5*, 3631–3636.
- (457) Pluth, M. D.; Bergman, R. G.; Raymond, K. N. Acid catalysis in basic solution: a supramolecular host promotes orthoformate hydrolysis. *Science* **2007**, *316*, 85–88.
- (458) Fujita, M.; Tominaga, M.; Hori, A.; Therrien, B. Coordination assemblies from a Pd (II)-cornered square complex. *Acc. Chem. Res.* **2005**, *38*, 369–378.
- (459) Fujita, M.; Nagao, S.; Iida, M.; Ogata, K.; Ogura, K. Palladium (II)-directed assembly of macrocyclic dinuclear complexes composed of (en) Pd<sup>2+</sup> and bis (4-pyridyl)-substituted bidentate ligands. Remarkable ability for molecular recognition of electron-rich aromatic guests. *J. Am. Chem. Soc.* **1993**, *115*, 1574–1576.
- (460) Yoshizawa, M.; Takeyama, Y.; Kusukawa, T.; Fujita, M. Cavity-Directed, Highly Stereoselective [2 + 2] Photodimerization of Olefins within Self-Assembled Coordination Cages. *Angew. Chem.* **2002**, *114*, 1403–1405.
- (461) Nishioka, Y.; Yamaguchi, T.; Yoshizawa, M.; Fujita, M. Unusual [2 + 4] and [2 + 2] cycloadditions of arenes in the confined cavity of self-assembled cages. *J. Am. Chem. Soc.* **2007**, *129*, 7000–7001.
- (462) Nishioka, Y.; Yamaguchi, T.; Kawano, M.; Fujita, M. Asymmetric [2 + 2] olefin cross photoaddition in a self-assembled host with remote chiral auxiliaries. *J. Am. Chem. Soc.* **2008**, *130*, 8160–8161.
- (463) Das, T.; Kumar, A.; Ghosh, P.; Maity, A.; Jaffer, S. S.; Purkayastha, P. Interaction of twisted intramolecular charge-transfer probe loaded silver nanoparticles with the hydrophobic nanocavities of cyclodextrins. *J. Phys. Chem. C* **2010**, *114*, 19635–19640.
- (464) Tabushi, I.; Fujita, K.; Yuan, L. C. Specific host-guest energy transfer by use of  $\beta$ -cyclodextrin. *Tetrahedron Lett.* **1977**, *18*, 2503–2506.
- (465) Schneider, H.-J.; Sangwan, N. K. Diels–Alder reactions in hydrophobic cavities: a quantitative correlation with solvophobicity and rate enhancements by macrocycles. *J. Chem. Soc., Chem. Commun.* **1986**, 1787–1789.
- (466) Akkilagunta, V. K.; Reddy, V. P.; Kakulapati, R. R. Aqueous-phase aerobic oxidation of alcohols by ru/c in the presence of cyclodextrin: one-pot biomimetic approach to quinoxaline synthesis. *Synlett* **2010**, *2010*, 2571–2574.
- (467) Narayana Murthy, S.; Madhav, B.; Prakash Reddy, V.; Rama Rao, K.; Nageswar, Y. V. D. An approach toward the synthesis of  $\beta$ -hydroxy sulfones on water. *Tetrahedron Lett.* **2009**, *50*, 5009–5011.
- (468) Tokumura, A. Metabolic pathways and physiological and pathological significances of lysolipid phosphate mediators. *J. Cell. Biochem.* **2004**, *92*, 869–881.

- (469) Tabushi, I.; Shimizu, N.; Sugimoto, T.; Shiozuka, M.; Yamamura, K. Cyclodextrin flexibly capped with metal ion. *J. Am. Chem. Soc.* **1977**, *99*, 7100–7102.
- (470) Singleton, M. L.; Reibenspies, J. H.; Daresbourg, M. Y. A cyclodextrin host/guest approach to a hydrogenase active site biomimetic cavity. *J. Am. Chem. Soc.* **2010**, *132*, 8870–8871.
- (471) Danielson, P. B. The cytochrome P450 superfamily: biochemistry, evolution and drug metabolism in humans. *Curr. Drug Metab.* **2002**, *3*, 561–597.
- (472) Schenning, A. P.; Lutje Spelberg, J. H.; Hubert, D. H.; Feiters, M. C.; Nolte, R. J. A supramolecular cytochrome P450 mimic. *Chem. - Eur. J.* **1998**, *4*, 871–880.
- (473) Cai, Y.; Liu, Y.; Lu, Y.; Gao, G.; He, M. Ionic manganese porphyrins with S-containing counter anions: mimicking cytochrome P450 activity for alkene epoxidation. *Catal. Lett.* **2008**, *124*, 334–339.
- (474) Beltman, J. B.; Marée, A. F.; de Boer, R. J. Analysing immune cell migration. *Nat. Rev. Immunol.* **2009**, *9*, 789–798.
- (475) Liang, C.-C.; Park, A. Y.; Guan, J.-L. In vitro scratch assay: a convenient and inexpensive method for analysis of cell migration in vitro. *Nat. Protoc.* **2007**, *2*, 329–333.
- (476) Kurosaka, S.; Kashina, A. Cell biology of embryonic migration. *Birth Defects Res., Part C* **2008**, *84*, 102–122.
- (477) Paxton, W. F.; Kistler, K. C.; Olmeda, C. C.; Sen, A.; St. Angelo, S. K.; Cao, Y.; Mallouk, T. E.; Lammert, P. E.; Crespi, V. H. Catalytic nanomotors: autonomous movement of striped nanorods. *J. Am. Chem. Soc.* **2004**, *126*, 13424–13431.
- (478) Nelson, B. J.; Kaliakatsos, I. K.; Abbott, J. J. Microrobots for minimally invasive medicine. *Annu. Rev. Biomed. Eng.* **2010**, *12*, 55–85.
- (479) Ghosh, A.; Fischer, P. Controlled propulsion of artificial magnetic nanostructured propellers. *Nano Lett.* **2009**, *9*, 2243–2245.
- (480) Ibele, M.; Mallouk, T. E.; Sen, A. Schooling Behavior of Light-Powered Autonomous Micromotors in Water. *Angew. Chem., Int. Ed.* **2009**, *48*, 3308–3312.
- (481) Magdanz, V.; Sanchez, S.; Schmidt, O. G. Development of a Sperm-Flagella Driven Micro-Bio-Robot. *Adv. Mater.* **2013**, *25*, 6581–6588.
- (482) Kline, T. R.; Paxton, W. F.; Mallouk, T. E.; Sen, A. Catalytic nanomotors: remote-controlled autonomous movement of striped metallic nanorods. *Angew. Chem.* **2005**, *117*, 754–756.
- (483) Catchmark, J. M.; Subramanian, S.; Sen, A. Directed rotational motion of microscale objects using interfacial tension gradients continually generated via catalytic reactions. *Small* **2005**, *1*, 202–206.
- (484) Paxton, W. F.; Sundararajan, S.; Mallouk, T. E.; Sen, A. Chemical locomotion. *Angew. Chem., Int. Ed.* **2006**, *45*, 5420–5429.
- (485) Liu, R.; Sen, A. Autonomous Nanomotor Based on Copper-Platinum Segmented Nanobattery. *J. Am. Chem. Soc.* **2011**, *133*, 20064–20067.
- (486) Garcia-Gradilla, V.; Sattayasamitsathit, S.; Soto, F.; Kuralay, F.; Yardimci, C.; Wiitala, D.; Galarnyk, M.; Wang, J. Ultrasound-Propelled Nanoporous Gold Wire for Efficient Drug Loading and Release. *Small* **2014**, *10*, 4154–4159.
- (487) Gao, W.; Wang, J. Synthetic micro/nanomotors in drug delivery. *Nanoscale* **2014**, *6*, 10486–10494.
- (488) Garcia-Gradilla, V.; Orozco, J.; Sattayasamitsathit, S.; Soto, F.; Kuralay, F.; Pourazary, A.; Katzenberg, A.; Gao, W.; Shen, Y.; Wang, J. Functionalized ultrasound-propelled magnetically guided nanomotors: Toward practical biomedical applications. *ACS Nano* **2013**, *7*, 9232–9240.
- (489) Wang, J.; Gao, W. Nano/microscale motors: biomedical opportunities and challenges. *ACS Nano* **2012**, *6*, 5745–5751.
- (490) Gao, W.; Kagan, D.; Pak, O. S.; Clawson, C.; Campuzano, S.; Chuluun-Erdene, E.; Shipton, E.; Fullerton, E. E.; Zhang, L.; Lauga, E.; et al. Cargo-Towing Fuel-Free Magnetic Nanoswimmers for Targeted Drug Delivery. *Small* **2012**, *8*, 460–467.
- (491) Wang, J. Biomolecule-Functionalized Nanowires: From Nanosensors to Nanocarriers. *ChemPhysChem* **2009**, *10*, 1748–1755.
- (492) Jurado-Sánchez, B.; Sattayasamitsathit, S.; Gao, W.; Santos, L.; Fedorak, Y.; Singh, V. V.; Orozco, J.; Galarnyk, M.; Wang, J. Self-Propelled Activated Carbon Janus Micromotors for Efficient Water Purification. *Small* **2015**, *11*, 499–506.
- (493) Li, J.; Singh, V. V.; Sattayasamitsathit, S.; Orozco, J.; Kaufmann, K.; Dong, R.; Gao, W.; Jurado-Sánchez, B.; Fedorak, Y.; Wang, J. Water-Driven Micromotors for Rapid Photocatalytic Degradation of Biological and Chemical Warfare Agents. *ACS Nano* **2014**, *8*, 11118–11125.
- (494) Orozco, J.; Vilela, D.; Valdés-Ramírez, G.; Fedorak, Y.; Escarpa, A.; Vazquez-Duhalt, R.; Wang, J. Efficient Biocatalytic Degradation of Pollutants by Enzyme-Releasing Self-Propelled Motors. *Chem. - Eur. J.* **2014**, *20*, 2866–2871.
- (495) Gao, W.; Feng, X.; Pei, A.; Gu, Y.; Li, J.; Wang, J. Seawater-driven magnesium based Janus micromotors for environmental remediation. *Nanoscale* **2013**, *5*, 4696–4700.
- (496) Orozco, J.; García-Gradilla, V.; D'Agostino, M.; Gao, W.; Cortés, A.; Wang, J. Artificial enzyme-powered microfish for water-quality testing. *ACS Nano* **2013**, *7*, 818–824.
- (497) Ganguly, A.; Yang, H.; Sharma, R.; Patel, K. D.; Cabral, F. The role of microtubules and their dynamics in cell migration. *J. Biol. Chem.* **2012**, *287*, 43359–43369.
- (498) Meyer, A. S.; Hughes-Alford, S. K.; Kay, J. E.; Castillo, A.; Wells, A.; Gertler, F. B.; Lauffenburger, D. A. 2D protrusion but not motility predicts growth factor-induced cancer cell migration in 3D collagen. *J. Cell Biol.* **2012**, *197*, 721–729.
- (499) Hammer, D. A.; Robbins, G. P.; Haun, J. B.; Lin, J. J.; Qi, W.; Smith, L. A.; Ghoroghchian, P. P.; Therien, M. J.; Bates, F. S. Leuko-polymerosomes. *Faraday Discuss.* **2008**, *139*, 129–141.
- (500) Magdanz, V.; Stoychev, G.; Ionov, L.; Sanchez, S.; Schmidt, O. Stimuli-Responsive Microjets with Reconfigurable Shape. *Angew. Chem., Int. Ed.* **2014**, *53*, 2673–2677.
- (501) Hong, Y.; Blackman, N. M.; Kopp, N. D.; Sen, A.; Velegol, D. Chemotaxis of nonbiological colloidal rods. *Phys. Rev. Lett.* **2007**, *99*, 178103.
- (502) Baraban, L.; Harazim, S. M.; Sanchez, S.; Schmidt, O. G. Chemotactic behavior of catalytic motors in microfluidic channels. *Angew. Chem.* **2013**, *125*, 5662–5666.
- (503) Wilson, D. A.; van Blaaderen, A.; Nolte, J. M. R.; van Hest, J. C. M.; de Nijs, B. Fuel concentration dependent movement of supramolecular catalytic nanomotors. *Nanoscale* **2013**, *5*, 1315–1318.
- (504) Wilson, D. A.; Nolte, R. J.; van Hest, J. C. Entrapment of metal nanoparticles in polymer stomatocytes. *J. Am. Chem. Soc.* **2012**, *134*, 9894–9897.
- (505) Wu, Y.; Wu, Z.; Lin, X.; He, Q.; Li, J. Autonomous movement of controllable assembled Janus capsule motors. *ACS Nano* **2012**, *6*, 10910–10916.
- (506) Wu, Y.; Si, T.; Lin, X.; He, Q. Near infrared-modulated propulsion of catalytic Janus polymer multilayer capsule motors. *Chem. Commun.* **2015**, *51*, 511–514.
- (507) Wu, Y.; Lin, X.; Wu, Z.; Möhwald, H.; He, Q. Self-propelled polymer multilayer Janus capsules for effective drug delivery and light-triggered release. *ACS Appl. Mater. Interfaces* **2014**, *6*, 10476–10481.
- (508) Wu, Z.; Wu, Y.; He, W.; Lin, X.; Sun, J.; He, Q. Self-Propelled Polymer-Based Multilayer Nanorockets for Transportation and Drug Release. *Angew. Chem., Int. Ed.* **2013**, *52*, 7000–7003.
- (509) Wu, Z.; Lin, X.; Wu, Y.; Si, T.; Sun, J.; He, Q. Near-infrared light-triggered “on/off” motion of polymer multilayer rockets. *ACS Nano* **2014**, *8*, 6097–6105.
- (510) Wu, Z.; Li, T.; Li, J.; Gao, W.; Xu, T.; Christianson, C.; Gao, W.; Galarnyk, M.; He, Q.; Zhang, L.; et al. Turning Erythrocytes into Functional Micromotors. *ACS Nano* **2014**, *8*, 12041–12048.
- (511) Ikezoe, Y.; Washino, G.; Uemura, T.; Kitagawa, S.; Matsui, H. Autonomous motors of a metal–organic framework powered by reorganization of self-assembled peptides at interfaces. *Nat. Mater.* **2012**, *11*, 1081–1085.
- (512) Ikezoe, Y.; Fang, J.; Wasik, T. L.; Uemura, T.; Zheng, Y.; Kitagawa, S.; Matsui, H. Peptide Assembly-Driven Metal–Organic Framework (MOF) Motors for Micro Electric Generators. *Adv. Mater.* **2015**, *27*, 288–291.

- (513) Dong, B.; Zhou, T.; Zhang, H.; Li, C. Y. Directed self-assembly of nanoparticles for nanomotors. *ACS Nano* **2013**, *7*, 5192–5198.
- (514) Dreyfus, R.; Baudry, J.; Roper, M. L.; Fermigier, M.; Stone, H. A.; Bibette, J. Microscopic artificial swimmers. *Nature* **2005**, *437*, 862–865.
- (515) Mori, N.; Kurabayashi, K.; Takeuchi, S. Artificial flagellates: Analysis of advancing motions of biflagellate micro-objects. *Appl. Phys. Lett.* **2010**, *96*, 083701.
- (516) Miettinen, H. M.; Gripentrog, J. M.; Jesaitis, A. J. Chemotaxis of Chinese hamster ovary cells expressing the human neutrophil formyl peptide receptor: role of signal transduction molecules and alpha $\beta$  integrin. *J. Cell Sci.* **1998**, *111*, 1921–1928.
- (517) Pollard, T. D.; Borisy, G. G. Cellular motility driven by assembly and disassembly of actin filaments. *Cell* **2003**, *112*, 453–465.
- (518) Robbins, G. P.; Saunders, R. L.; Haun, J. B.; Rawson, J.; Therien, M. J.; Hammer, D. A. Tunable leuko-polymersomes that adhere specifically to inflammatory markers. *Langmuir* **2010**, *26*, 14089–14096.
- (519) Peng, F.; Tu, Y.; van Hest, J.; Wilson, D. A. Self-Guided Supramolecular Cargo-Loaded Nanomotors with Chemotactic Behavior towards Cells. *Angew. Chem., Int. Ed.* **2015**, *54* (40), 11662–11665.
- (520) Sengupta, S.; Dey, K. K.; Muddana, H. S.; Tabouillet, T.; Ibele, M. E.; Butler, P. J.; Sen, A. Enzyme molecules as nanomotors. *J. Am. Chem. Soc.* **2013**, *135*, 1406–1414.
- (521) Dey, K. K.; Das, S.; Poyton, M. F.; Sengupta, S.; Butler, P. J.; Cremer, P. S.; Sen, A. Chemotactic separation of enzymes. *ACS Nano* **2014**, *8*, 11941–11949.
- (522) Morgan, A. R.; Dawson, A. B.; Mckenzie, H. S.; Skelhon, T. S.; Beanland, R.; Franks, H. P.; Bon, S. A. Chemotaxis of catalytic silica-manganese oxide "matchstick" particles. *Materials Horizons* **2014**, *1* (1), 65–68.
- (523) Dey, K. K.; Bhandari, S.; Bandyopadhyay, D.; Basu, S.; Chattopadhyay, A. The pH Taxis of an Intelligent Catalytic Microbot. *Small* **2013**, *9*, 1916–1920.
- (524) Singh, A. K.; Dey, K. K.; Chattopadhyay, A.; Mandal, T. K.; Bandyopadhyay, D. Multimodal chemo-magnetic control of self-propelling microbots. *Nanoscale* **2014**, *6*, 1398–1405.
- (525) Dhar, P.; Cao, Y.; Kline, T.; Pal, P.; Swayne, C.; Fischer, T. M.; Miller, B.; Mallouk, T. E.; Sen, A.; Johansen, T. H. Autonomously moving local nanoprobe in heterogeneous magnetic fields. *J. Phys. Chem. C* **2007**, *111*, 3607–3613.
- (526) Khalil, I. S.; Magdanz, V.; Sanchez, S.; Schmidt, O. G.; Abelmann, L.; Misra, S. Engineering in Medicine and Biology Society (EMBC), 2013 35th Annual International Conference of the IEEE; IEEE: Piscataway, NJ, 2013; pp 5299–5302.
- (527) Zhao, G.; Pumera, M. Magnetotactic artificial self-propelled nanojets. *Langmuir* **2013**, *29*, 7411–7415.
- (528) Springer, T. A. Adhesion receptors of the immune system. *Nature* **1990**, *346*, 425–434.
- (529) Usta, O. B.; Alexeev, A.; Zhu, G.; Balazs, A. C. Modeling microcapsules that communicate through nanoparticles to undergo self-propelled motion. *ACS Nano* **2008**, *2*, 471–476.
- (530) Solon, J.; Streicher, P.; Richter, R.; Brochard-Wyart, F.; Bassereau, P. Vesicles surfing on a lipid bilayer: Self-induced haptotactic motion. *Proc. Natl. Acad. Sci. U. S. A.* **2006**, *103*, 12382–12387.
- (531) Hammer, D. A.; Kamat, N. P. Towards an artificial cell. *FEBS Lett.* **2012**, *586*, 2882–2890.
- (532) Blain, J. C.; Szostak, J. W. Progress toward synthetic cells. *Annu. Rev. Biochem.* **2014**, *83*, 615–640.
- (533) Szostak, J. W.; Bartel, D. P.; Luisi, P. L. Synthesizing life. *Nature* **2001**, *409*, 387–390.
- (534) Chen, I. A.; Walde, P. From self-assembled vesicles to protocells. *Cold Spring Harbor Perspect. Biol.* **2010**, *2*, a002170.
- (535) Oberholzer, T.; Wick, R.; Luisi, P. L.; Biebricher, C. K. Enzymatic RNA replication in self-reproducing vesicles: an approach to a minimal cell. *Biochem. Biophys. Res. Commun.* **1995**, *207*, 250–257.
- (536) Kurihara, K.; Tamura, M.; Shohda, K.-i.; Toyota, T.; Suzuki, K.; Sugawara, T. Self-reproduction of supramolecular giant vesicles combined with the amplification of encapsulated DNA. *Nat. Chem.* **2011**, *3*, 775–781.
- (537) Oberholzer, T.; Albrizio, M.; Luisi, P. L. Polymerase chain reaction in liposomes. *Chem. Biol.* **1995**, *2*, 677–682.
- (538) Chakrabarti, A. C.; Breaker, R. R.; Joyce, G. F.; Deamer, D. W. Production of RNA by a polymerase protein encapsulated within phospholipid vesicles. *J. Mol. Evol.* **1994**, *39*, 555–559.
- (539) Zhu, T. F.; Szostak, J. W. Coupled growth and division of model protocell membranes. *J. Am. Chem. Soc.* **2009**, *131*, 5705–5713.
- (540) Zhu, T. F.; Adamala, K.; Zhang, N.; Szostak, J. W. Photochemically driven redox chemistry induces protocell membrane pearlizing and division. *Proc. Natl. Acad. Sci. U. S. A.* **2012**, *109*, 9828–9832.
- (541) Chen, I. A.; Szostak, J. W. A kinetic study of the growth of fatty acid vesicles. *Biophys. J.* **2004**, *87*, 988–998.
- (542) Walde, P.; Goto, A.; Monnard, P.-A.; Wessicken, M.; Luisi, P. L. Oparin's reactions revisited: Enzymic synthesis of poly (adenylic acid) in micelles and self-reproducing vesicles. *J. Am. Chem. Soc.* **1994**, *116*, 7541–7547.
- (543) Murtas, G. Internal lipid synthesis and vesicle growth as a step toward self-reproduction of the minimal cell. *Syst. Synth. Biol.* **2010**, *4*, 85–93.
- (544) Terasawa, H.; Nishimura, K.; Suzuki, H.; Matsuura, T.; Yomo, T. Coupling of the fusion and budding of giant phospholipid vesicles containing macromolecules. *Proc. Natl. Acad. Sci. U. S. A.* **2012**, *109*, 5942–5947.
- (545) Sunami, T.; Caschera, F.; Morita, Y.; Toyota, T.; Nishimura, K.; Matsuura, T.; Suzuki, H.; Hanczyc, M. M.; Yomo, T. Detection of association and fusion of giant vesicles using a fluorescence-activated cell sorter. *Langmuir* **2010**, *26*, 15098–15103.
- (546) Stano, P.; Luisi, P. L. Achievements and open questions in the self-reproduction of vesicles and synthetic minimal cells. *Chem. Commun.* **2010**, *46*, 3639–3653.
- (547) Hanczyc, M. M.; Fujikawa, S. M.; Szostak, J. W. Experimental models of primitive cellular compartments: Encapsulation, growth, and division. *Science* **2003**, *302*, 618–622.
- (548) Luisi, P. L.; Stano, P. Synthetic biology: Minimal cell mimicry. *Nat. Chem.* **2011**, *3*, 755–756.
- (549) Mills, D.; Peterson, R.; Spiegelman, S. An extracellular Darwinian experiment with a self-duplicating nucleic acid molecule. *Proc. Natl. Acad. Sci. U. S. A.* **1967**, *58*, 217.
- (550) Schrum, J. P.; Zhu, T. F.; Szostak, J. W. The origins of cellular life. *Cold Spring Harbor Perspect. Biol.* **2010**, *2*, a002212.
- (551) Margulis, L. *Symbiosis in Cell Evolution: Microbial Communities in the Archean and Proterozoic Eons*; W. H. Freeman: New York, 1993.
- (552) Schrödinger, E. *What is life? The Physical Aspect of the Living Cell*; The Cambridge University Press: Cambridge, U.K., 1944.
- (553) Ruiz-Mirazo, K.; Briones, C.; de la Escosura, A. Prebiotic systems chemistry: new perspectives for the origins of life. *Chem. Rev.* **2014**, *114*, 285–366.
- (554) Whitesides, G. M.; Grzybowski, B. Self-assembly at all scales. *Science* **2002**, *295*, 2418–2421.
- (555) Mattia, E.; Otto, S. Supramolecular systems chemistry. *Nat. Nanotechnol.* **2015**, *10*, 111–119.
- (556) Korevaar, P. A.; George, S. J.; Markvoort, A. J.; Smulders, M. M.; Hilbers, P. A.; Schenning, A. P.; De Greef, T. F.; Meijer, E. Pathway complexity in supramolecular polymerization. *Nature* **2012**, *481*, 492–496.
- (557) Klajn, R.; Bishop, K. J.; Grzybowski, B. A. Light-controlled self-assembly of reversible and irreversible nanoparticle suprastructures. *Proc. Natl. Acad. Sci. U. S. A.* **2007**, *104*, 10305–10309.
- (558) Klajn, R.; Wesson, P. J.; Bishop, K. J.; Grzybowski, B. A. Writing Self-Erasing Images using Metastable Nanoparticle "Inks". *Angew. Chem., Int. Ed.* **2009**, *48*, 7035–7039.
- (559) Emond, M.; Le Saux, T.; Allemand, J. F.; Pelupessy, P.; Plisson, R.; Jullien, L. Energy propagation through a protometabolism leading to the local emergence of singular stationary concentration profiles. *Chem. - Eur. J.* **2012**, *18*, 14375–14383.

- (560) Krabbenborg, S. O. *Surface Gradients under Electrochemical Control*; Universiteit Twente: Enschede, The Netherlands, 2014.
- (561) Whitesides, G. M.; Grzybowski, B. A.; Stone, H. A. Dynamic self-assembly of magnetized, millimetre-sized objects rotating at a liquid-air interface. *Nature* **2000**, *405*, 1033–1036.
- (562) Swan, J. W.; Bauer, J. L.; Liu, Y.; Furst, E. M. Directed colloidal self-assembly in toggled magnetic fields. *Soft Matter* **2014**, *10*, 1102–1109.
- (563) Grzybowski, B. A.; Campbell, C. J. Complexity and dynamic self-assembly. *Chem. Eng. Sci.* **2004**, *59*, 1667–1676.
- (564) Grzybowski, B. A.; Whitesides, G. M. Macroscopic synthesis of self-assembled dissipative structures. *J. Phys. Chem. B* **2001**, *105*, 8770–8775.
- (565) Tretiakov, K. V.; Bishop, K. J.; Grzybowski, B. A. Additivity of the excess energy dissipation rate in a dynamically self-assembled system. *J. Phys. Chem. B* **2009**, *113*, 7574–7578.
- (566) Grzybowski, B. A.; Wilmer, C. E.; Kim, J.; Browne, K. P.; Bishop, K. J. Self-assembly: from crystals to cells. *Soft Matter* **2009**, *5*, 1110–1128.
- (567) Timonen, J. V.; Latikka, M.; Leibler, L.; Ras, R. H.; Ikkala, O. Switchable static and dynamic self-assembly of magnetic droplets on superhydrophobic surfaces. *Science* **2013**, *341*, 253–257.
- (568) Eelkema, R.; van Esch, J. H. Catalytic control over the formation of supramolecular materials. *Org. Biomol. Chem.* **2014**, *12*, 6292–6296.
- (569) Boekhoven, J.; Poolman, J. M.; Maity, C.; Li, F.; van der Mee, L.; Minkenberg, C. B.; Mendes, E.; van Esch, J. H.; Eelkema, R. Catalytic control over supramolecular gel formation. *Nat. Chem.* **2013**, *5*, 433–437.
- (570) Boekhoven, J.; Brizard, A. M.; Kowlgi, N. K.; Koper, J. M.; Elkema, R.; van Esch, J. H. Dissipative Self-Assembly of a Molecular Gelator by Using a Chemical Fuel. *Angew. Chem.* **2010**, *122*, 4935–4938.
- (571) Debnath, S.; Roy, S.; Ulijn, R. V. Peptide nanofibers with dynamic instability through nonequilibrium biocatalytic assembly. *J. Am. Chem. Soc.* **2013**, *135*, 16789–16792.
- (572) von Maltzahn, G.; Min, D. H.; Zhang, Y.; Park, J. H.; Harris, T. J.; Sailor, M.; Bhatia, S. N. Nanoparticle Self-Assembly Directed by Antagonistic Kinase and Phosphatase Activities. *Adv. Mater.* **2007**, *19*, 3579–3583.
- (573) Dambeniek, A.; Vu, P.; Fyles, T. Dissipative assembly of a membrane transport system. *Chem. Sci.* **2014**, *5*, 3396–3403.
- (574) Gibson, D. G.; Glass, J. I.; Lartigue, C.; Noskov, V. N.; Chuang, R.-Y.; Algire, M. A.; Benders, G. A.; Montague, M. G.; Ma, L.; Moodie, M. M.; et al. Creation of a bacterial cell controlled by a chemically synthesized genome. *Science* **2010**, *329*, 52–56.
- (575) Nardin, C.; Widmer, J.; Winterhalter, M.; Meier, W. Amphiphilic block copolymer nanocontainers as bioreactors. *Eur. Phys. J. E: Soft Matter Biol. Phys.* **2001**, *4*, 403–410.
- (576) Chalmeau, J.; Monina, N.; Shin, J.; Vieu, C.; Noireaux, V.  $\alpha$ -Hemolysin pore formation into a supported phospholipid bilayer using cell-free expression. *Biochim. Biophys. Acta, Biomembr.* **2011**, *1808*, 271–278.
- (577) Vargo, K. B.; Parthasarathy, R.; Hammer, D. A. Self-assembly of tunable protein suprastructures from recombinant oleosin. *Proc. Natl. Acad. Sci. U. S. A.* **2012**, *109*, 11657–11662.
- (578) Raper, S. E.; Chirmule, N.; Lee, F. S.; Wivel, N. A.; Bagg, A.; Gao, G.-p.; Wilson, J. M.; Batshaw, M. L. Fatal systemic inflammatory response syndrome in a ornithine transcarbamylase deficient patient following adenoviral gene transfer. *Mol. Genet. Metab.* **2003**, *80*, 148–158.
- (579) Martino, C.; Kim, S. H.; Horsfall, L.; Abbaspourrad, A.; Rosser, S. J.; Cooper, J.; Weitz, D. A. Protein expression, aggregation, and triggered release from polymersomes as artificial cell-like structures. *Angew. Chem., Int. Ed.* **2012**, *51*, 6416–6420.
- (580) Pietrini, A. V.; Luisi, P. L. Cell-free protein synthesis through solubilisate exchange in water/oil emulsion compartments. *Chem-BioChem* **2004**, *5*, 1055–1062.
- (581) Choi, H.-J.; Montemagno, C. D. Artificial organelle: ATP synthesis from cellular mimetic polymersomes. *Nano Lett.* **2005**, *5*, 2538–2542.
- (582) Elani, Y.; Law, R. V.; Ces, O. Vesicle-based artificial cells as chemical microreactors with spatially segregated reaction pathways. *Nat. Commun.* **2014**, *5*, 530510.1038/ncomms6305.
- (583) Li, M.; Harbron, R. L.; Weaver, J. V.; Binks, B. P.; Mann, S. Electrostatically gated membrane permeability in inorganic protocells. *Nat. Chem.* **2013**, *5*, S29–S36.
- (584) Semenov, S. N.; Wong, A. S.; van der Made, R. M.; Postma, S. G.; Groen, J.; van Roekel, H. W.; de Greef, T. F.; Huck, W. T. Rational design of functional and tunable oscillating enzymatic networks. *Nat. Chem.* **2015**, *7*, 160–165.
- (585) Schmidli, P. K.; Schurtenberger, P.; Luisi, P. L. Liposome-mediated enzymatic synthesis of phosphatidylcholine as an approach to self-replicating liposomes. *J. Am. Chem. Soc.* **1991**, *113*, 8127–8130.